

~~CONFIDENTIAL~~

UNCLASSIFIED

NATIONAL ADVISORY COMMITTEE FOR AERONAUTICS

RESEARCH MEMORANDUM

INVESTIGATION OF AN NACA 4-(5)(05)-041 FOUR-BLADE

PROPELLER WITH SEVERAL SPINNERS AT

MACH NUMBERS UP TO 0.90

By Robert M. Reynolds, Donald A. Buell,
and John H. Walker

SUMMARY

An investigation has been made to determine the aerodynamic characteristics of an NACA 4-(5)(05)-041 four-blade propeller in combination with NACA 1-series and extended cylindrical spinners for a wide range of blade angles at Mach numbers up to 0.90. Included are data for the propeller operating at negative thrust at low forward speeds and operating at near-static conditions. A description of the 1000-horsepower propeller dynamometer used to obtain the data is included in the report.

The performance of the propeller in combination with two different NACA 1-series spinners having maximum diameters of 7.20 and 6.51 inches is compared with the performance of the propeller in combination with long (14 feet ahead of the propeller) cylindrical spinners having diameters of 7.20 and 12.00 inches. The majority of the data were obtained at a Reynolds number of 1.5 million per foot, based on the tunnel-datum airspeed. At the lower Mach numbers, data were also obtained at a Reynolds number of 3.0 million per foot.

Substantially lower propeller efficiency was obtained for the propeller with the NACA 1-series spinners as compared to that obtained for the propeller with the extended cylindrical spinners. The difference in efficiencies amounted to as much as 15 percent at the highest Mach number and blade angle of these tests. This difference is attributed to a general decrease in the section lift-drag ratios for the elements of the blade inboard of 0.7 radius, due to the higher resultant Mach numbers and the accompanying reduced section angles of attack for these portions of the blades in the presence of the 1-series spinner. The lower efficiency of the propeller with the 1-series spinner is indicative of the importance of establishing the pitch distribution of the propeller and

~~CONFIDENTIAL~~

UNCLASSIFIED

the location of the propeller with respect to the spinner with due regard to the flow field about the spinner.

The results show that, in general, the effects of compressibility on maximum efficiency are similar to those previously reported for the NACA 4-(4)(06)-04, 4-(5)(08)-03, and 4-(3)(08)-03 two-blade propellers. For the propeller with the 7.20-inch-diameter, 1-series spinner, the adverse effects of compressibility did not become apparent up to a Mach number of about 0.7 for a blade angle of 65° . For this blade angle and Mach number the maximum efficiency was 79 percent.

INTRODUCTION

In response to a need for data concerning the high-speed characteristics of propellers and propeller-spinner-cowling combinations suitable for use with gas turbine engines of large horsepower, two types of investigations have been made: the first, directed at improving the high-speed efficiency of propellers, and the second, investigating means for providing efficient air induction to turbine engines.

Research on the effects of compressibility, camber, sweep, thickness ratio, and dual rotation on propeller performance at high speeds is reported in references 1 through 8. Inasmuch as these studies were made with cylindrical spinners, they do not provide information regarding practical propeller-spinner installations.

Data are also available for use in the design of aerodynamically efficient spinner-cowling combinations. Reference 9 presents a procedure, from the results of tests at low speed, for the selection of spinner-cowling combinations for specific high-speed requirements, the validity of which has been subsequently shown for high speeds in references 10 and 11. These references present data only for the basic spinner-cowling combinations in the absence of propellers, and as such are not directly applicable to the design of propeller-spinner-cowling combinations.

To obtain data more directly useful for design purposes, an investigation was undertaken in the Ames 12-foot pressure wind tunnel to ascertain the aerodynamic characteristics of representative propeller-spinner-cowling combinations. One phase of this investigation is the determination of the characteristics of the propeller-spinner combination, in the absence of a cowling. This report presents the basic characteristics of an NACA 4-(5)(05)-041 propeller in combination with an NACA 1-series spinner. Another phase of the investigation, the internal pressure-recovery characteristics of an NACA D-type spinner-cowling combination as affected by the operation of the propeller, has been reported in reference 12.

Presented herein are the force-test results for the NACA 4-(5)(05)-041 four-blade, single-rotation propeller with NACA 1-series spinners having diameters of 7.20 and 6.51 inches. A comparison is presented of the results obtained with the propeller in combination with the 1-series spinners, with two extended cylindrical spinners (7.20 and 12.00 inches in diameter), and with the results of other propeller investigations (references 1, 2, and 4). These tests were conducted at blade angles from 15° to 70° and free-stream Mach numbers from 0.90 to 0.10, at a constant Reynolds number of 1.5 million per foot. Data are also included for the propeller in negative thrust, for operation at near-static conditions, and for operation at a Reynolds number of 3.0 million per foot.

SYMBOLS

b blade width, feet

c_{l_d} blade-section design lift coefficient

C_P power coefficient $\left(\frac{P}{\rho n^3 D^5} \right)$

C_T thrust coefficient $\left(\frac{T}{\rho n^2 D^4} \right)$

D propeller diameter, feet

$\frac{b}{D}$ blade-width ratio

h maximum thickness of blade section, feet

$\frac{h}{b}$ blade-thickness ratio

J advance-diameter ratio $\left(\frac{V_0}{nD} \right)$

M_d tunnel-datum Mach number

M_l local Mach number

M_r	reference Mach number used in correlation of local Mach number surveys
M_t	tip Mach number $\left[M_d \sqrt{1 + \left(\frac{\pi}{J} \right)^2} \right]$
n	propeller rotational speed, revolutions per second
P	power, foot-pounds per second
r	blade-section radius, feet
R	propeller-tip radius, feet
Rn	Reynolds number per foot $\left(\frac{\rho V}{\mu} \right)$
T	thrust, pounds
T_c	thrust coefficient $\left(\frac{T}{\rho V^2 D^2} \right)$
V	tunnel-datum velocity (tunnel airspeed uncorrected for tunnel-wall constraint), feet per second
V_o	equivalent free-air velocity (tunnel-datum airspeed corrected for tunnel-wall constraint), feet per second
β	section blade angle, degrees
$\beta_{0.75R}$	section blade angle at the 0.75 radius, degrees
η	efficiency $\left(\frac{T V_o}{P} \right)$ or $\left(\frac{C_T}{C_p} J \right)$
η_{max}	maximum efficiency
μ	viscosity of air, slugs per foot-second
ρ	mass density of air, slugs per cubic foot

APPARATUS AND CALIBRATIONS

1000-Horsepower Propeller Dynamometer

The 1000-horsepower single-rotation propeller dynamometer used in these tests in the Ames 12-foot pressure wind tunnel is shown for the 1-series and extended cylindrical spinners in figures 1 and 2, respectively. The external dimensions of the dynamometer are given in table I. A detailed description of the dynamometer is presented in appendix A.

Propeller and Spinners

Propeller.- The four-blade propeller used in this investigation has the blade designation NACA 4-(5)(05)-041. This designation indicates a 4-foot-diameter propeller having values of the design parameters at 0.7 radius as follows: section design lift coefficient, 0.50; section thickness ratio, 0.050; and solidity per blade, 0.041.

The propeller blade form was established through use of the design charts in reference 13 for the following full-scale requirements:

Operating altitude, feet	35,000
Flight Mach number (cruise)	0.80
Power at design altitude and speed, horsepower . .	5,600

The full-scale propeller, selected to comply with the design conditions, would be a four-blade, single-rotation propeller having a diameter of 23 feet, NACA 16-series blade sections, and an optimum load distribution at an advance-diameter ratio of 3.7 with a blade angle of 60° at 0.75 radius. The model propeller blade (fig. 3) had the form depicted in figure 4. The dashed lines in figure 4 show the revisions made to the portions of the blades inboard of a 4.5-inch radius to permit the extension of the propeller blade sections to the surface of the 6.51-inch-diameter, 1-series spinner described later.

Spinners.- The major portion of the investigation was made using a spinner having a maximum diameter of 7.20 inches (15 percent of the propeller diameter) and a total length of 13.73 inches. The forward portion of the spinner, 10.8 inches or 1.5 times the spinner diameter in length, was contoured to the NACA 1-series profile (reference 9). The rear portion of the spinner was cylindrical, having a length of 2.93 inches and a diameter of 7.20 inches. This spinner is designated as the 7.20-inch-diameter, 1-series spinner and is shown in figure 1. The coordinates of the spinner are given in the first part of table I. The propeller plane of rotation was 10.8 inches behind the spinner nose.

Limited tests were made with the propeller in combination with an NACA 1-46.5-047 spinner (reference 12), designated herein as the 6.51-inch-diameter, 1-series spinner. The installation of this spinner was similar to that for the 7.20-inch-diameter, 1-series spinner. The nose of the spinner was 4.20 inches ahead of the propeller plane of rotation.

Additional tests were made with the propeller in combination with two cylindrical spinners, extended approximately 14 feet ahead of the propeller (fig. 2). These spinners were 7.20 and 12.00 inches in diameter and are designated as the 7.20- and 12.00-inch-diameter, extended cylindrical spinners. The nose portions of these spinners were NACA 1-series bodies of revolution having lengths equal to 3 times the spinner diameters.

All tests were made with the propeller blade sections extended to the spinner surface and with the gaps between the propeller blades and the spinner sealed.

Calibrations

Calibrations were made of the thrust gages, the torquemeter, and the tunnel air stream in the vicinity of the dynamometer. A detailed description of the equipment and methods used in making the calibrations and a discussion of the calibration results are presented in appendix B.

TESTS

Propeller thrust, torque, and rotational speed were measured for the various propeller-spinner combinations at the blade angles and tunnel Mach numbers listed in table II. For reference, table III is a tabulation of the range of tunnel stagnation temperatures corresponding to the Mach numbers in table II.

Each run was made at a fixed value of tunnel Mach number and blade angle, with the rotational speed varied to provide a suitable range of advance-diameter ratios. Each run was initiated near the zero-thrust condition, and the rotational speed was increased (or decreased for the negative-thrust runs, footnote 3 in table II) until one of the operating limits was reached. There were four factors which limited the range of operation of the propeller:

1. Maximum capacity of the thrust gages (1500 or 750 pounds, see appendix B)

2. Maximum capacity of the torquemeter (800 pound-feet)
3. Maximum rotational speed permitted by structural characteristics of the propeller (6000 rpm for tests with the 7.20-inch-diameter, 1-series spinner; 5000 rpm for all other tests, subsequent to modification of the inner portions of the blades, see section Apparatus and Calibrations)
4. Aural indication of stalling of the propeller

With the exception of the runs noted in footnote 2 in table II, all tests were made at a Reynolds number of 1.5 million per foot, based on the tunnel-datum airspeed.

REDUCTION OF DATA

Propeller Thrust

Propeller thrust as used herein is the algebraic difference between the resultant longitudinal force produced by the propeller-spinner combination and the resultant longitudinal force produced by the spinner alone at the same air velocity and density. The methods used in determining the propeller thrust are discussed in detail in appendix C.

Propeller Torque

Dynamic calibrations of the torquemeter, discussed in appendix B, show that for a given rotational speed the sensitivity of the torquemeter varied about 2 percent (see calibration constant, table IV) between the three groups of calibrations (1 to 25, 26 to 39, and 40 to 44, table IV) made at different stages during the tests. In computing the propeller torque, the variation of the calibration constant with rotational speed was taken as a straight line having a slope equal to that obtained by treating the results of dynamic calibrations 1 to 25, table IV, by the method of least squares and having a value of the calibration constant at zero rotational speed equal to the average of the calibration constants of the static calibrations, table V (excluding calibrations 1, 2, and 6).

Datum Mach Number

From the calibrations of the tunnel air stream, discussed in detail in appendix B, the tunnel-datum Mach number was taken as the average Mach number over the propeller disc area for the extended cylindrical spinners. The same variation of datum Mach number with reference Mach number (appendix B) used in the reduction of the data for the 7.20-inch-diameter, extended cylindrical spinner was used for the reduction of the data for the 7.20- and 6.51-inch-diameter, 1-series spinners.

Tunnel-Wall Correction

The tunnel-datum velocity (and consequently the advance-diameter ratio and propeller efficiency) has been corrected for the effect of tunnel-wall constraint on the air-stream velocity at the propeller plane by use of the method described in reference 1. The ratio of the free-air velocity to the tunnel-datum velocity determined experimentally using the method of reference 1 for a 4-foot-diameter propeller in the Ames 12-foot pressure wind tunnel is compared in figure 5 with the theoretical values obtained from the method of reference 14. The good agreement, even at negative thrust, between the experimentally determined values and the theoretical values confirms the validity of the method of reference 1.

As used herein, the tunnel Mach numbers (M_d , M_l , M_r , M_t) are not corrected for tunnel-wall constraint. The free-air Mach number, however, can be obtained by applying the tunnel-wall corrections (fig. 5) to the tunnel-datum Mach number. At Mach numbers above 0.59, $T_c/1-M_d^2$ does not exceed 0.15, so the tunnel-wall correction is less than 1 percent. In the exact use of the propeller data presented herein, however, the tunnel-datum Mach number should be corrected to the free-air Mach number wherever small changes in Mach number produce large changes in the results.

Accuracy of Results

Analysis of the accuracy of the separate measurements of thrust, torque, and air-stream velocity has indicated that errors in the propeller efficiencies reported herein are probably less than 2 percent, but

could be as large as 4 percent if a maximum error in the indicated torque is assumed as a possibility from the torquemeter calibration data. Repeat tests have shown consistent agreement of the propeller efficiencies within 2 percent.

RESULTS

The characteristics of the NACA 4-(5)(05)-041 propeller in combination with the 7.20-inch-diameter, 1-series spinner are presented in figures 6 through 9. The variation, with advance-diameter ratio, of the propeller thrust coefficient, power coefficient, efficiency, and tip Mach number is shown in figure 6 for various blade angles at tunnel-datum Mach numbers between 0.90 and 0.10. Figure 7 shows the negative-thrust characteristics of the propeller for blade angles of 15° , 0° , and -15° at datum Mach numbers of 0.20 and 0.10. The results obtained in operation of the propeller at blade angles of 20° , 15° , 10° , and 0° at near-static conditions are presented in figure 8. Figure 9 presents a comparison of the thrust coefficients, power coefficients, and efficiency of the propeller for a blade angle of 50° at Reynolds numbers of 1.5 and 3.0 million per foot and datum Mach numbers between 0.59 and 0.29.

The characteristics of the propeller in combination with the 6.51-inch-diameter, 1-series spinner, the 7.20-inch-diameter, extended cylindrical spinner, and the 12.00-inch-diameter, extended cylindrical spinner are presented in figures 10, 11, and 12, respectively.

For the propeller with the 7.20-inch-diameter, 1-series spinner, the variation of maximum efficiency with Mach number, tip Mach number, and advance-diameter ratio is shown in figures 13, 14, and 15, respectively. For the propeller with the extended cylindrical spinners, the variation of maximum efficiency with Mach number and advance-diameter ratio is shown in figures 16 and 17, respectively.

Figure 18 presents the effect of Mach number on the maximum efficiency of the NACA 4-(5)(05)-041 propeller, in combination with various spinners, compared with the results from the propeller investigations reported in references 2 and 4, all for a blade angle of 60° at 0.75 radius.

DISCUSSION

The data presented in the figures showing the characteristics of the propeller (with the 7.20-inch-diameter, 1-series spinner) in negative

thrust (fig. 7) and in operation at near-static conditions (fig. 8) are believed to be self-explanatory and therefore are not discussed in detail. It may be noted, however, that values of 2.3 and 1.4 for the ratio of the thrust coefficient to the power coefficient, for blade angles of 5° and 20° , respectively (see fig. 8(b)), correspond to values of 6.0 and 3.7 pounds of thrust per horsepower, respectively, for the design value of nD (211).

For Mach numbers between 0.59 and 0.29 and for a blade angle of 50° , increasing the Reynolds number from 1.5 million to 3.0 million per foot had a negligible effect on the performance of the propeller (fig. 9).

Propeller Efficiency With the NACA 1-Series Spinners

Effect of Mach number on maximum efficiency.- In general, the effect of Mach number on the maximum efficiency of the NACA 4-(5)(05)-041 propeller with the 7.20-inch-diameter, 1-series spinner (fig. 13) is similar to the results reported for investigations of two-blade propellers (references 1, 2, and 4). For blade angles greater than 40° , the highest values of maximum efficiency obtained at each blade angle showed a progressive reduction with increasing blade angle, decreasing from 86 percent at a blade angle of 40° to 79 percent at a blade angle of 65° (fig. 13). The Mach number at which marked efficiency losses, due to adverse compressibility effects, became apparent increased with increasing blade angle, up to a blade angle of 65° . The highest Mach number at which the propeller operated without marked compressibility losses at a blade angle of 65° was about 0.7, at which condition the propeller efficiency was 79 percent. With the occurrence of severe compressibility losses, associated with supersonic resultant section Mach numbers and consequent reduced section lift-drag ratios, the rate of loss of efficiency increased with increasing blade angle.

Figure 14, which presents the variation of maximum efficiency with tip Mach number for blade angles greater than 40° , indicates primarily that the loss in efficiency due to compressibility began at about the same tip Mach number, approximately 0.8, regardless of the blade angle.

The variation of maximum efficiency with Mach number for the propeller in combination with the 6.51-inch-diameter, 1-series spinner was essentially identical, within the limits of experimental accuracy of these tests, to the results (fig. 13) shown for the propeller with the 7.20-inch-diameter, 1-series spinner.

Effect of advance-diameter ratio on maximum efficiency.- The effect of advance-diameter ratio on the maximum efficiency of the NACA 4-(5)(05)-041

propeller, at constant Mach numbers (fig. 15), was also similar to the results reported for investigations of two-blade propellers (references 1, 2, and 4). Figure 15 shows the same general phenomena discussed in these references; namely, that for operation of the propeller at subcritical Mach numbers, highest efficiencies are obtained at relatively high advance-diameter ratios but, as the Mach number is increased to supercritical values, the highest efficiencies are obtained at low advance-diameter ratios. The Mach number for the change from operation at high advance-diameter ratio to operation at low advance-diameter ratio for highest efficiencies was about 0.75 for the propeller with the 7.20-inch-diameter, 1-series spinner. As in the investigations reported in references 1, 2, and 4, maximum efficiency at Mach numbers above 0.8 was obtained in operation of the propeller at the lower blade angles and advance-diameter ratios (figs. 6(a), 6(b), and 6(c)), for which conditions the resultant Mach number was greater than unity for most of the blade elements.

Analysis of the data presented in figure 6 indicates that at the design conditions (0.80 Mach number, 5600 horsepower, 23-foot diameter, 3.7 advance-diameter ratio, 35,000-foot altitude) the propeller blade angle at the 0.75 radius would be $62-1/2^\circ$ and the efficiency would be 55 percent. This efficiency is about 2 percent less than the maximum that would be attained with this propeller at the design Mach number and advance-diameter ratio (see fig. 15). Further analysis of the data in figure 6 indicates that by operating the propeller at a lower value of advance-diameter ratio, 2.4, the same power could be absorbed by a 13-foot-diameter propeller with an efficiency of 61 percent.

Propeller Efficiency With the Extended Cylindrical Spinners

As shown in figures 16 and 17, the general effects of Mach number and advance-diameter ratio on the maximum efficiency of the propeller with the 7.20- and 12.00-inch-diameter, extended cylindrical spinners are similar to those previously discussed for the propeller with the 1-series spinners. The Mach number for the change from operation at high advance-diameter ratio to operation at low advance-diameter ratio for highest efficiencies is about 0.82 for the propeller with the 7.20-inch-diameter, extended cylindrical spinner (fig. 17(a)) and about 0.83 for the propeller with the 12.00-inch-diameter, extended cylindrical spinner (fig. 17(b)).

Comparison of the Maximum Efficiency of the Propeller With 1-Series Spinners and With Cylindrical Spinners

Comparison of the maximum efficiency of the propeller in combination with the cylindrical spinners (fig. 16) with the maximum efficiency of the propeller with the 1-series spinner (fig. 13) shows that generally higher efficiencies were obtained for the propeller with the cylindrical spinners, and that the highest efficiencies were obtained with the 12.00-inch-diameter, cylindrical spinner. Values of the maximum efficiency for the various propeller-spinner combinations at datum Mach numbers between 0.85 and 0.60 are shown for comparison in the following table:

VALUES OF MAXIMUM EFFICIENCY, η_{\max} , AT SEVERAL
DATUM MACH NUMBERS FOR THE VARIOUS SPINNERS

[Values in parentheses are estimated by extrapolation]

Ma	Blade angle at 0.75 radius, $\beta_{0.75R}$ (deg)								
	65°			60°			55°		
	1	2	3	1	2	3	1	2	3
0.85	0.49	(0.59)	(0.64)	----	----	----	----	----	----
.80	.57	.70	.72	0.59	(0.67)	(0.69)	----	----	----
.75	.68	.78	.79	.67	.76	.76	0.64	(0.69)	(0.72)
.70	.79	.82	.83	.76	.82	.83	.73	.80	.80
.60	.79	.85	.85	.81	.84	.85	.82	.86	.86
Row	SPINNER								
1	7.20-inch-diameter, 1-series spinner								
2	7.20-inch-diameter, extended cylindrical spinner								
3	12.00-inch-diameter, extended cylindrical spinner								

In general, the increment in efficiency between the cylindrical and 1-series spinners increased with either increasing Mach number for a given blade angle or increasing blade angle for a given Mach number. The difference in performance of the propeller with the 7.20-inch-diameter, cylindrical spinner and with the 7.20-inch-diameter, 1-series spinner is primarily attributable to the different radial Mach number distributions in the plane of the propeller for the spinners, as discussed in appendix B. The difference in propeller efficiencies with the 7.20- and 12.00-inch-diameter, cylindrical spinners is partly attributable to the different radial Mach number distributions in the plane of the propeller with the two spinners (see appendix B) and partly attributable to the enclosure of a portion of the thick, inner portions of the propeller blades within the

larger spinner. By use of the method of reference 15, calculations were made of the distribution of thrust and torque loading on the blade for the cylindrical and 1-series spinners of the same diameter. Although only of qualitative value, these calculations indicated that the lower efficiency with the 1-series spinner was due to the fact that the blade elements inboard of 0.7 radius were operating at lower lift-drag ratios, brought about by the higher resultant Mach numbers and the accompanying reduced section angles of attack for these portions of the blade. As shown in figures 15 and 17, the maximum efficiency decreased from about 67 percent for the propeller with the 12.00-inch-diameter, cylindrical spinner to about 65 percent with the 7.20-inch-diameter, cylindrical spinner and to about 61 percent with the 7.20-inch-diameter, 1-series spinner, for Mach numbers of 0.83, 0.82, and 0.78, respectively (Mach numbers for which there was little variation of maximum efficiency with advance-diameter ratio). This decrease in maximum efficiency indicates that average values of the section lift-drag ratios were lower for the propeller in combination with the 1-series spinners than for the propeller with the cylindrical spinners.

In figure 18 the variation of maximum efficiency with Mach number for the NACA 4-(5)(05)-041 four-blade propeller, with various spinners, is compared to similar data, reported in references 2 and 4, for the NACA 4-(4)(06)-04, 4-(5)(08)-03, and 4-(3)(08)-03 two-blade propellers with 13.00-inch-diameter, cylindrical spinners. The Mach number at which losses in efficiency due to compressibility began was about the same (0.7) for the NACA 4-(5)(05)-041 propeller with the 12.00-inch-diameter, cylindrical spinner and the NACA 4-(4)(06)-04 propeller with a 13.00-inch-diameter, cylindrical spinner, as might be expected in view of the small differences in camber and thickness between the two blades. Also as might be expected for the thinner blades, at Mach numbers greater than about 0.7 the rate of loss of efficiency with increasing Mach number was not as great for the NACA 4-(5)(05)-041 propeller as for either the NACA 4-(4)(06)-04 or 4-(5)(08)-03 propeller. The trend of the data indicates that at some Mach number in excess of 0.8, the NACA 4-(5)(05)-041 propeller with the 12.00-inch-diameter, cylindrical spinner would have a higher maximum efficiency than either the NACA 4-(4)(06)-04 or 4-(5)(08)-03 propeller. At the subcritical Mach numbers at least part of the difference in maximum efficiency between the NACA 4-(5)(05)-041 propeller with the 12.00-inch-diameter, cylindrical spinner and the NACA 4-(4)(06)-04 propeller is attributable to the difference in total solidity of the two propellers. References 16 and 17 indicate that increasing the solidity of a propeller by increasing the number of blades, in this case from two blades to four blades, can result in a decrease in maximum efficiency of the order of 3 percent.

CONCLUSIONS

An investigation of an NACA 4-(5)(05)-041 four-blade, single-rotation propeller in combination with NACA 1-series and extended cylindrical spinners at Mach numbers up to 0.90 and blade angles of 70° to 15° indicated the following results:

1. Substantially lower efficiencies were obtained for the propeller in combination with the NACA 1-series spinners as compared with those obtained for the propeller in combination with the extended cylindrical spinners. The difference in efficiencies amounted to as much as 15 percent at the highest Mach number and blade angle of these tests.

2. As a corollary of item 1 above, it may be concluded that the efficiency of a propeller in combination with a practical spinner, such as the NACA 1-series spinners, is likely to be considerably less than that indicated by wind-tunnel tests of propellers with cylindrical spinners, unless the pitch distribution and the location of the propeller with respect to the spinner are established with due regard to the local flow about the spinner, or unless the spinner is shaped to provide more uniform flow in the region of the propeller.

3. For the propeller in combination with the 7.20-inch-diameter, 1-series spinner, the highest Mach number at which compressibility had not caused a decrease in maximum efficiency was about 0.7 for a blade angle of 65°. For this blade angle and Mach number the maximum efficiency was 79 percent.

4. In general, the effects of compressibility on the maximum propeller efficiency were similar to those reported for blade designs such as the NACA 4-(4)(06)-04, the NACA 4-(5)(08)-03, and the NACA 4-(3)(08)-03 two-blade propellers.

Ames Aeronautical Laboratory
National Advisory Committee for Aeronautics
Moffett Field, Calif.

APPENDIX A

THE 1000-HORSEPOWER PROPELLER DYNAMOMETER OF THE
AMES 12-FOOT PRESSURE WIND TUNNEL

GENERAL ARRANGEMENT

A drawing and photographs of the single-rotation propeller dynamometer are presented in figure 1. A cutaway view of the internal mechanism is presented in figure 19 and the external dimensions are given in table I. The dynamometer has a rating of 1000 horsepower at 6600 revolutions per minute. Speed control of the 2-pole induction motor is accomplished by means of a variable-frequency power supply.

The dynamometer is made up of two major subassemblies, the fixed external housing and the floating dynamometer unit, interconnected structurally at two flexure-pivot supports. The fixed external housing is comprised of the shroud, main housing, tail cone, support struts, shroud for the box beam, thrust strain-gage members, and motor-stator torque-restraining member. The components of the floating dynamometer unit are the spinner, propeller-hub assembly, drive shaft, torquemeter, motor, box beam (for support of electrical, lubricant, air, and coolant leads), inside member of the mercury seal, and the dynamometer housing.

The flexure pivots carry, in tension, the weight of the floating unit and provide restraint against lateral motion. When the flexure pivots and their supports are deflected longitudinally by a thrust load, they produce a moment equal and opposite to the moment produced by the weight of the floating dynamometer unit. This subassembly, as suspended on the flexure pivot supports, is thus neutrally stable longitudinally.

Restraint of the floating dynamometer unit against longitudinal motion is accomplished by means of a pair of cantilever beams with strain gages. These beams are fixed to the main housing and linked to the dynamometer housing. The links are parallel to and equidistant from the dynamometer center line.

The manner in which the motor stator is mounted in the dynamometer housing permits nearly frictionless longitudinal movement of the floating dynamometer unit without the motor-stator torque reaction being transmitted through the flexure pivots to the fixed housing. The motor stator is supported on trunnion bearings and is restrained against rotational movement by a pair of forked torque arms which are attached to the motor stator and fit over a corresponding pair of radial ball bearings supported by the fixed structure. The reaction forces in the arms

form a couple about the center line of the dynamometer. The inner races of the radial bearings are continuously rotated by a motor drive in order that only the difference between the rolling friction of the bearings is present in the thrust system.

Control of the air pressure inside of the dynamometer is maintained during its operation. Air is introduced for operation of the torque-meter and through the oil-mist lubrication system for the motor and drive shaft bearings. Air and oil mist is scavenged from the dynamometer by vacuum pumps. Three pressure seals (see fig. 19) are employed to separate the inside of the dynamometer from the wind tunnel. A flexible, neoprene pressure seal joins the floating dynamometer unit to the fixed shroud a short distance behind the propeller spinner. A carbon ring, bonded to a molded-neoprene diaphragm and spring retained against the back face of the rear propeller-hub taper collar, provides a pressure seal between the dynamometer housing and the rotating drive shaft. A mercury pressure seal, beneath the box-beam shroud and the floor of the test section, separates the interior of the dynamometer from the wind-tunnel balance chamber.

All electrical, lubricant, air, and coolant leads entering the dynamometer pass through air-tight packing glands in the floating member of the mercury pressure seal. The leads swing freely in a long loop from the floating member of the mercury seal to brackets which secure them to stationary structure in the balance chamber.

INSTRUMENTATION

Thrust

The thrust acting on the dynamometer is measured by means of two resistance-type strain gages mounted on cantilever beams. Two alternate sets of strain gages are in use, having thrust capacities of 1500 and 750 pounds per pair. The output of the strain-gage system is indicated on a self-balancing potentiometer. Calibrations of the strain gages (see appendix B) are made to ascertain the factors relating the potentiometer readings to the applied thrust loads.

Pressure measurements, made to determine the pressure forces on the system, are described in appendix C.

Torque

The torque produced in the propeller shaft is measured by means of a General Electric Company variable-inductance-type torquemeter with a capacity of 800 pound-feet. Essentially, the torquemeter consists of a torque-transmitting shaft which is flanged at each end to permit attachment between the driving and driven units of the dynamometer. Between the end flanges, the shaft is housed concentrically within a reference tube, one end of which is rigidly attached to the shaft. The other, or free, end of the reference tube is held concentric with the shaft by means of a spoke-like flexure-pivot arrangement and contains a series of windings about a stator core. A toothed flange, integral with the shaft and aligned with the stator core, constitutes the rotor portion of the torquemeter. Twisting of the shaft under a torque load results in an angular displacement of the toothed flange with respect to the stator core. The magnetic field between the stator and rotor is thereby altered and a change in current in the exciting windings occurs. This current is transmitted through slip rings to brushes and is indicated by means of a manual-balancing potentiometer. Calibrations of the torquemeter (see appendix B) are made to ascertain the factors relating the potentiometer readings to applied torque loads.

Rotational Speed

The rotational speed of the drive shaft is measured by means of the frequency of the current produced by a variable-reluctance alternating-current generator mounted on the back end of the motor shaft. The current is transmitted to a frequency meter which indicates the rotational speed within an accuracy of 0.05 percent in the range between 240 and 6600 rpm.

APPENDIX B

CALIBRATIONS

CALIBRATION OF THE THRUST GAGES

Calibrations of the thrust gages were made by applying known thrust loads to the propeller shaft after the dynamometer was installed complete with all fairings, leads, hoses, etc., in the wind tunnel. All calibration data were treated uniformly by use of the method of least squares to obtain straight-line calibrations (reference 18). For the most part, the error in indicated thrust was within 1 percent of the applied load, except in the small-load range where larger percentage errors would be expected.

CALIBRATION OF THE TORQUEMETER

Calibrations of the torquemeter together with a potentiometer were made to determine the characteristics of the torquemeter when subjected to torque loads while stationary (static calibrations) and while rotating (dynamic calibrations). In each calibration the ratio of applied torque to the potentiometer reading was constant for a given rotational speed and the data was treated uniformly by the method of least squares for fitting a straight line. The results of typical dynamic and static calibrations are presented in tables IV and V, respectively. For individual calibrations, either static or dynamic, the error in indicated torque was within 1/2 percent of the applied torque, except in the small-load range. The dynamic calibrations were divided into three groups (1-25, 26-39, and 40-44, table IV), each group having been made at a different stage of the test. For each group of calibrations, the calibration constant varied linearly with the rotational speed, with a probable error of about 1/4 percent. However, there was a variation of about 2 percent in the general magnitude of the calibration constant obtained in the three groups of dynamic calibrations. The calibration constants for zero rotational speed as extrapolated from the dynamic calibrations showed fair agreement with the slopes obtained in the static calibrations. There were no significant differences between dynamic calibrations made with the propeller shaft rotating under combined thrust and torque loads and dynamic calibrations made with no thrust loads.

CALIBRATION OF THE TUNNEL AIR STREAM

Figure 20 shows the locations of the survey-tube and wall static-pressure orifices at which the local Mach number was determined by stream surveys for both the 1-series and extended cylindrical spinners. The local Mach number distribution on the surface of the 1-series spinner and the forebody of the dynamometer was measured on a mock-up of the dynamometer.

The 25 static-pressure orifices along the tunnel wall (see fig. 20) were the only orifices common to all the stream surveys made for the various dynamometer installations. As a means of correlating the various surveys, the average of the local Mach numbers at the five wall orifices on the left side of the dynamometer and immediately adjacent to the propeller plane of rotation was used as a reference Mach number. The regular variation of the local Mach number along the tunnel wall for the various spinners may be seen by comparison of the data listed in table VI.

Typical longitudinal Mach number variations at several radii and for several reference Mach numbers are shown for the 7.20-inch-diameter, 1-series spinner, the 7.20-inch-diameter, extended cylindrical spinner, and the 12.00-inch-diameter, extended cylindrical spinner in figures 21, 22, and 23, respectively. The longitudinal and radial local Mach number variations obtained with the dynamometer mock-up are shown in figures 24 and 25, respectively. Figure 26 was derived from the data in figures 21 to 25 and shows the radial variation of the local Mach number at the propeller plane of rotation.

In order to obtain a theoretical confirmation of the radial and longitudinal Mach number gradients measured by tunnel air-stream surveys, the dynamometer body was represented by a longitudinal source-sink distribution of varying strength in a uniform flow field. Calculations of the radial and longitudinal Mach number gradients induced in various planes by the assumed source-sink distribution were made using the equations developed in reference 19, modified for compressibility effects as indicated in reference 20. The results of these calculations confirm the general magnitude and trend of the radial and longitudinal Mach number gradients and indicate that the radial variation of Mach number in the plane of the propeller, for the extended cylindrical spinner installations, was due to the presence of the dynamometer body downstream of the propeller.

The tunnel-datum Mach number was taken as the average Mach number over the propeller disc, obtained by integration of the local Mach numbers shown in figures 26(b) and 26(c) replotted versus the square of the radius between the limits of the spinner surface and the propeller

tip. Figure 27 shows the variation of the datum Mach number with the reference Mach number for the extended cylindrical spinners.

From figure 26 it is apparent that the difference between the radial variation of Mach number for the 7.20-inch-diameter, 1-series spinner and the 7.20-inch-diameter, extended cylindrical spinner (figs. 26(a) and 26(b)) was due to the local effects of the 1-series spinner, since the local Mach numbers between 25- and 72-inches radii were identical for both spinners. Since any difference in propeller performance caused by these local effects of the 1-series spinner should be chargeable to the propeller-spinner combination, the variation of the datum Mach number with reference Mach number for the 7.20- and 6.51-inch-diameter, 1-series spinners was assumed to be the same as that for the 7.20-inch-diameter, extended cylindrical spinner (fig. 27).

It is of interest to note in figures 21(a), 21(b), and 24 that at the propeller plane of rotation (10.8 inches behind the nose of the 7.20-inch-diameter, 1-series spinner) the inner portions of the blades were subjected to about the maximum Mach numbers measured. A more uniform radial velocity distribution, approaching that for the 7.20-inch-diameter cylindrical spinner, would have been obtained had the propeller been somewhat farther from the spinner nose.

APPENDIX C

PROPELLER THRUST AS AFFECTED BY SPINNER DRAG
AND SPINNER PRESSURE FORCES

As used herein, the propeller thrust is the indicated thrust of the propeller-spinner combination plus the spinner-drag tare and minus the thrust created by pressures acting between the floating and fixed members of the apparatus. As an aid in defining the various forces contributing to the resultant propeller thrust, cutaway views of the various spinners are presented in figure 28.

The following equations were used in the reduction of the propeller data:

For the 7.20- and 6.51-inch-diameter, 1-series spinners (fig. 28(a)),

$$T_P = T_{SG} + D_S - T_{P_1} - T_{P_2} \quad (1)$$

For the cylindrical spinners (figs. 28(b) and 28(c)),

$$T_P = T_{SG} + D_S - T_{P_1} - T_{P_2} + T_{P_3} + T_{P_4} \quad (2)$$

The notations used in the above equations represent the quantities listed below:

For the 7.20- and 6.51-inch-diameter, 1-series spinners (fig. 28(a)):

T_P	propeller thrust, pounds
T_{SG}	reaction force exerted by the thrust gages on the floating portion of the dynamometer, pounds
D_S	spinner-drag tare force measured at the same airspeeds and densities as those for the propeller tests, assuming a spinner base-pressure equal to the free-stream static pressure, pounds
T_{P_1}	$(p_1 - p_0) A_1$
T_{P_2}	$(p_2 - p_0) A_2$
A_1	cross-sectional area of the portion of the spinner outside the neoprene pressure seal, including half the frontal area of the neoprene pressure seal, square feet

- A_2 cross-sectional area of the portion of the spinner inside the neoprene pressure seal, including half the frontal area of the neoprene pressure seal, square feet
- P_0 free-stream static pressure computed using the datum Mach number, pounds per square foot
- P_1 static pressure outside the neoprene pressure seal, pounds per square foot
- P_2 static pressure inside the neoprene pressure seal, pounds per square foot

For the extended cylindrical spinners (figs. 28(b) and 28(c)):

$\left. \begin{array}{l} T_P, T_{SG}, T_{P_1} \\ T_{P_2}, A_1, A_2 \\ P_0, P_1, P_2 \end{array} \right\}$ same as for the 1-series spinners

- D_S spinner-drag tare force measured at the same airspeeds and densities as those for the propeller tests, pounds
- $T_{P_3} \quad (P_3 - P_0) A_3$
- $T_{P_4} \quad (P_4 - P_0) A_4$
- A_3 cross-sectional area of the portion of the spinner outside the labyrinth, including half the frontal area of the labyrinth, square feet
- A_4 cross-sectional area of the portion of the spinner inside the labyrinth, including half the frontal area of the labyrinth, square feet
- P_3 static pressure outside the labyrinth, pounds per square foot
- P_4 static pressure inside the labyrinth, pounds per square foot

All pressure measurements were indicated on multitube, liquid-in-glass manometers and recorded simultaneously by photographic means. For all the spinners, the static pressure P_1 was measured at a single location outside the neoprene pressure seal (fig. 28).

For the 12.00-inch-diameter cylindrical spinner, the static pressure p_1 was measured at 12 additional locations, 6 radial locations at each of 2 positions 180° apart, just behind the rear face of the spinner. The variation in the pressure p_1 at the 12 locations was less than 1 pound per square foot. For all spinners, the pressure p_2 was measured inside and immediately adjacent to the neoprene pressure seal and also at three widely separated locations inside the dynamometer. No data were recorded until the static pressures at all four locations inside the dynamometer were equalized. Control of the internal dynamometer pressure (appendix A) was maintained in a manner such that the pressure p_2 inside the neoprene seal was always less than the pressure p_1 outside the seal. For both cylindrical spinners, the pressure p_3 was measured at 4 locations, equally spaced circumferentially outside the labyrinth. Also for both cylindrical spinners, the pressure p_4 was measured at 4 locations, three of which were equally spaced circumferentially inside the labyrinth with the remaining one on the axis of rotation. There was no significant circumferential variation in pressure either inside or outside the labyrinth, but average values of the pressure p_4 were generally 2 pounds per square foot less than average values of p_3 .

The spinner-drag tare forces were measured by operating the dynamometer, complete except for the propeller blades, in the wind tunnel at conditions nearly identical to those for the propeller tests and were computed from the preceding equations with T_p equal to zero. For the 1-series spinners, with and without the propeller, the spinner-drag tare (and, consequently, the resultant longitudinal thrust) was adjusted for computational purposes to correspond to a spinner-base pressure equal to the static pressure of the free stream (see definition of T_{p_1} and T_{p_2}). This procedure determined the magnitude of the spinner-drag tare but had no influence on the propeller thrust. It may be noted that the spinner-drag tare forces for all the spinners except the 12.00-inch-diameter cylindrical spinner include the skin-friction drag of the cylindrical portion of the dynamometer behind the spinner, back to and including the cover plates over the neoprene pressure seal (see fig. 28). The spinner-drag tare forces as evaluated from the tare runs were found to be independent of rotational speed and, for constant Reynolds number, dependent on tunnel Mach number only. Figure 29 shows the variation of the spinner-drag tare forces with datum Mach number for the various spinners. While these data are somewhat erratic, the scatter for the most part is only of the order of $1/2$ pound, which is the order of accuracy of the thrust gages. Values of the spinner-drag tare force from the faired curves of figure 29 were applied in computing the propeller thrust.

Maximum and average values of the spinner-drag tare and of the four spinner-gap pressure terms are listed in the following table as percentages of the propeller thrust for the various spinners at conditions near maximum efficiency operation of the propeller:

Spinner	D_S		T_{p_1}		T_{p_2}		T_{p_3}		T_{p_4}	
	Max	Av.	Max	Av.	Max	Av.	Max	Av.	Max	Av.
7.20-inch-diameter, 1-series spinner	2	1	4	2	3	2	-	-	-	-
6.51-inch-diameter, 1-series spinner	1	- ^a	1	1	6	4	-	-	-	-
7.20-inch-diameter, cylindrical spinner	2	1	4	2	8	5	- ^a	- ^a	1	1
12.00-inch-diameter, cylindrical spinner	3	2	4	3	6	5	4	2	8	5

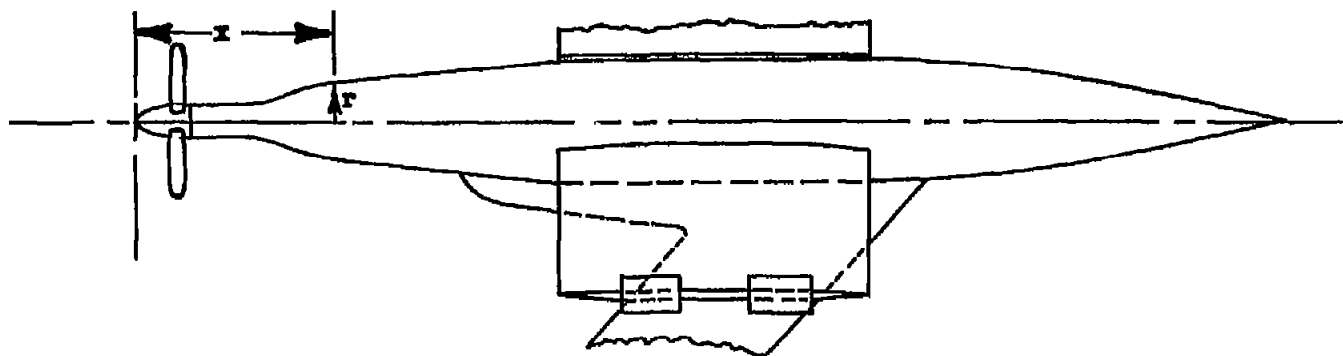
^aLess than 1/2 percent.

REFERENCES

1. Delano, James Benjamin, and Carmel, Melvin M.: Investigation of the NACA 4-(5)(08)-03 Two-Blade Propeller at Forward Mach Numbers to 0.925. NACA RM L9G06a, 1949.
2. Delano, James Benjamin, and Morgan, Francis G., Jr.: Investigation of the NACA 4-(3)(08)-03 Two-Blade Propeller at Forward Mach Numbers to 0.925. NACA RM L9I06, 1949.
3. Carmel, Melvin M., Morgan, Francis G., Jr., and Coppolino, Domenic A.: Effect of Compressibility and Camber as Determined from an Investigation of the NACA 4-(3)(08)-03 and 4-(5)(08)-03 Two-Blade Propellers up to Forward Mach Numbers of 0.925. NACA RM L50D28, 1950.
4. Delano, James Benjamin, and Harrison, Daniel E.: Investigation of the NACA 4-(4)(06)-04 Two-Blade Propeller at Forward Mach Numbers to 0.925. NACA RM L9I07, 1949.
5. Delano, James B., and Harrison, Daniel E.: Investigation of the NACA 4-(4)(06)-057-45A and NACA 4-(4)(06)-057-45B Two-Blade Swept Propellers at Forward Mach Numbers to 0.925. NACA RM L9L05, 1950.
6. Delano, James B., and Carmel, Melvin M.: Investigation of the NACA 4-(0)(03)-045 and NACA 4-(0)(08)-045 Two-Blade Propellers at Forward Mach Numbers to 0.925. NACA RM L9L06a, 1950.
7. Carmel, Melvin M., and Milillo, Joseph R.: Investigation of the NACA 4-(0)(03)-045 Two-Blade Propeller at Forward Mach Numbers to 0.925. NACA RM L50A31a, 1950.
8. Platt, Robert J., Jr., and Shumaker, Robert A.: Investigation of the NACA 3-(3)(05)-05 Eight-Blade Dual-Rotating Propeller at Forward Mach Numbers to 0.925. NACA RM L50D21, 1950.
9. Nichols, Mark R., and Keith, Arvid L., Jr.: Investigation of a Systematic Group of NACA 1-Series Cowlings With and Without Spinners. NACA Rep. 950, 1949. (Formerly NACA RM L8A15)
10. Pendley, Robert E., and Smith, Norman F.: An Investigation of the Characteristics of Three NACA 1-Series Nose Inlets at Subcritical and Supercritical Mach Numbers. NACA RM L8L06, 1949.
11. Pendley, Robert E., and Robinson, Harold L.: An Investigation of Several NACA 1-Series Nose Inlets with and without Protruding Central Bodies at High-Subsonic Mach Numbers and at a Mach Number of 1.2. NACA RM L9L23a, 1950.

12. Sammonds, Robert I., and Molk, Ashley J.: Effects of Propeller-Spinner Junction on the Pressure-Recovery Characteristics of an NACA I-Series D-Type Cowl in Combination with a Four-Blade Single-Rotation Propeller at Mach Numbers Up to 0.83 and at an Angle of Attack of 0° . NACA RM A52D01a, 1952.
13. Crigler, John L., and Talkin, Herbert W.: Propeller Selection from Aerodynamic Considerations. NACA ACR July, 1942.
14. Young, A. D.: Note on the Application of the Linear Perturbation Theory to Determine the Effect of Compressibility on the Wind Tunnel Constraint on a Propeller. TN No. Aero. 1539, RAE (British) 1944.
15. Crigler, John L.: Comparison of Calculated and Experimental Propeller Characteristics for Four-, Six-, and Eight-Blade Single-Rotating Propellers. NACA ACR 4B04, 1944.
16. Hartman, Edwin P., and Biermann, David: The Aerodynamic Characteristics of Full-Scale Propellers Having 2, 3, and 4 Blades of Clark Y and R.A.F. 6 Airfoil Sections. NACA Rep. 640, 1938.
17. Lock, C.N.H., Bateman, H., and Nixon, H. L.: Wind Tunnel Tests of High Pitch Airscrews. Pt. 1. R. & M. No. 1673, British A.R.C., 1935.
18. Mills, Frederick Cecil: Statistical Methods. Henry Holt and Company, Inc., 1938.
19. Prandtl, L.: Applications of Modern Hydrodynamics to Aeronautics. NACA Rep. 116, 1921.
20. Boltz, Frederick W., and Beam, Benjamin H.: The Effects of Compressibility on the Pressures on a Body of Revolution and on the Aerodynamic Characteristics of a Wing-Nacelle Combination Consisting of the Body of Revolution Mounted on a Swept-Back Wing. NACA RM A50E09, 1950.

TABLE I.- COORDINATES OF THE DYNAMOMETER WITH THE 7.20-INCH-DIAMETER, 1-SERIES SPINNER
[Coordinates in inches]



Distance from nose of spinner, x	Radius from center of rotation, r	Distance from nose of spinner, x	Radius from center of rotation, r	Distance from nose of spinner, x	Radius from center of rotation, r	Distance from nose of spinner, x	Radius from center of rotation, r
0.000	0.000	2.052	1.847	8.856	3.523	42.85	7.65
.043	.239	2.268	1.946	9.936	3.587	44.77	8.05
.086	.336	2.484	2.040	10.584	3.599	46.69	8.38
.162	.458	2.700	2.129	10.800	3.600	48.63	8.65
.270	.597	3.024	2.256	28.691	3.600	50.21	8.81
.378	.719	3.456	2.413	28.913	3.603	95.96	13.00
.486	.827	3.996	2.593	29.413	3.626	99.46	13.00
.648	.972	4.536	2.753	29.913	3.675	171.46	13.00
.864	1.145	5.076	2.898	30.413	3.749	191.46	12.47
1.080	1.301	5.616	3.028	30.913	3.850	211.46	10.78
1.296	1.443	6.048	3.122	31.413	3.978	231.46	8.00
1.512	1.572	6.912	3.284	31.892	4.126	251.46	4.06
1.729	1.688	7.992	3.437	40.956	7.188	265.46	0.00

¹End of 1-series spinner profile; cylindrical portion of spinner extends to x, 13.73.



TABLE II.- BLADE ANGLES AND TUNNEL MACH NUMBERS FOR TESTS OF THE NACA 4-(5)(05)-041 PROPELLER
IN COMBINATION WITH VARIOUS SPINNERS

28

Datum Mach number	Blade angle at 0.75 radius, β 0.75 R, deg.											
	70	65	60	55	50	40	30	20	15	10	0	-15
0.90	a	a	a	a	---	---	---	---	---	---	---	---
.86	a	a	a	a	---	---	---	---	---	---	---	---
¹ .82	a	acd	abod	a	---	---	---	---	---	---	---	---
¹ .78	a	acd	abod	a	a	---	---	---	---	---	---	---
¹ .73	a	acd	a cd	acd	a	---	---	---	---	---	---	---
¹ .68	a	acd	abod	acd	a	---	---	---	---	---	---	---
.64	---	---	---	a	a	---	---	---	---	---	---	---
.59	---	acd	abod	acd	² ab	---	---	---	---	---	---	---
.49	---	---	a	a	² a	a	---	---	---	---	---	---
.39	---	---	a	a	² ab	ab	a	---	---	---	---	---
.29	---	---	---	---	² a	ab	a	---	---	---	---	---
.20	---	---	---	---	---	ab	a	a	a	---	³ a	³ a
.10	---	---	---	---	---	---	---	a	³ a	---	³ a	³ a
(approx) 0	---	---	---	---	---	---	---	a	a	a	a	---
<p style="text-align: center;"><u>SPINNERS</u></p> <p>a. 7.20-inch-diameter, 1-series spinner b. 6.51-inch-diameter, 1-series spinner c. 7.20-inch-diameter, extended cylindrical spinner d. 12.00-inch-diameter, extended cylindrical spinner</p>												

¹ Datum Mach numbers for spinner d are 0.01 higher than these values

² Combinations investigated at a Reynolds number of 3.0 million per foot (spinner a only)

³ Combinations investigated with the propeller in negative thrust.



NACA RM A52119a

TABLE III.- RANGE OF TUNNEL STAGNATION TEMPERATURE FOR THE VARIOUS TESTS
[Degrees Fahrenheit, in order from high to low J]

Datum Noch number	spinner	Blade angle at 0.75 radius, 80.752 deg											
		75	65	60	55	50	40	30	20	15	10	0	-15
0.90	a	109-142	100-140	112-143	116-128	---	---	---	---	---	---	---	---
.85	a	120-140	116-140	131-151	115-130	---	---	---	---	---	---	---	---
.82	a	122-143	113-137	114-135	124-135	---	---	---	---	---	---	---	---
.82	b	---	---	116-130	---	---	---	---	---	---	---	---	---
.82	c	---	122-138	113-126	---	---	---	---	---	---	---	---	---
.83	d	---	122-138	113-126	---	---	---	---	---	---	---	---	---
.78	a	112-137	109-136	108-129	123-137	115-122	---	---	---	---	---	---	---
.78	b	---	---	112-129	---	---	---	---	---	---	---	---	---
.78	c	---	113-134	113-127	---	---	---	---	---	---	---	---	---
.79	d	---	116-133	114-123	---	---	---	---	---	---	---	---	---
.73	a	110-135	85-118	115-126	110-124	112-126	---	---	---	---	---	---	---
.73	c	---	114-135	126-136	114-127	---	---	---	---	---	---	---	---
.74	d	---	112-133	112-130	127-139	---	---	---	---	---	---	---	---
.68	a	85-120	108-117	104-118	104-118	105-113	---	---	---	---	---	---	---
.68	b	---	---	119-126	---	---	---	---	---	---	---	---	---
.68	c	---	125-140	107-119	123-133	---	---	---	---	---	---	---	---
.69	d	---	130-142	119-144	126-132	---	---	---	---	---	---	---	---
.64	a	---	---	---	126-128	112-120	---	---	---	---	---	---	---
.59	a	---	94-106	98-105	102-110	94-102	---	---	---	---	---	---	---
.59 ¹	b	---	---	116-119	---	115-130	---	---	---	---	---	---	---
.59	c	---	124-128	115-118	123-123	104-109	---	---	---	---	---	---	---
.59	d	---	126-129	130-130	121-123	---	---	---	---	---	---	---	---
.49	a	---	---	85- 93	91- 94	93-100	75- 81	---	---	---	---	---	---
.49 ¹	b	---	---	---	---	102-111	---	---	---	---	---	---	---
.39	a	---	---	80- 82	83- 88	87- 89	79- 82	71- 73	---	---	---	---	---
.39 ¹	b	---	---	---	---	86- 94	---	---	---	---	---	---	---
.39	c	---	---	---	---	94- 95	91- 94	---	---	---	---	---	---
.29	a	---	---	---	---	80- 80	76- 78	74- 77	---	---	---	---	---
.29 ¹	b	---	---	---	---	83- 85	93- 94	---	---	---	---	---	---
.20	a	---	---	---	---	---	74- 78	74- 74	66- 67	58- 61	---	60- 66	49- 63
.20	b	---	---	---	---	---	92- 89	---	---	---	---	---	---
.10	a	---	---	---	---	---	---	---	68- 66	57- 43	---	62- 62	51- 56
(Approx.) 0	a	---	---	---	---	---	---	---	63- 63	61- 74	52- 57	63- 61	---

SPINNER

- a. 7.20-inch-diameter, 3-series spinner
- b. 6.51-inch-diameter, 1-series spinner
- c. 7.20-inch-diameter, extended cylindrical spinner
- d. 12.00-inch-diameter, extended cylindrical spinner

¹Combinations investigated at a Reynolds number of 3.0 million per foot.

TABLE IV.- SUMMARY OF THE RESULTS OF DYNAMIC CALIBRATIONS OF THE TORQUEMETER

Calibration	Rotational speed (rpm)	Calibration constant (lb-ft/count)	Intercept (lb-ft)	Probable error (lb-ft)	Number of points defining line
5	1000	1.1415	-1.4	0.7	16
8	1000	1.1483	-1.6	.6	16
13	1000	1.1451	-1.2	.8	16
16	1000	1.1540	-3.0	.8	16
21	1000	1.1543	-1.1	.5	16
27	1000	1.1663	-1.1	1.7	13
36	1000	1.1588	-.6	.5	16
41	1000	1.1727	.6	1.3	15
1	2000	1.1510	-1.1	.7	16
6	2000	1.1504	.6	.5	16
9	2000	1.1525	1.4	.7	16
17	2000	1.1549	3.4	.7	16
22	2000	1.1552	-.7	.4	16
28	2000	1.1632	-2.9	3.4	13
37	2000	1.1723	-1.7	.4	16
40	2000	1.1678	3.6	1.6	16
2	3000	1.1492	-.2	.8	16
7	3000	1.1532	.6	1.0	15
10	3000	1.1591	1.3	.5	16
18	3000	1.1597	2.3	1.0	16
23	3000	1.1641	1.5	.7	16
29	3000	1.1743	1.8	2.2	14
33	3000	1.1810	2.0	.6	16
42	3000	1.1769	1.4	1.4	15
30	3500	1.1628	.5	.8	16
34	3500	1.1789	2.9	.6	16
3	4000	1.1578	3.9	1.6	16
11	4000	1.1674	4.2	.6	16
14	4000	1.1640	3.9	1.1	16
19	4000	1.1628	3.9	1.0	16
24	4000	1.1674	3.7	.9	16
31	4000	1.1773	5.4	1.0	16
35	4000	1.1794	3.1	1.1	16
43	4000	1.1852	3.8	.8	15
32	4500	1.1871	.3	.7	16
38	4500	1.1858	2.3	1.1	16
4	5000	1.1704	4.6	.8	16
12	5000	1.1764	2.3	.9	16
15	5000	1.1733	5.9	.6	16
20	5000	1.1720	6.7	.7	16
25	5000	1.1790	3.7	.9	16
26	5000	1.1820	4.1	1.1	16
44	5000	1.1976	7.7	1.4	15
39	5500	1.1933	2.1	.6	16

TABLE V.- SUMMARY OF THE RESULTS OF STATIC CALIBRATIONS OF THE TORQUEMETER

Calibration	Calibration constant (lb-ft/count)	Intercept (lb-ft)	Probable error (lb-ft)	Number of points defining line
1	1.1698	0.0	1.0	27
2	1.1706	-.3	.7	27
3	1.1306	-1.0	.5	27
4	1.1328	-.3	.5	27
5	1.1251	-.9	.5	27
6	1.1703	-.9	.9	21
7	1.1334	-.5	1.0	21
8	1.1290	.3	.4	21
9	1.1283	.6	.3	21
10	1.1419	-.5	.4	21
11	1.1370	-1.0	.6	21

NACA

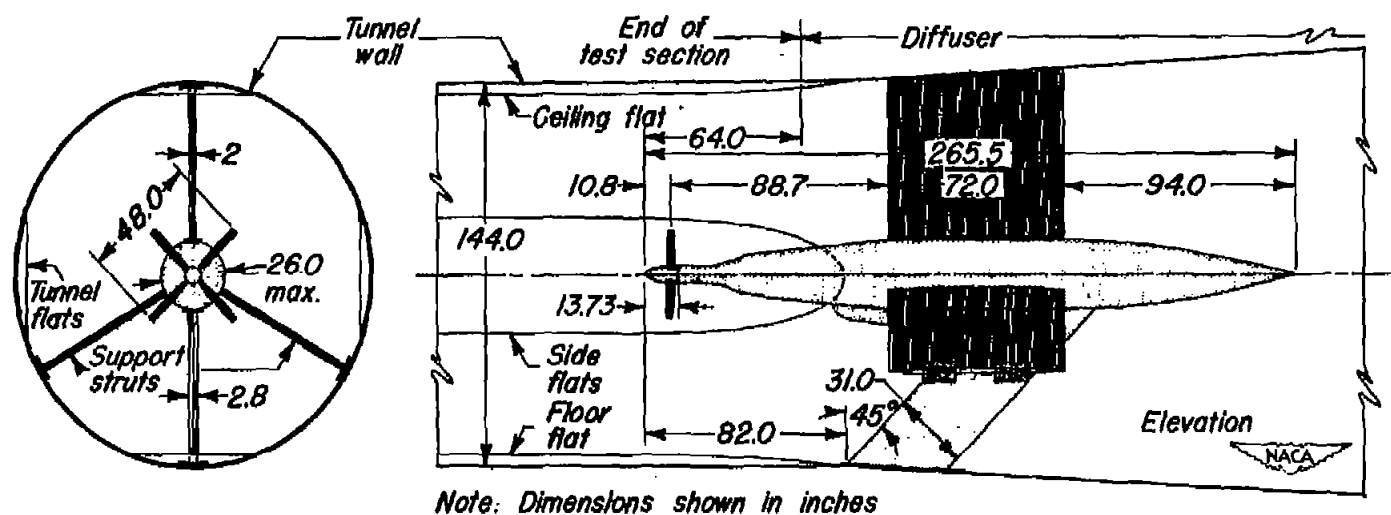
TABLE VI.- COMPARISON OF THE LOCAL MACH NUMBERS AT THE TUNNEL WALL FOR VARIOUS SPINNERS
[Longitudinal stations positive downstream of propeller]

8

Longitudinal station, in. from propeller	Approx. $M_1, 0.90$				Approx. $M_1, 0.88$				Approx. $M_1, 0.84$			
	①	②	③	④	①	②	③	④	①	②	③	④
-16.8	0.890	0.888	0.909	0.893	0.869	0.867	0.870	0.872	0.829	0.830	0.834	0.836
-8.8	.900	.900	.919	.903	.879	.879	.880	.881	.838	.840	.842	.847
-0.8	.898	.895	.909	.892	.876	.873	.872	.872	.836	.835	.835	.838
7.2	.893	.891	.903	.886	.872	.870	.869	.867	.833	.833	.833	.835
13.2	.898	.893	.905	.886	.876	.872	.870	.868	.838	.836	.835	.836
23.2	.915	.912	.920	.898	.894	.893	.887	.880	.854	.855	.851	.849
31.2	.891	.892	.898	.874	.870	.872	.866	.857	.833	.836	.832	.827
39.2	.908	.901	.901	.875	.887	.881	.869	.859	.849	.843	.835	.829
Longitudinal station, in. from propeller	Approx. $M_1, 0.80$				Approx. $M_1, 0.75$				Approx. $M_1, 0.60$			
	①	②	③	④	①	②	③	④	①	②	③	④
-16.8	0.790	0.791	0.792	0.795	0.733	0.743	0.740	0.743	0.598	0.599	0.594	0.591
-8.8	.797	.801	.800	.803	.741	.751	.747	.749	.603	.605	.600	.596
-0.8	.796	.796	.793	.795	.740	.747	.743	.744	.602	.601	.597	.592
7.2	.793	.795	.791	.793	.743	.746	.741	.742	.601	.601	.595	.592
13.2	.797	.797	.793	.794	.742	.748	.743	.743	.603	.603	.598	.593
23.2	.814	.815	.808	.808	.758	.767	.758	.757	.614	.617	.594	.593
31.2	.794	.798	.791	.789	.739	.750	.754	.740	.602	.602	.598	.592
39.2	.809	.805	.794	.791	.754	.757	.745	.742	.612	.610	.601	.594
<p style="text-align: center;">SPINNER</p> <p>① 7.20-inch-diameter, l-series spinner</p> <p>② 7.20-inch-diameter, l-series spinner on dynamometer mock-up</p> <p>③ 7.20-inch-diameter, extended cylindrical spinner</p> <p>④ 12.00-inch-diameter, extended cylindrical spinner</p>												

NACA RM A52119a

NACA



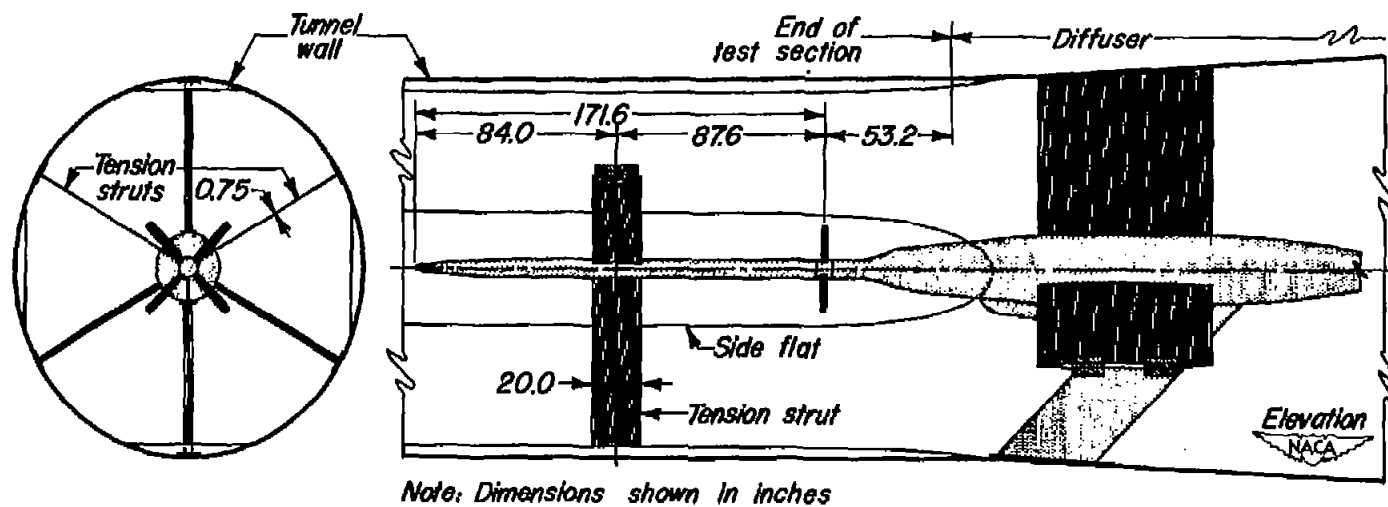
(a) General arrangement of the dynamometer.

Figure 1.—The 1000-horsepower propeller dynamometer in the Ames 12-foot pressure wind tunnel.



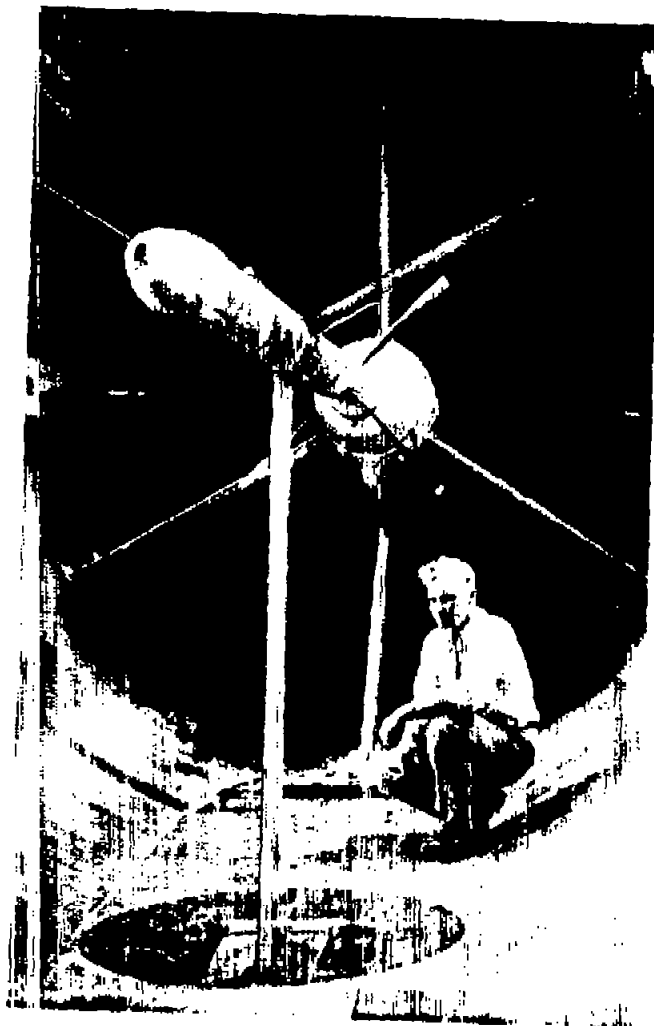
(b) Photographs of the dynamometer.

Figure 1.- Concluded.



(a) General arrangement of the extended cylindrical spinners.

Figure 2.- The extended cylindrical spinners with the 1000-horsepower propeller dynamometer.



(b) Photographs of the extended cylindrical spinners.

Figure 2.- Concluded.

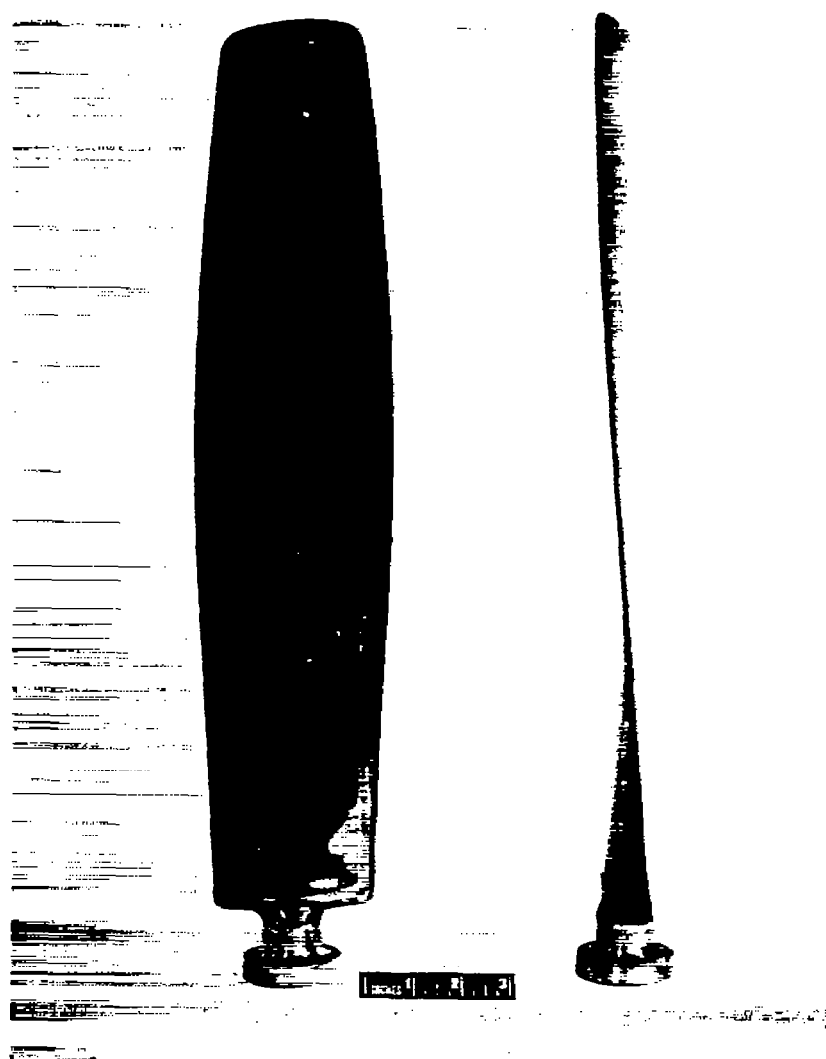


Figure 3.—The NACA 4-(5)(05)-041 propeller.

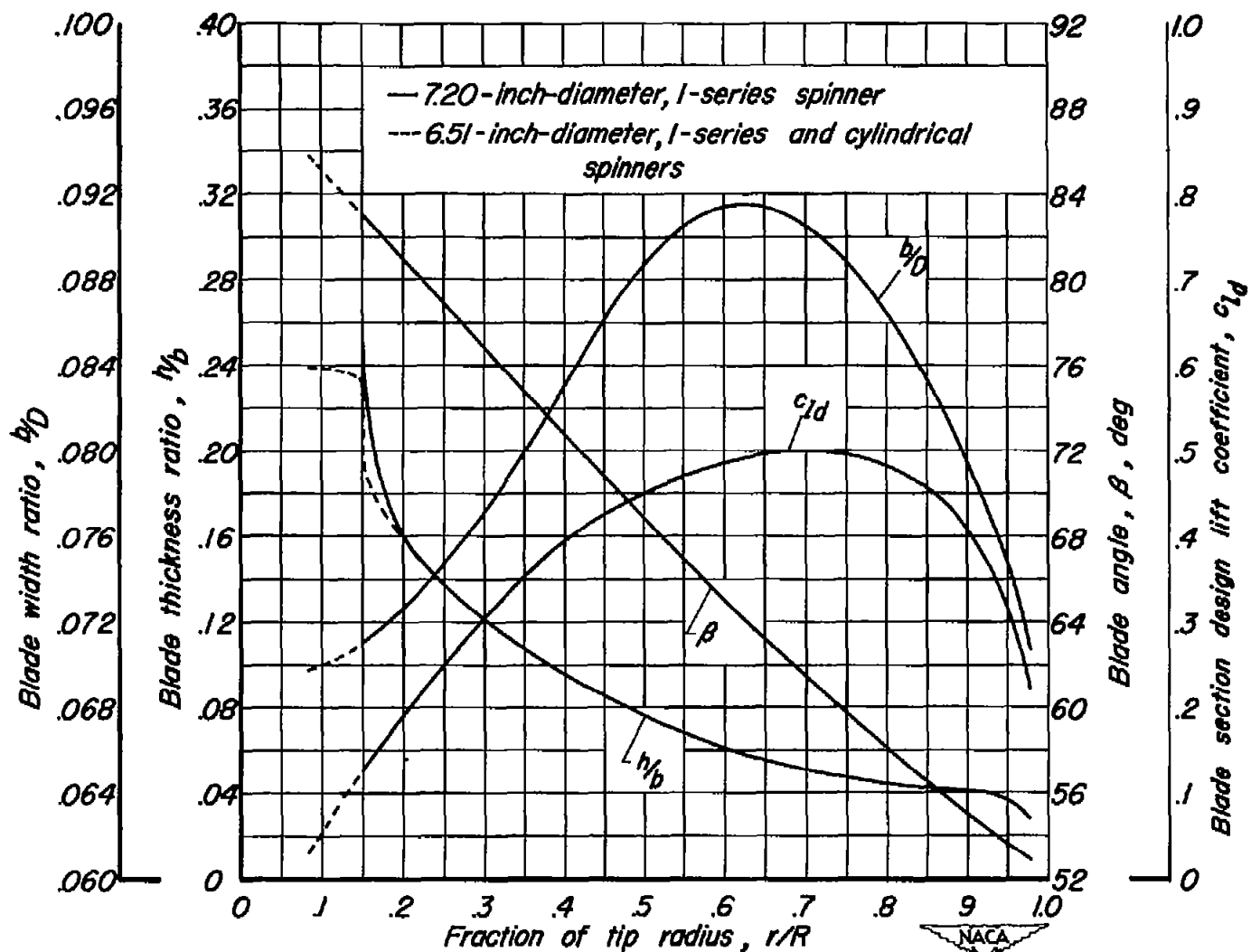


Figure 4.-Planform and blade-form curves for the NACA 4-(5)(05)-041 propeller.

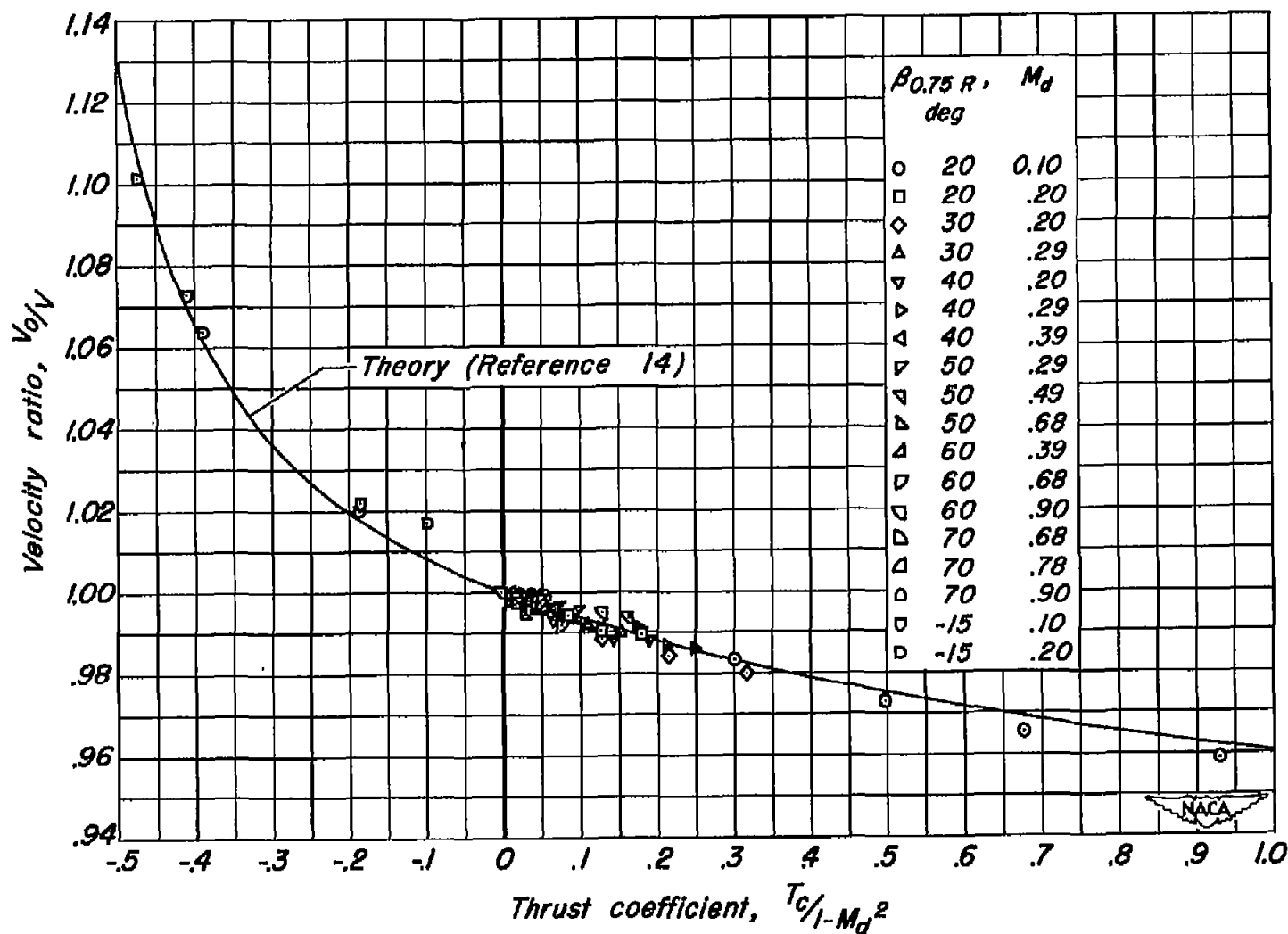


Figure 5.—Tunnel-wall-interference correction for a 4-foot-diameter propeller in the Ames 12-foot pressure wind tunnel.

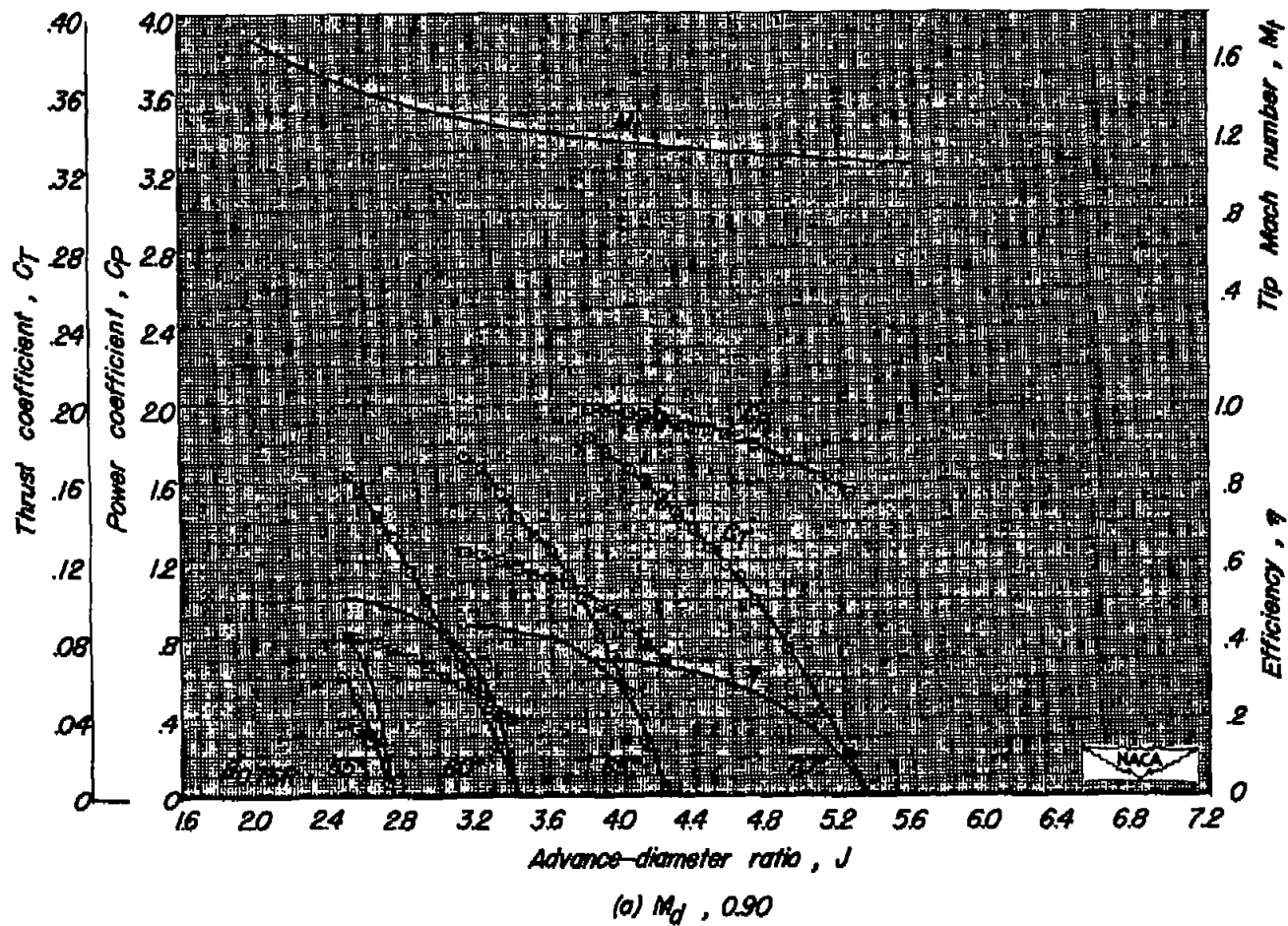
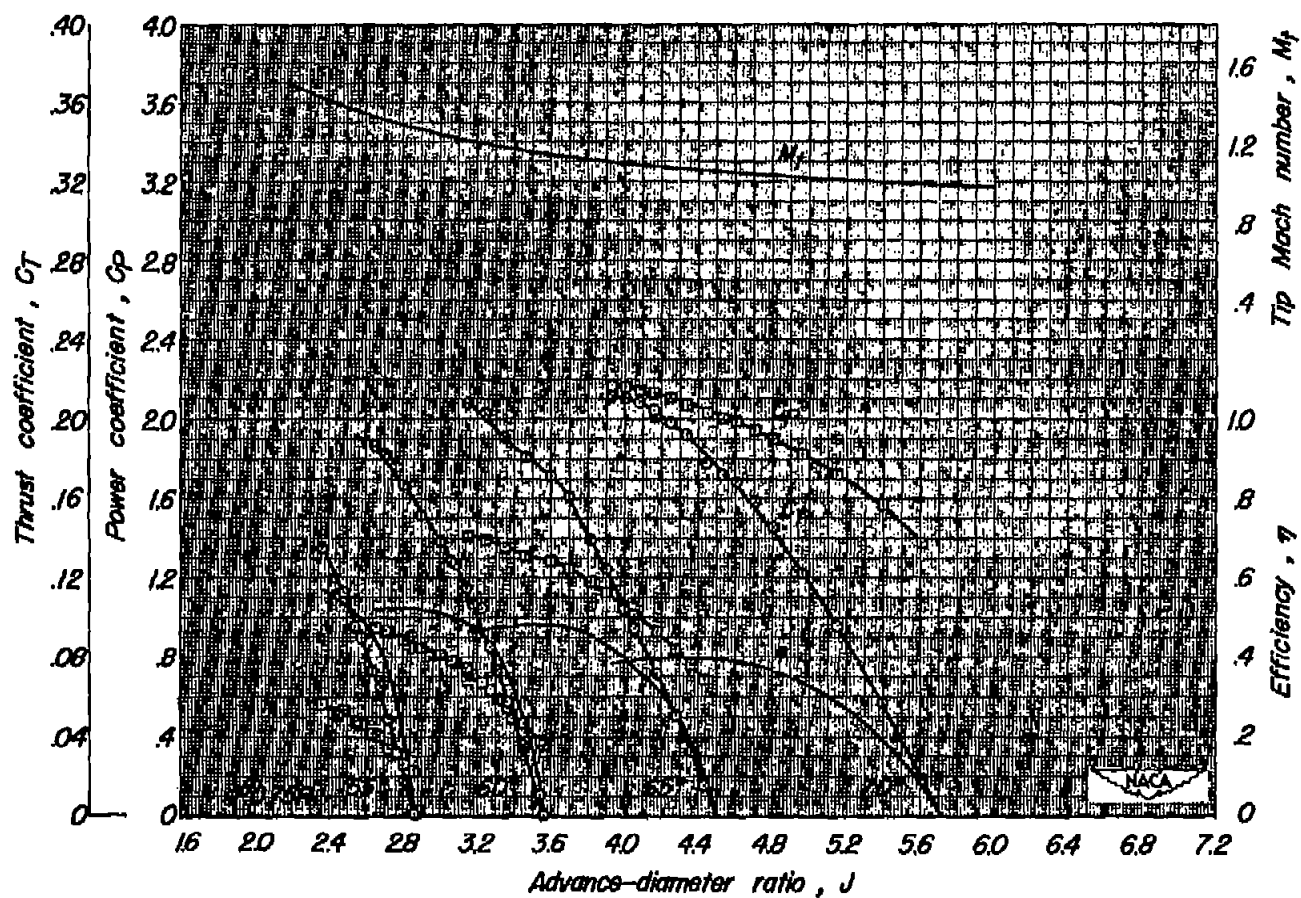
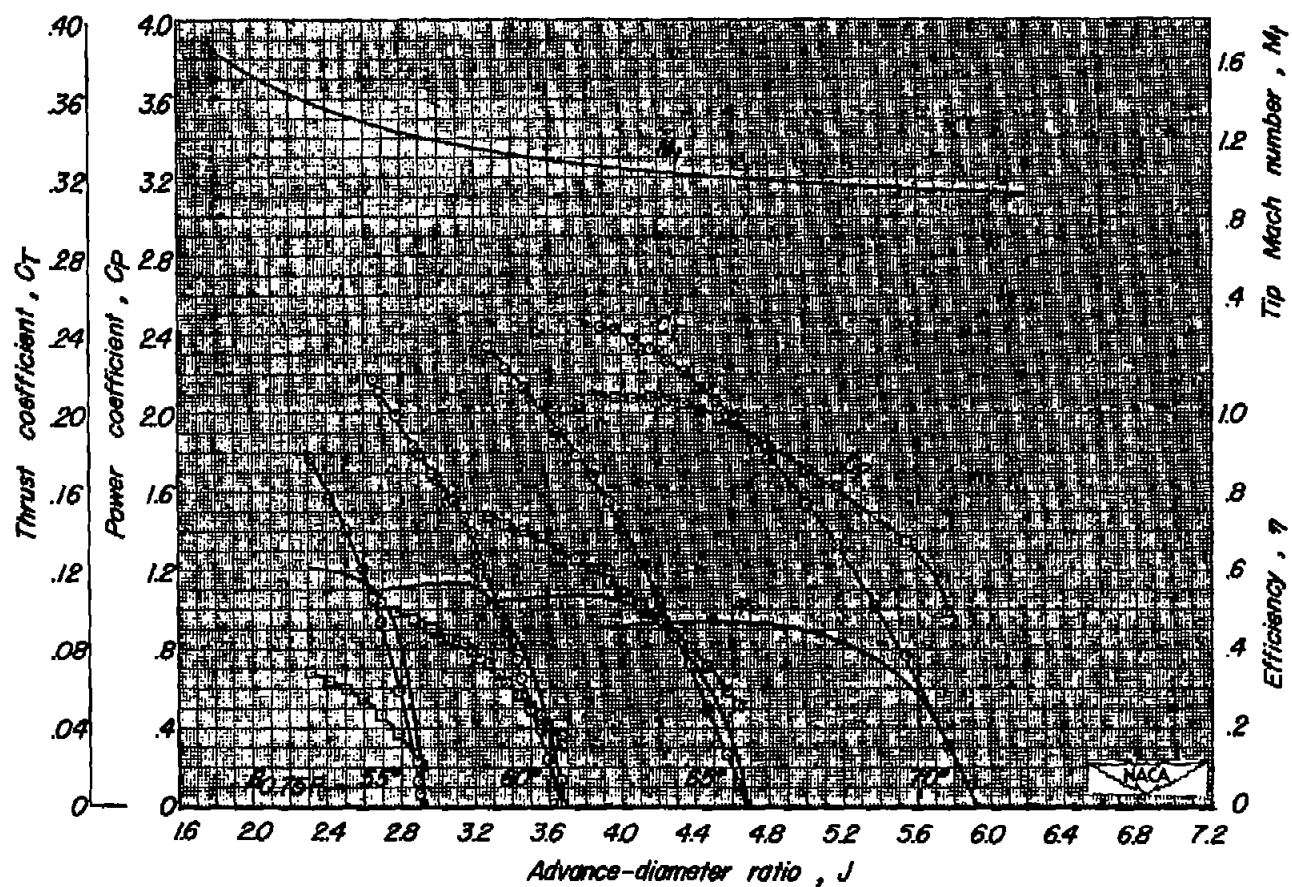


Figure 6.-Characteristics of the NACA 4-(5)05-041 propeller. 7.20-inch-diameter, 1-series spinner.



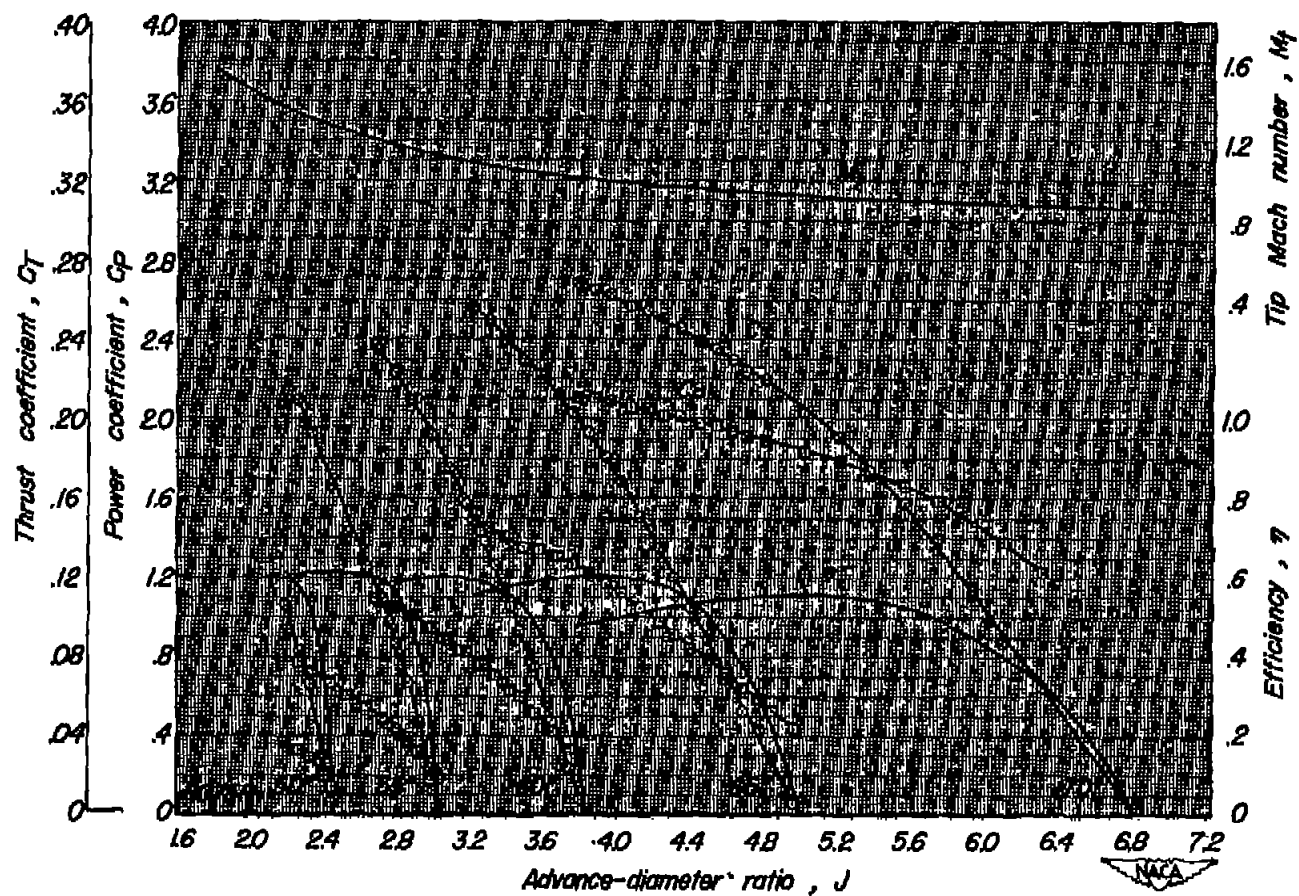
(b) M_T , 0.86

Figure 6 - Continued.



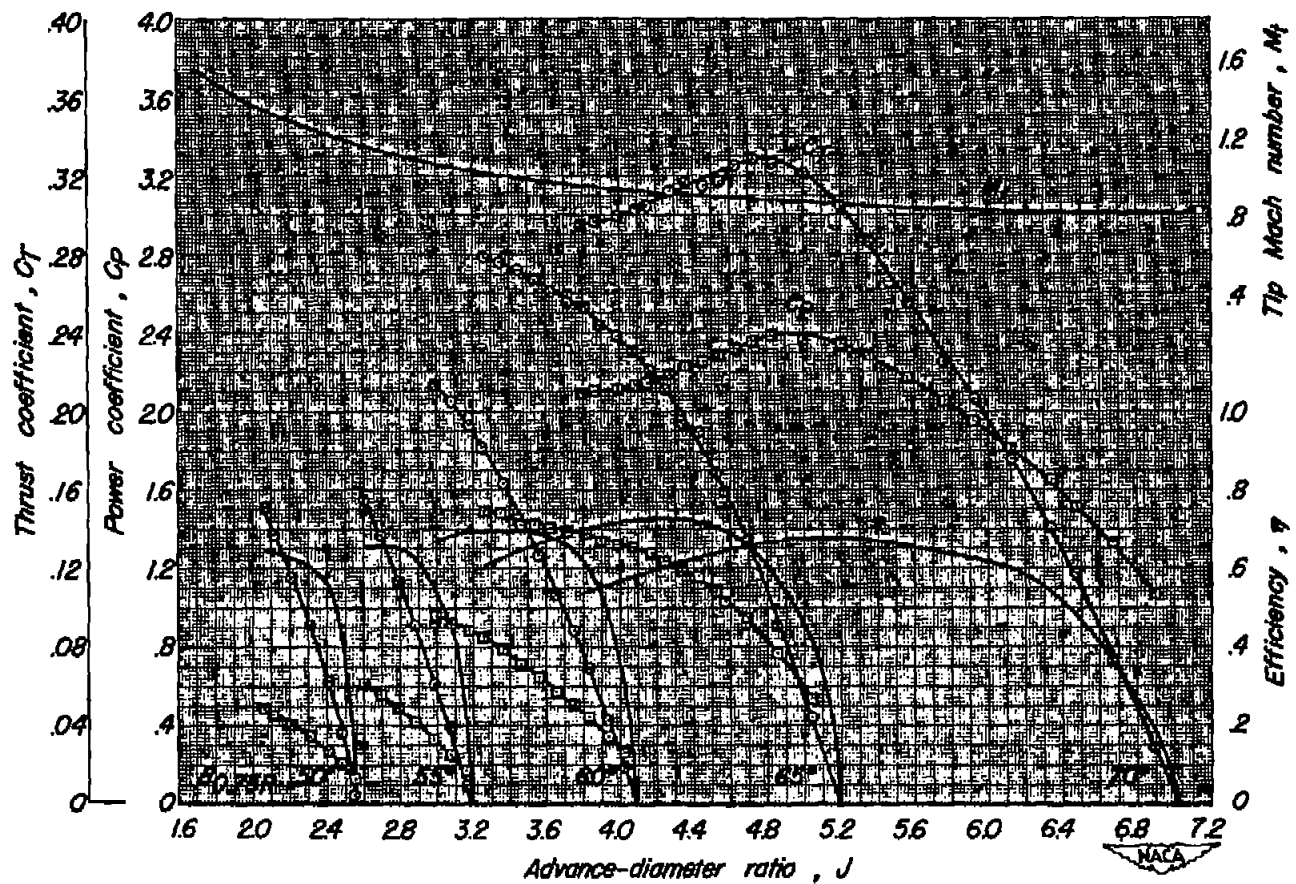
(c) $M_t = 0.82$

Figure 6 -Continued.



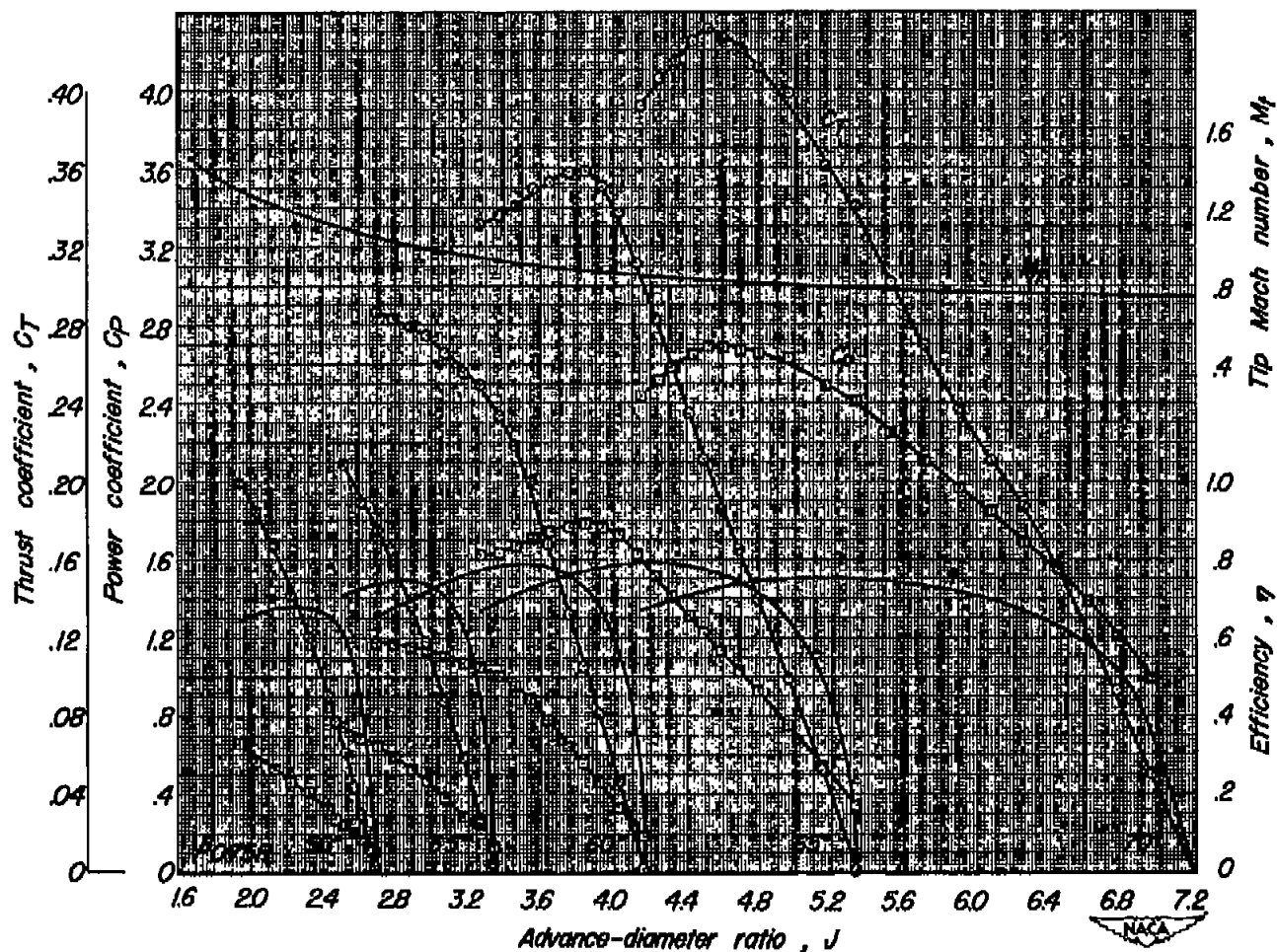
(d) M_d , 0.78

Figure 6.-Continued.



(e) $M_d, 0.73$

Figure 6.-Continued.



(f) $M_d, 0.68$

Figure 6-Continued.

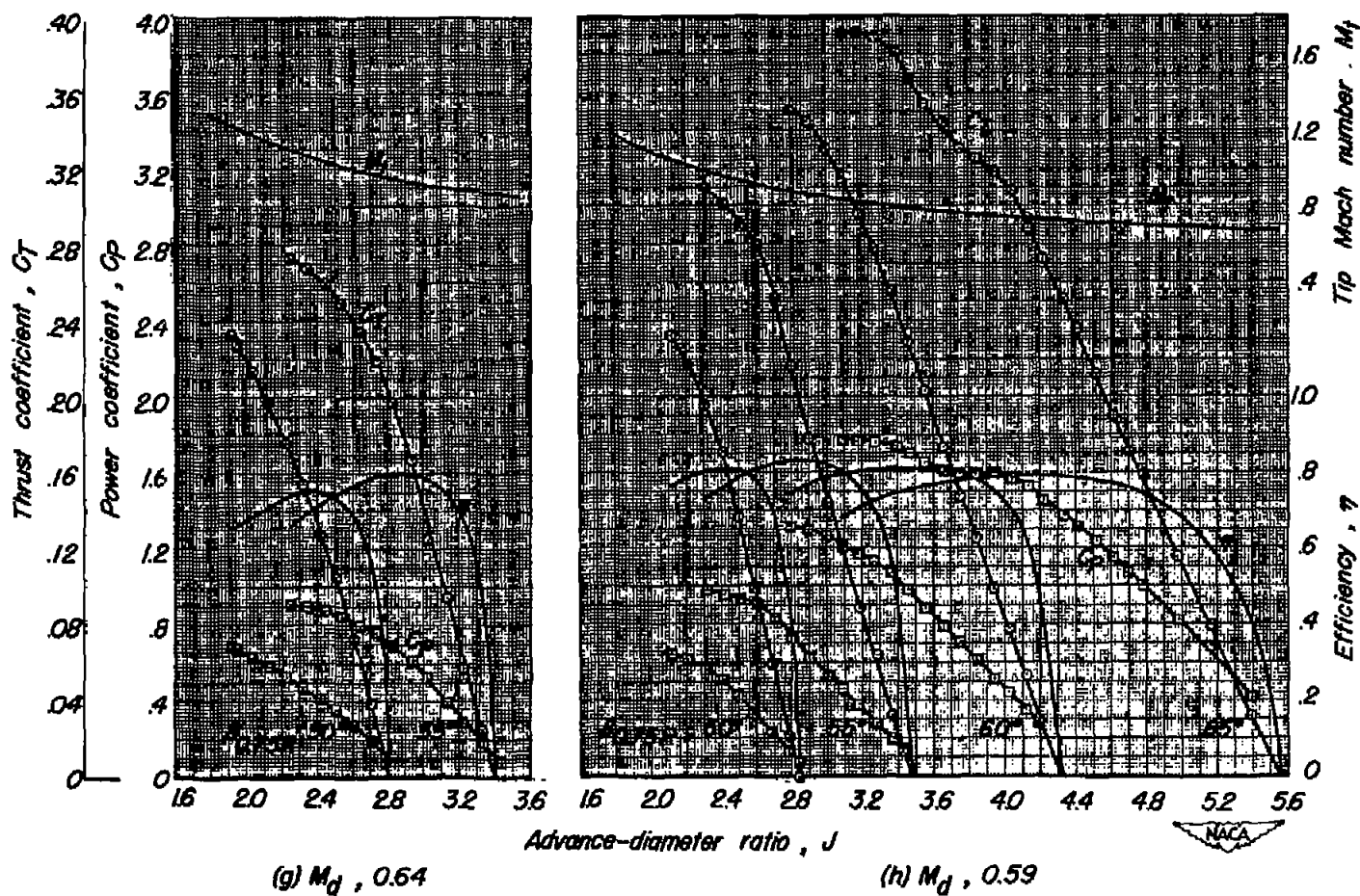
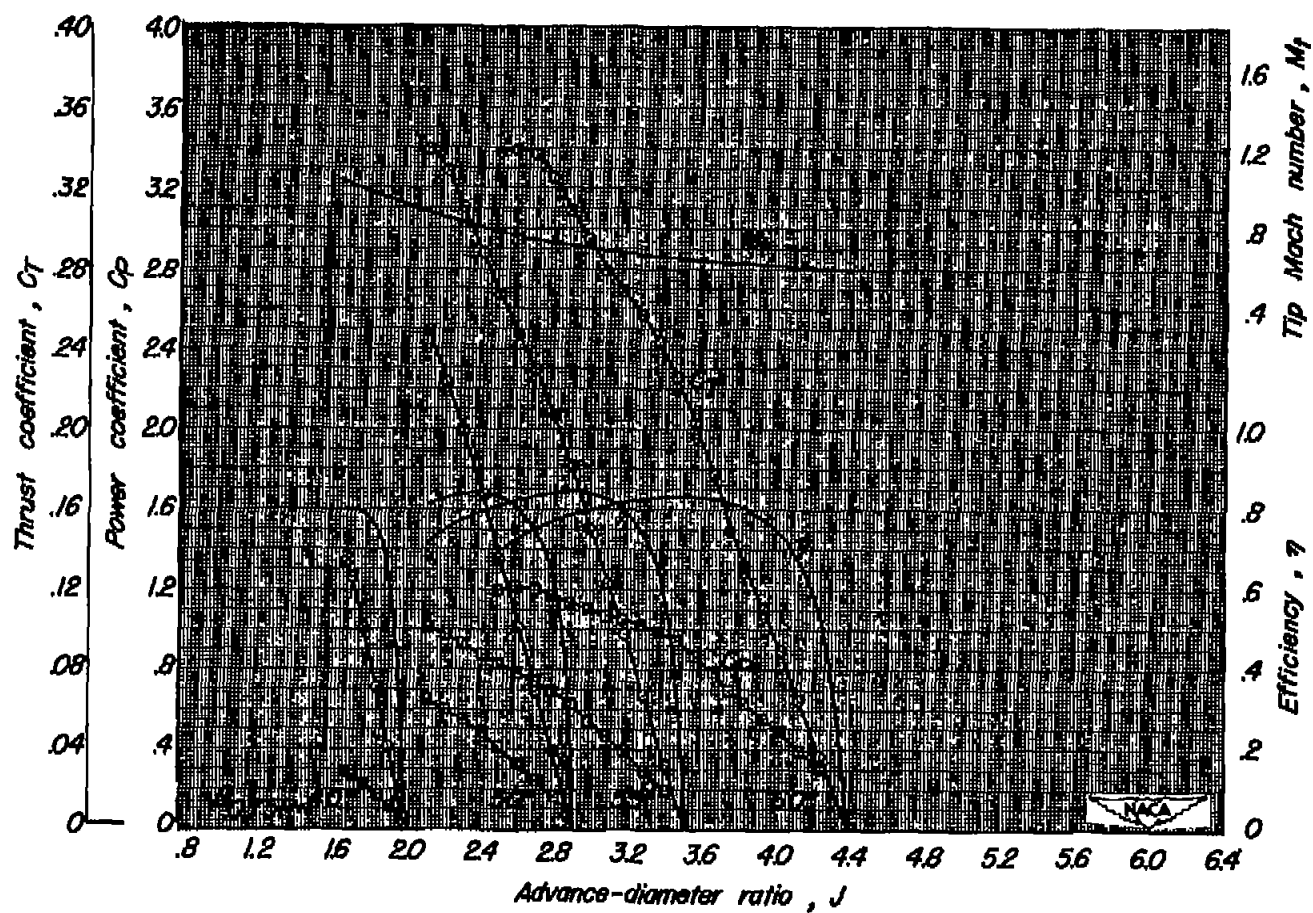
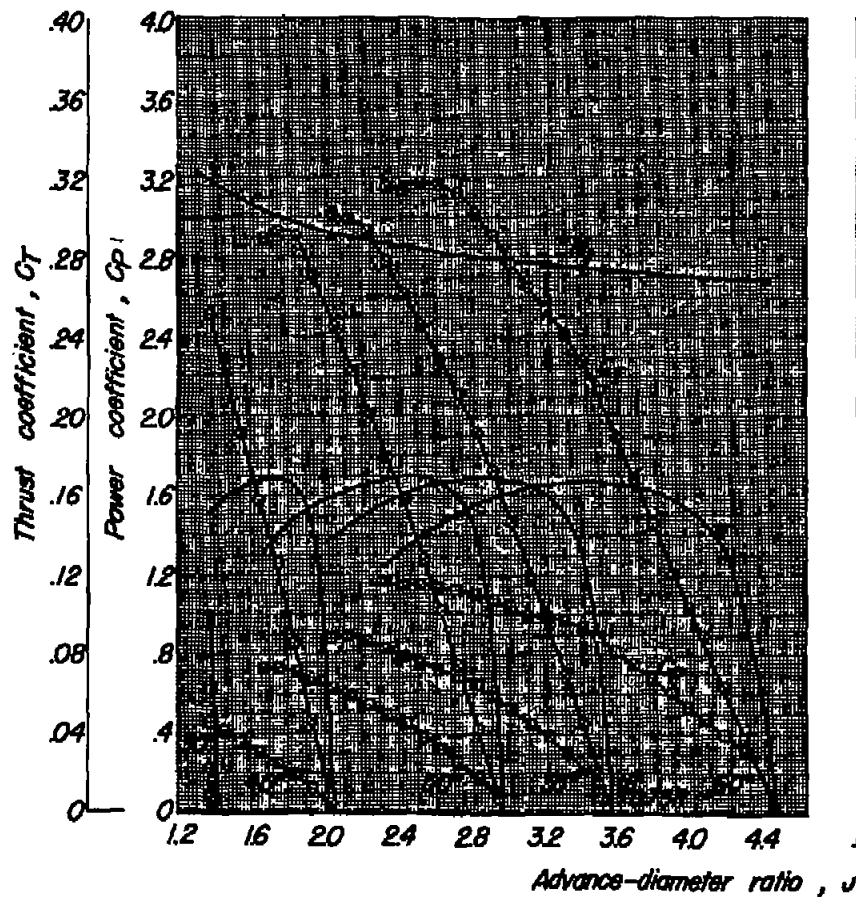


Figure 6 - Continued.

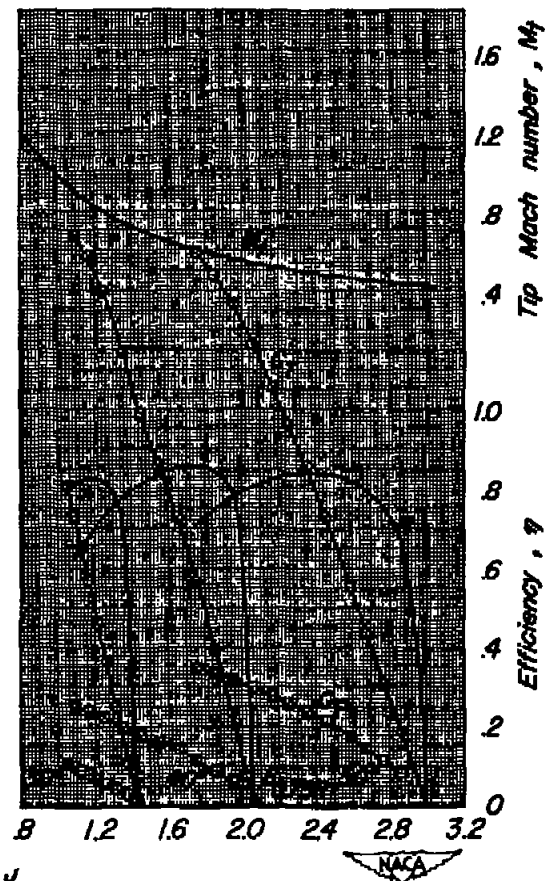


(i) $M_T, 0.49$

Figure 6.-Continued.



(j) $M_d, 0.39$



(k) $M_d, 0.29$

Figure 6.-Continued.

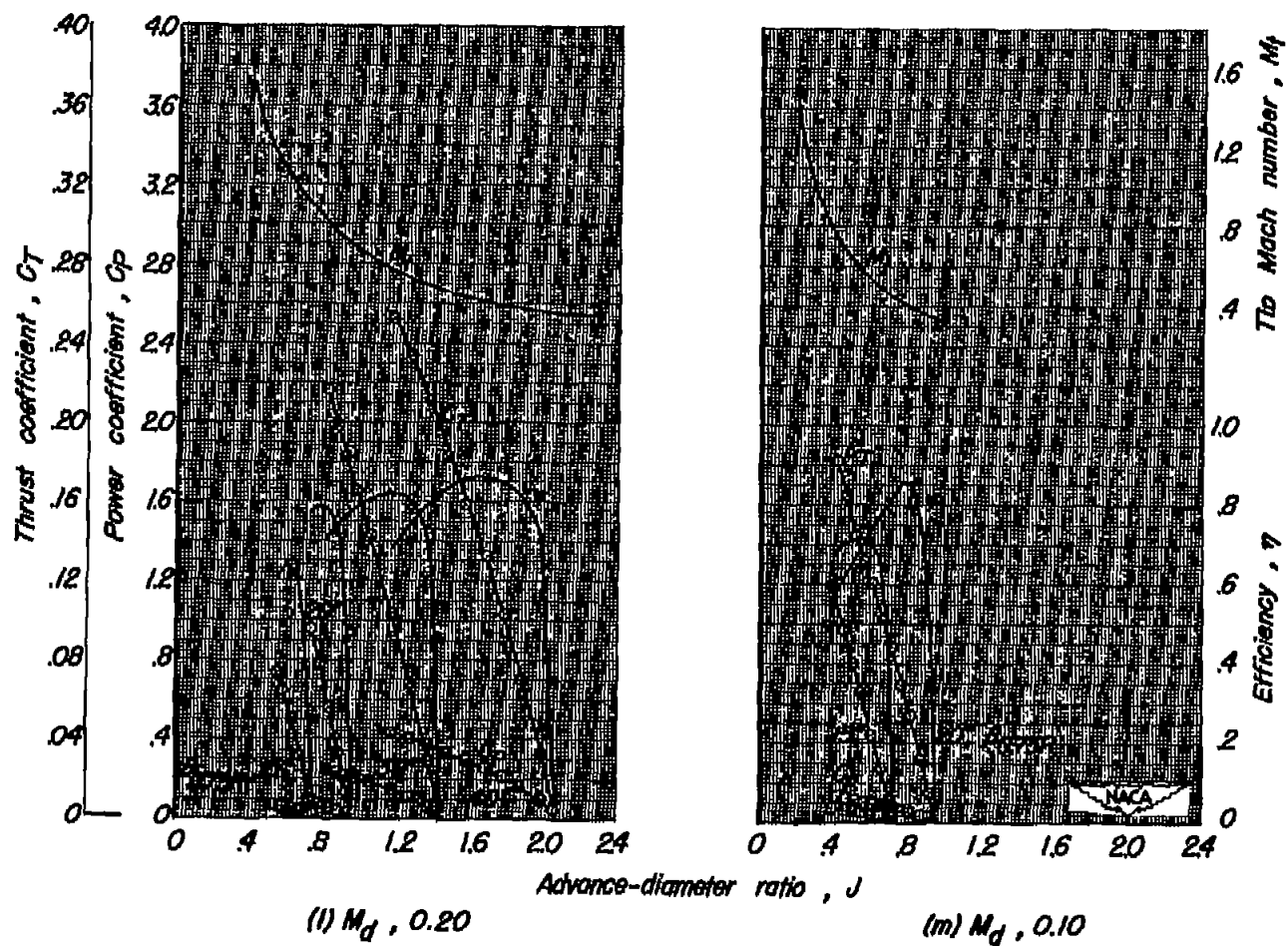


Figure 6.- Concluded.

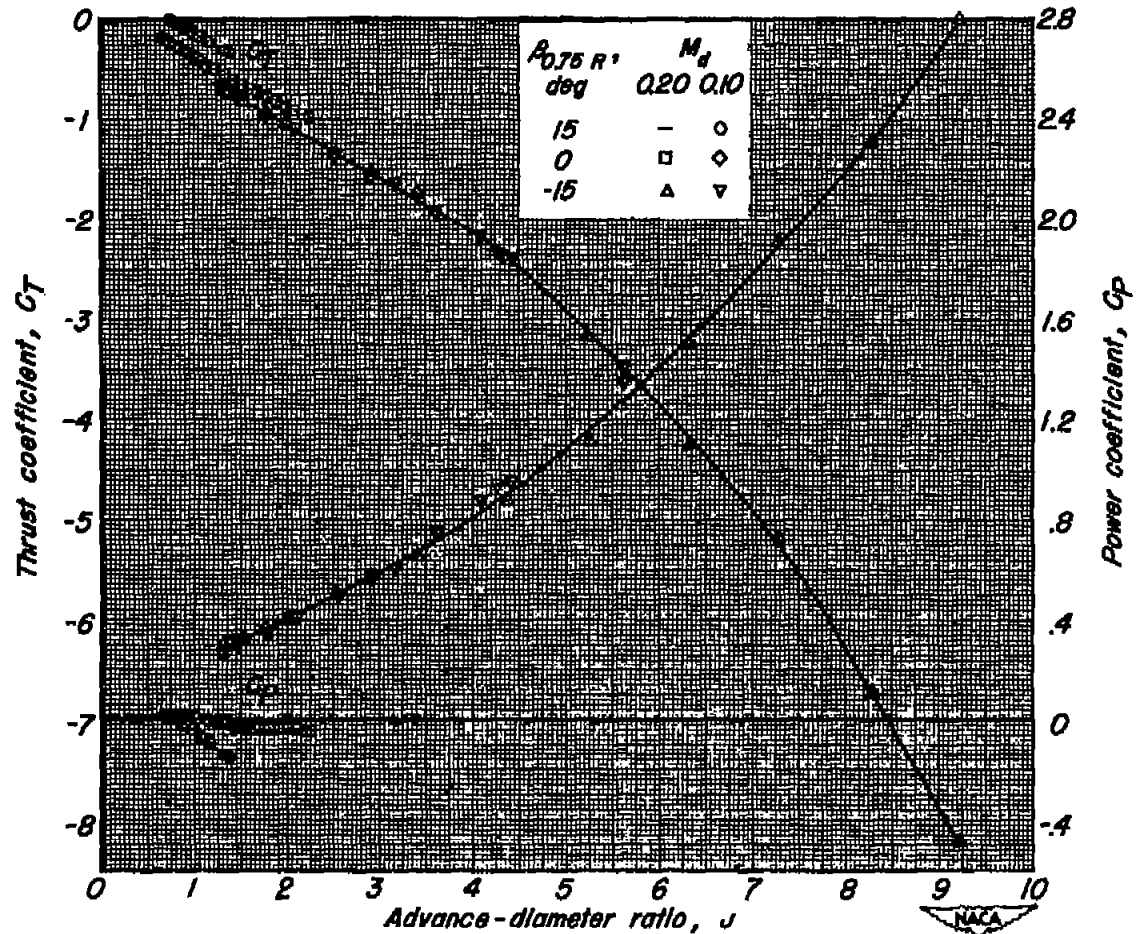
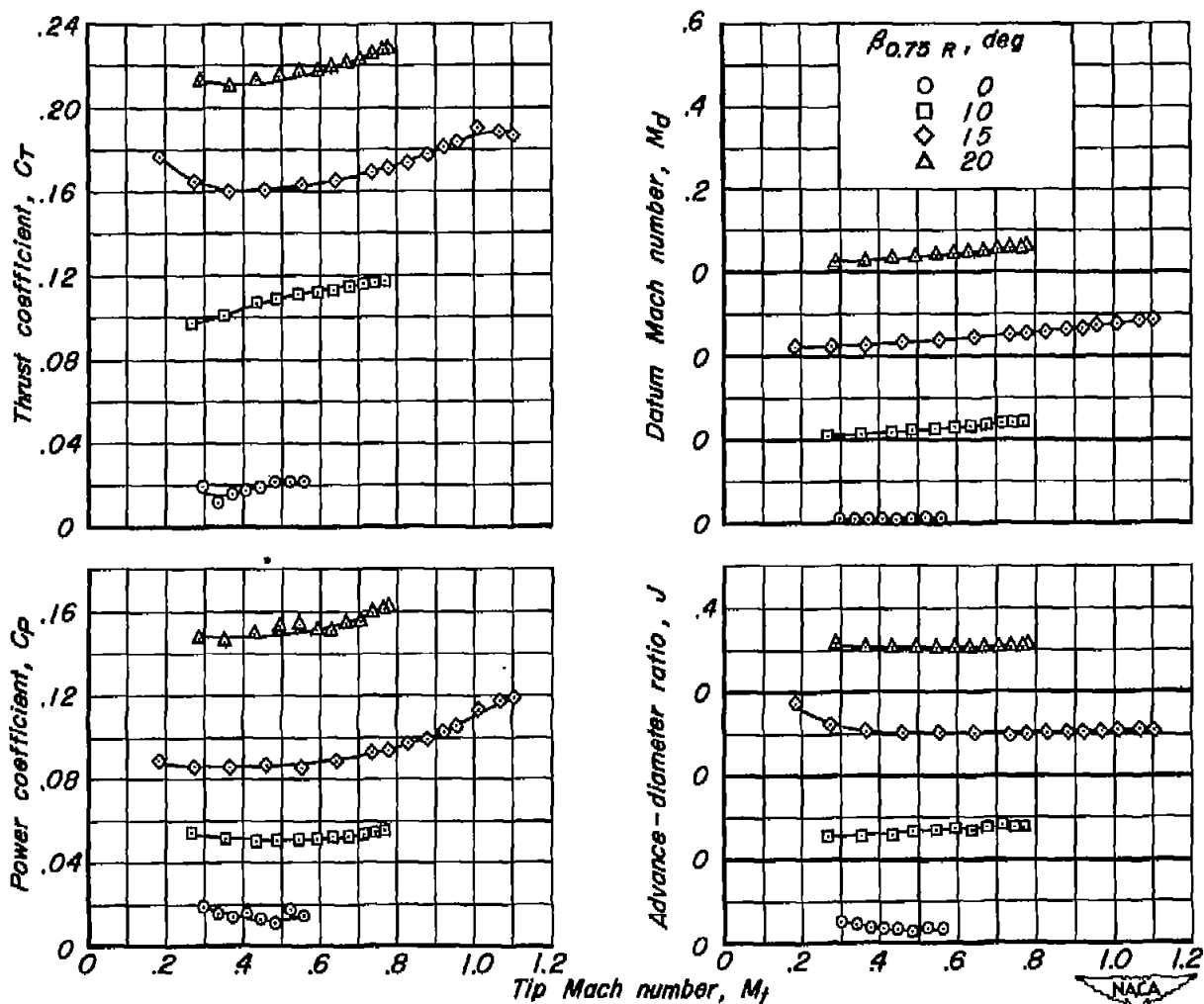
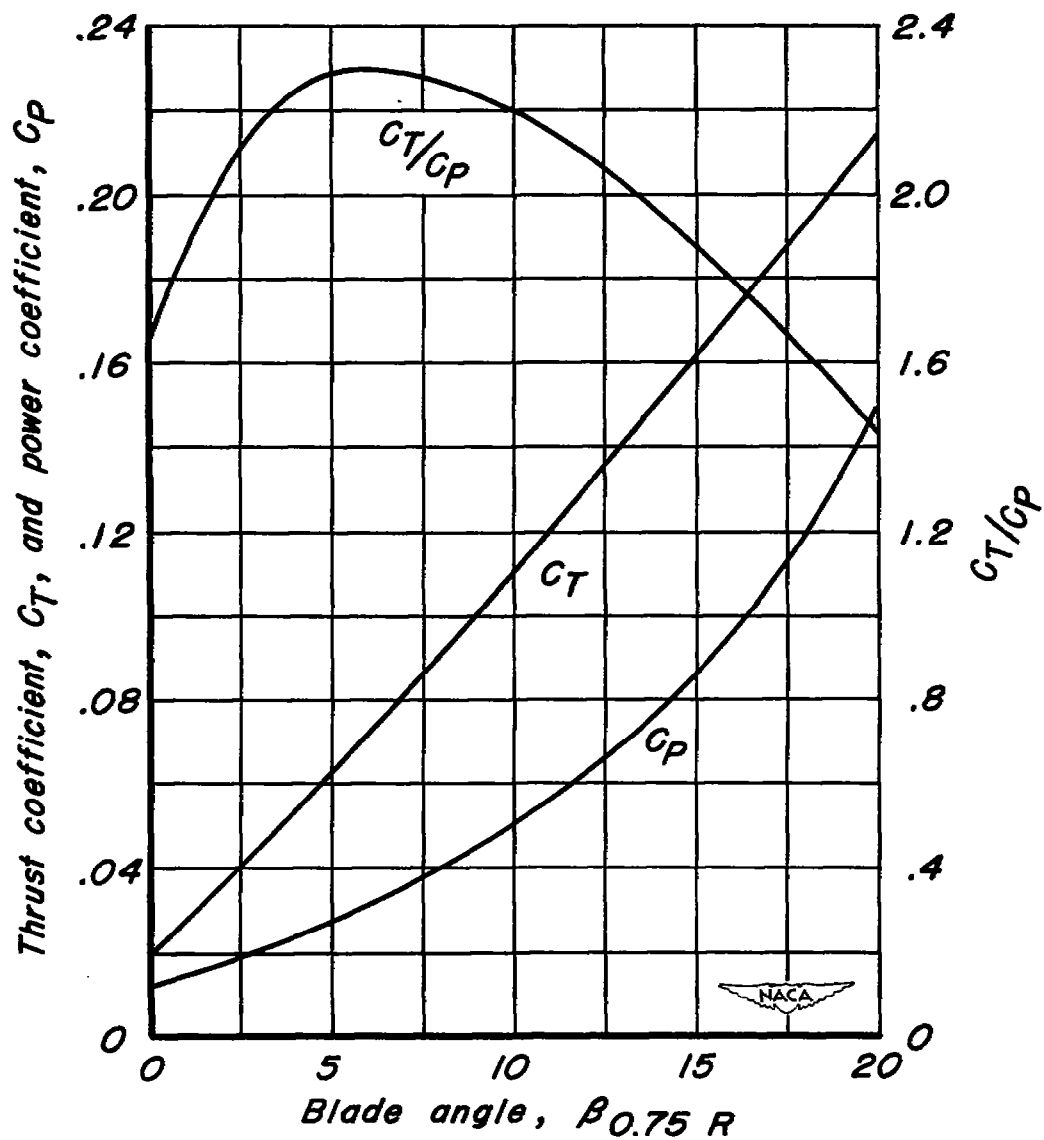


Figure 7.- Characteristics of the NACA 4-(5)05-041 propeller in negative thrust, 7.20-inch-diameter, 1-series spinner.



(a) Variation of thrust coefficient, power coefficient, datum Mach number, and advance-diameter ratio with propeller tip Mach number.

Figure 8.- Characteristics of the NACA 4-(5)(05)-041 propeller at low advance-diameter ratios and datum Mach numbers, 7.20-inch-diameter, 1-series spinner.



(b) Variation of thrust coefficient, power coefficient, and the ratio of thrust coefficient to power coefficient with propeller blade angle. M_t , 0.50.

Figure 8.—Concluded.

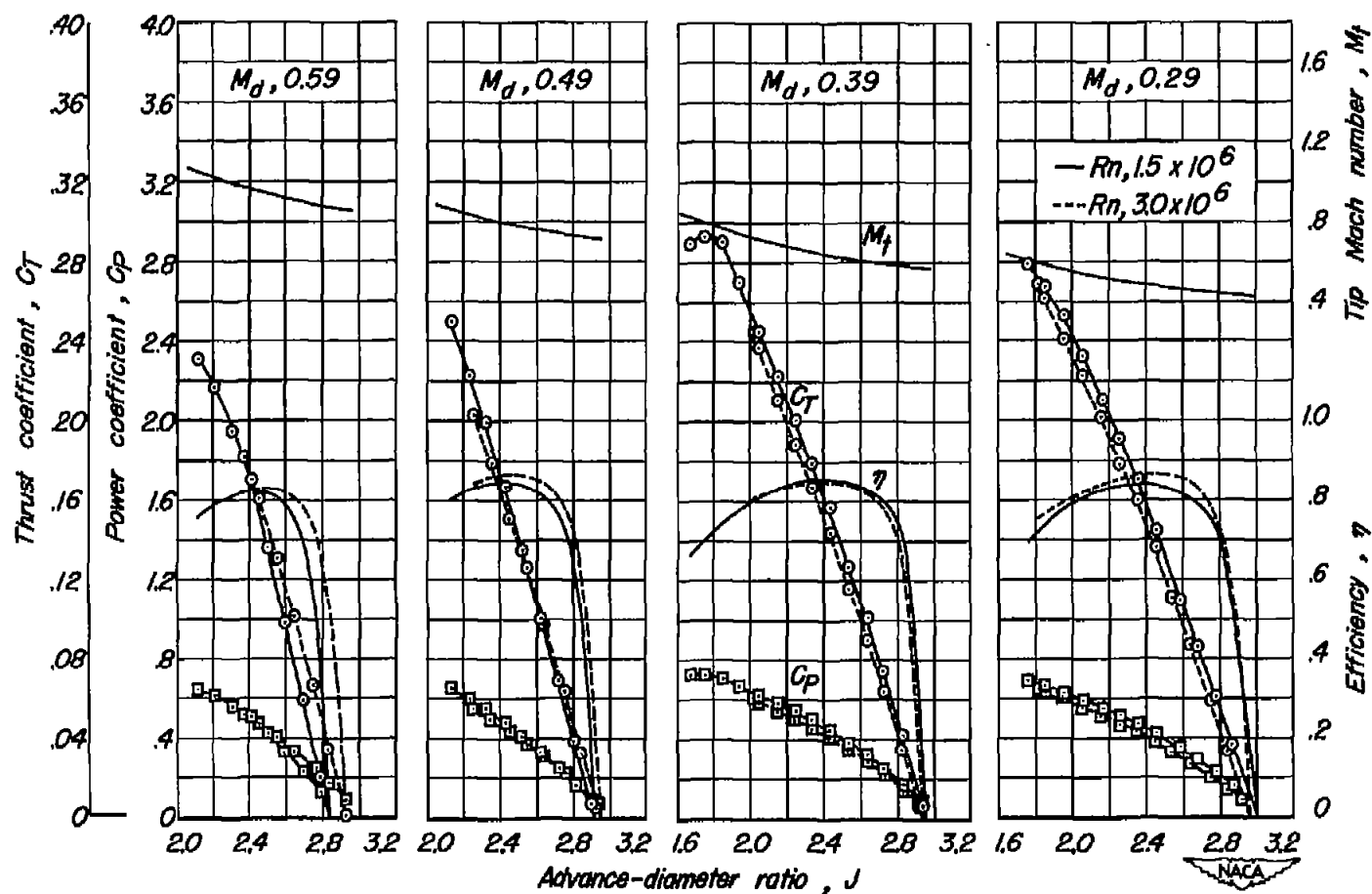


Figure 9 .-The effect of Reynolds number on the characteristics of the NACA 4-(5)(05)-041 propeller with the 7.20-inch-diameter, 1-series spinner; $\beta_{0.75R}, 50^\circ$.

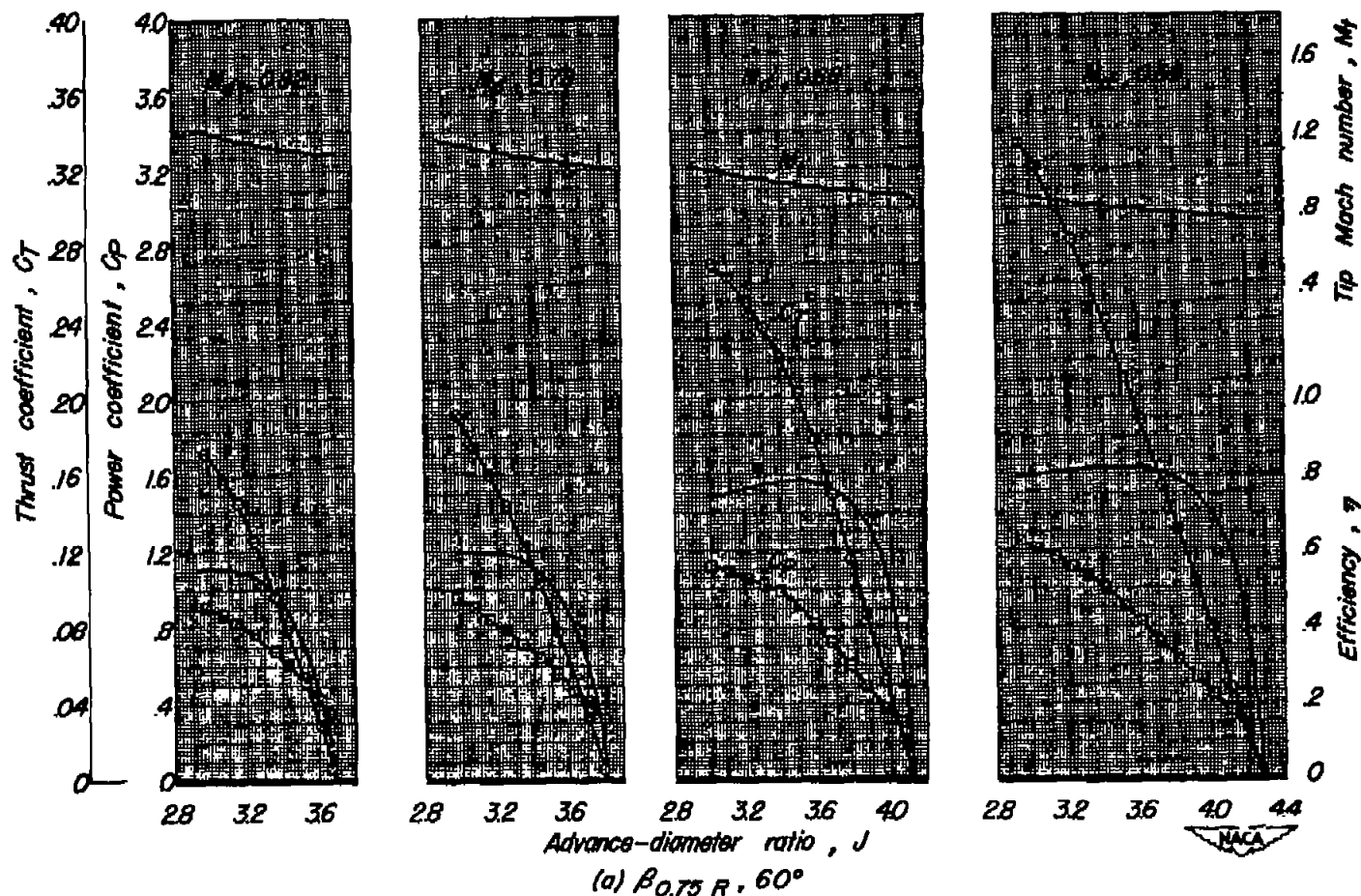
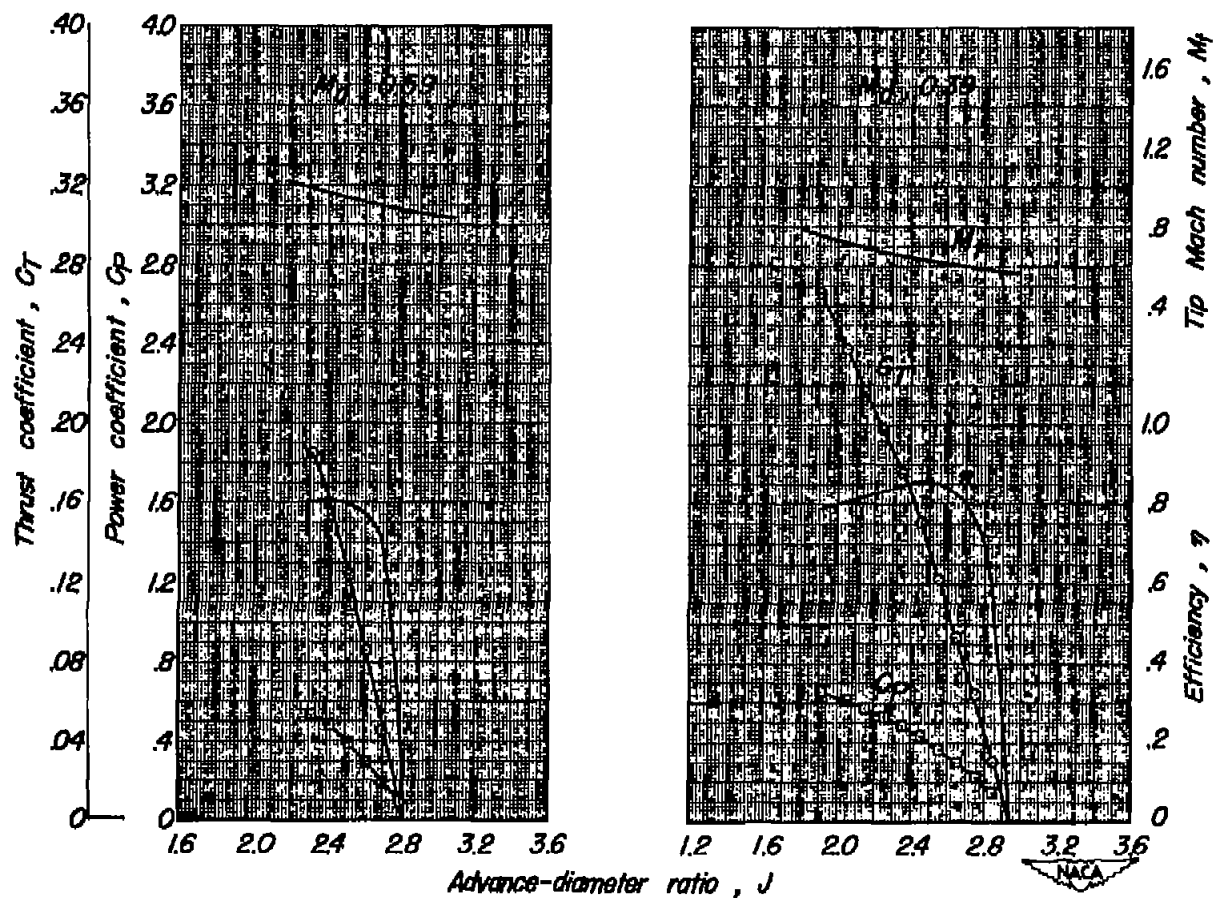
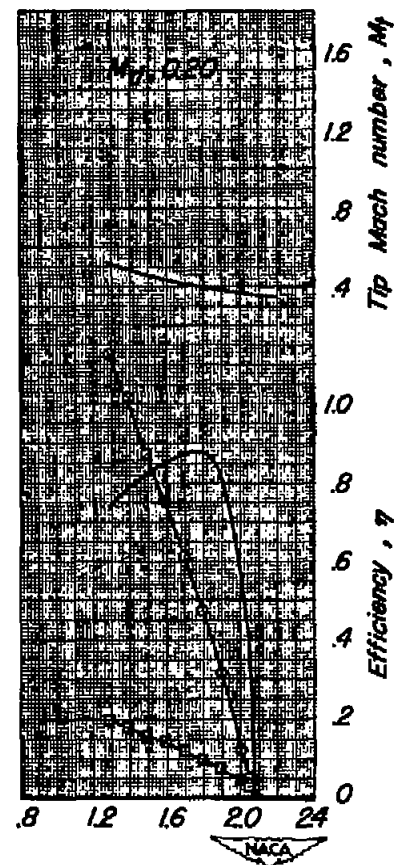
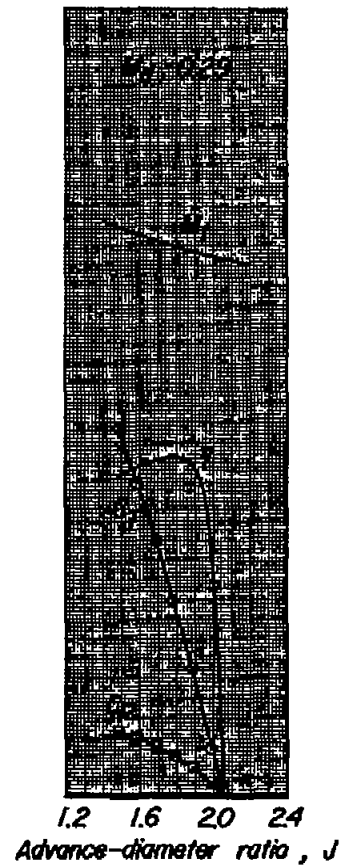
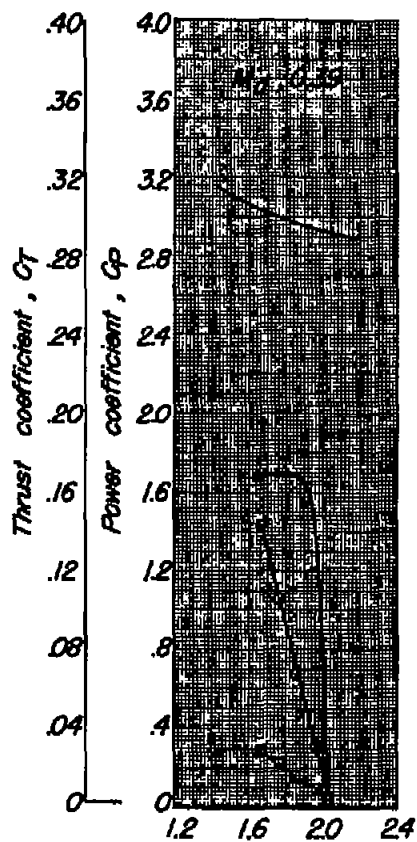


Figure 10-Characteristics of the NACA 4-(5)(05)-041 propeller, 6.51-inch-diameter, 1-series spinner.



(b) $\beta_{0.75 R}, 50^\circ$

Figure 10.-Continued.



(c) $\beta_{0.75} R, 40^\circ$

Figure 10.-Concluded.

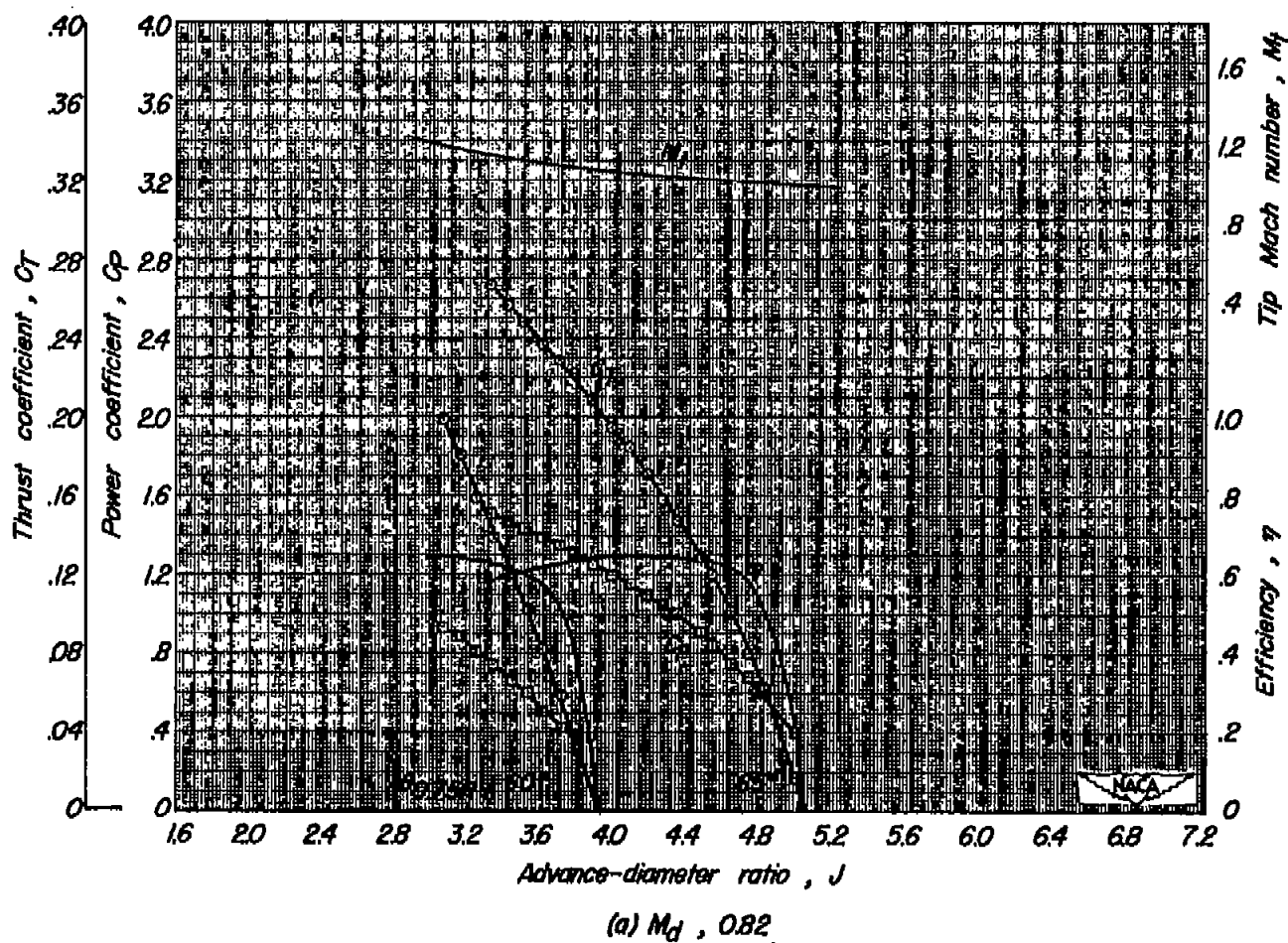
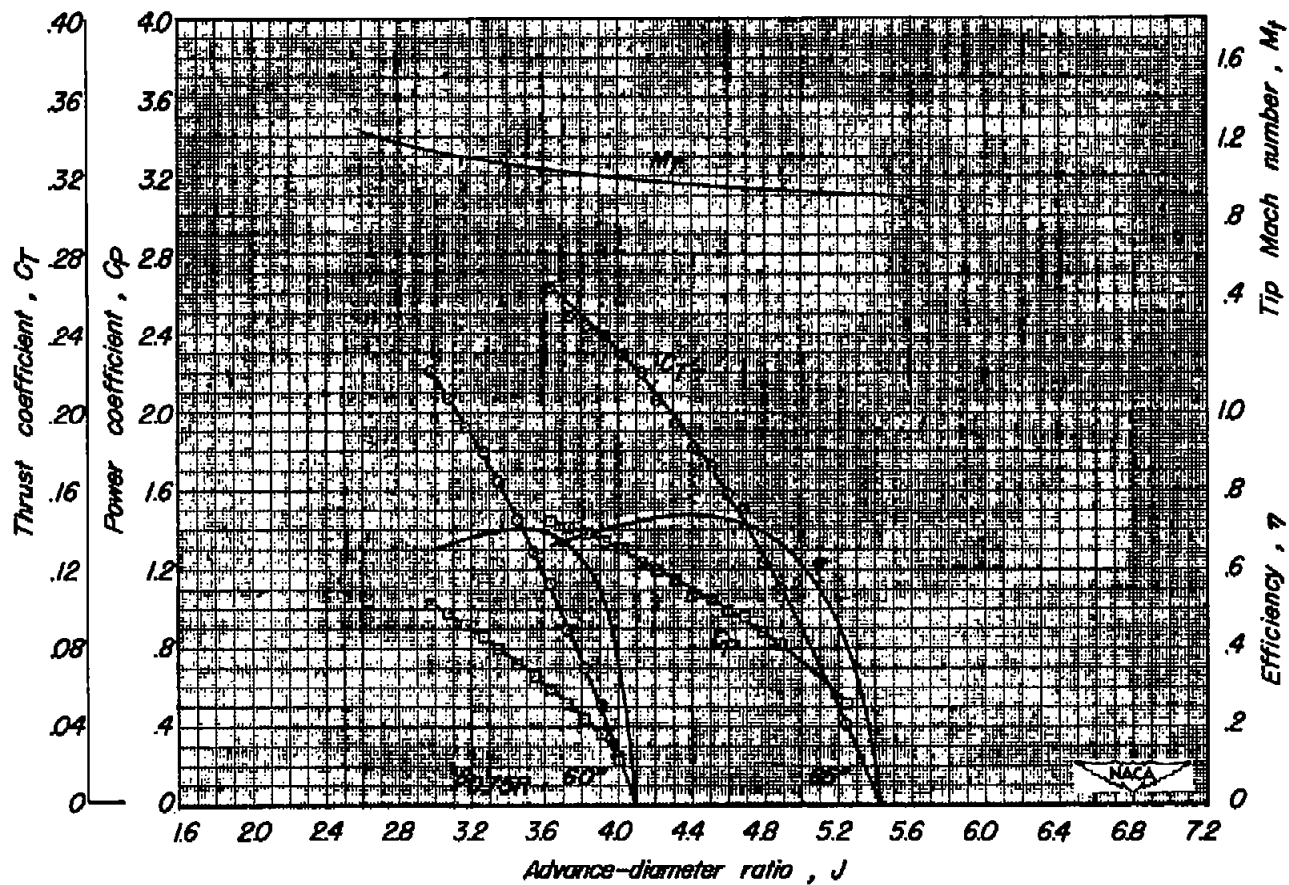
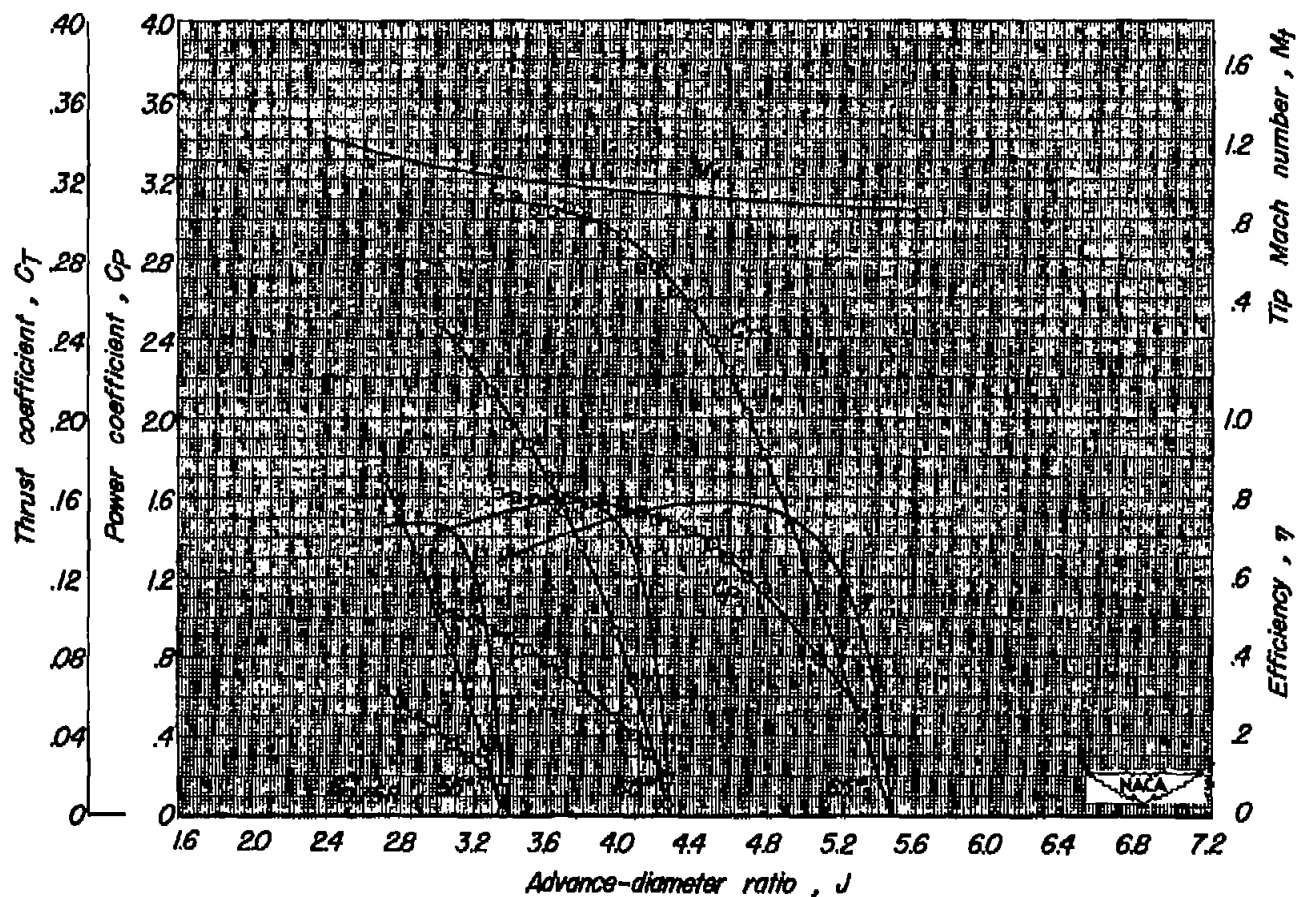


Figure 11 - Characteristics of the NACA 4-(5)(05)-041 propeller, 720-inch-diameter, extended cylindrical spinner.



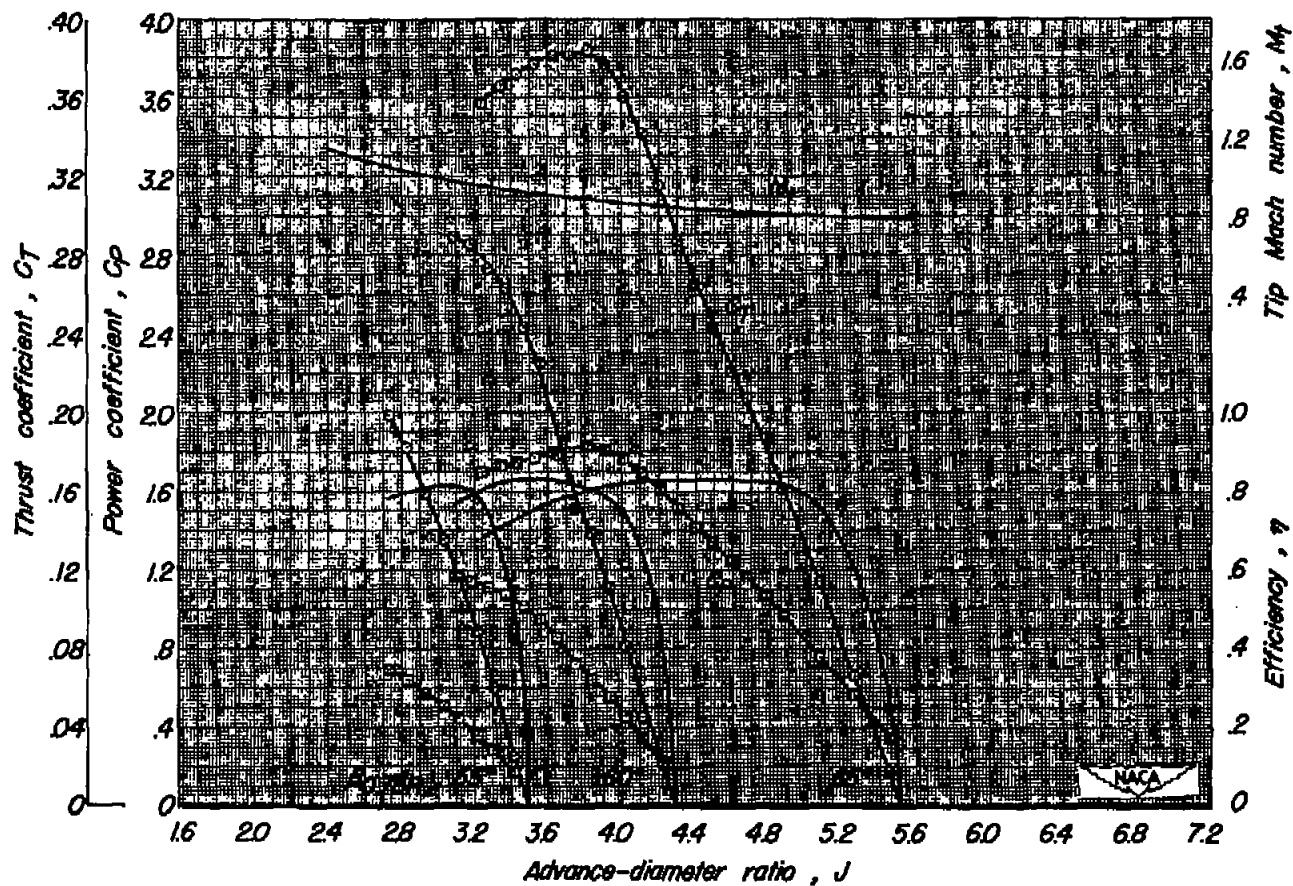
(b) M_d , 0.78

Figure 11 -Continued.



(c) M_d , 0.73

Figure 11 - Continued.



(d) $M_t, 0.68$

Figure 11 - Continued.

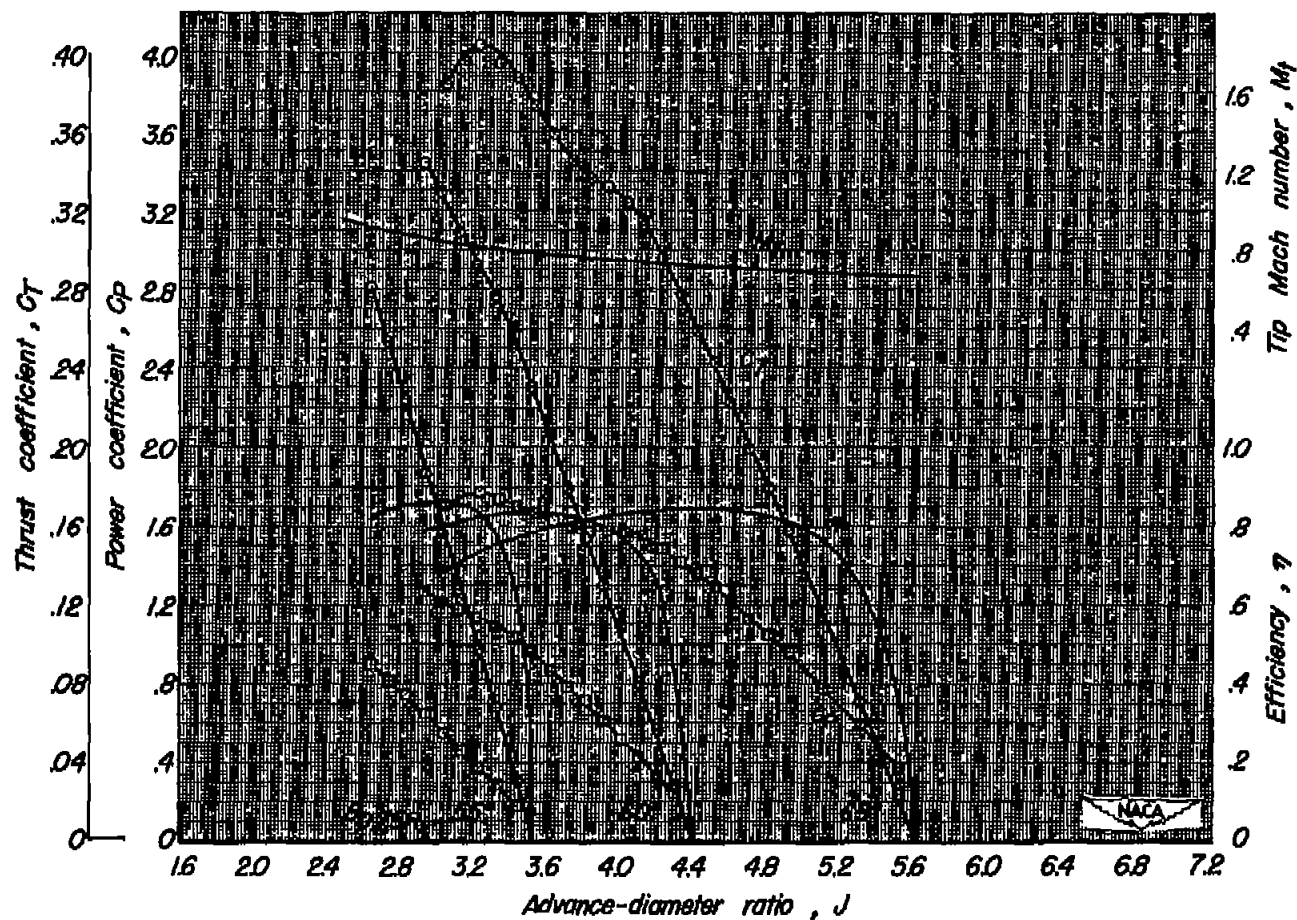
(e) $M_d, 0.59$

Figure 11.-Concluded.

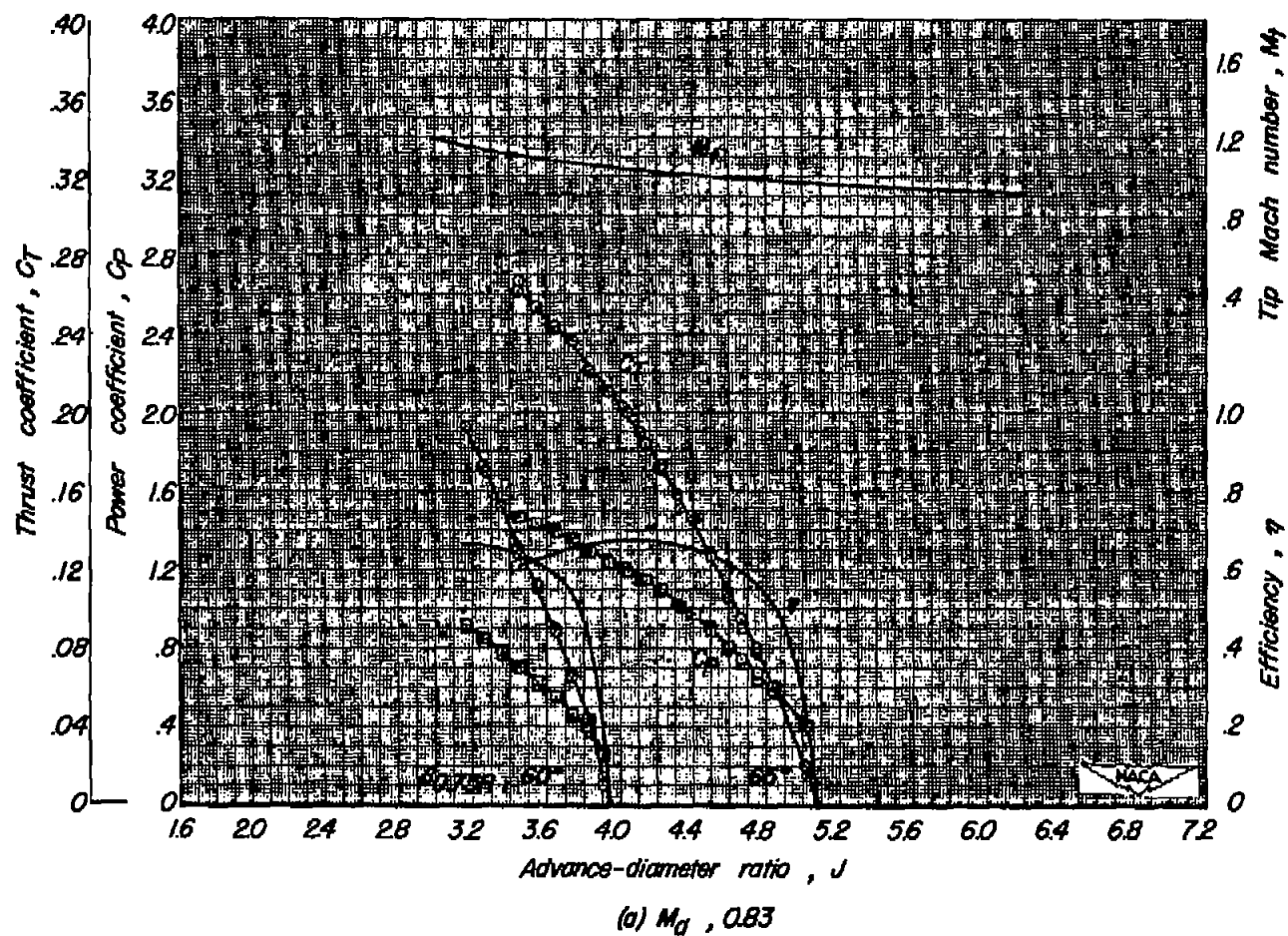


Figure 12.-Characteristics of the NACA 4-(5)(05)-041 propeller, 12.00-inch-diameter, extended cylindrical spinner.

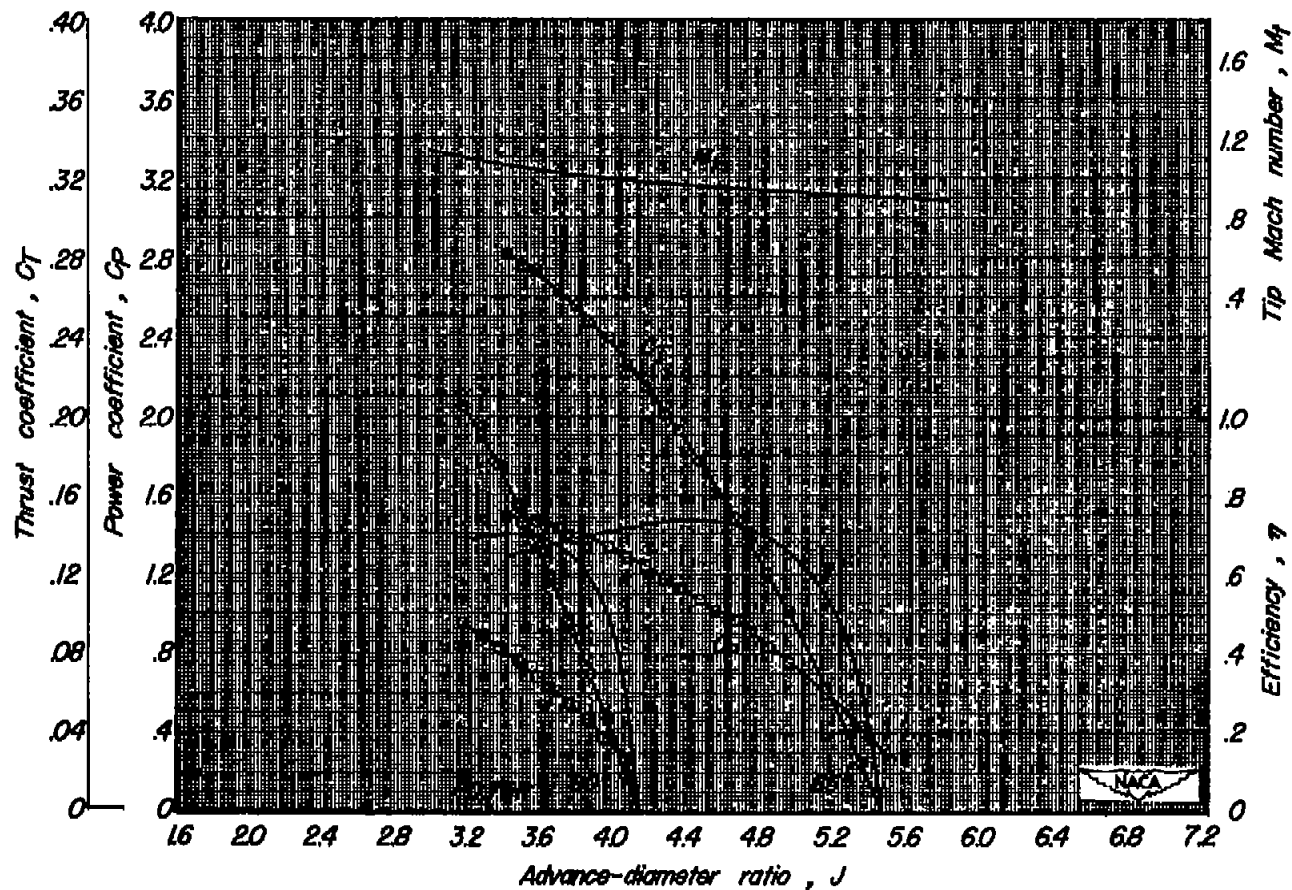
(b) $M_d, 0.79$

Figure 12.-Continued.

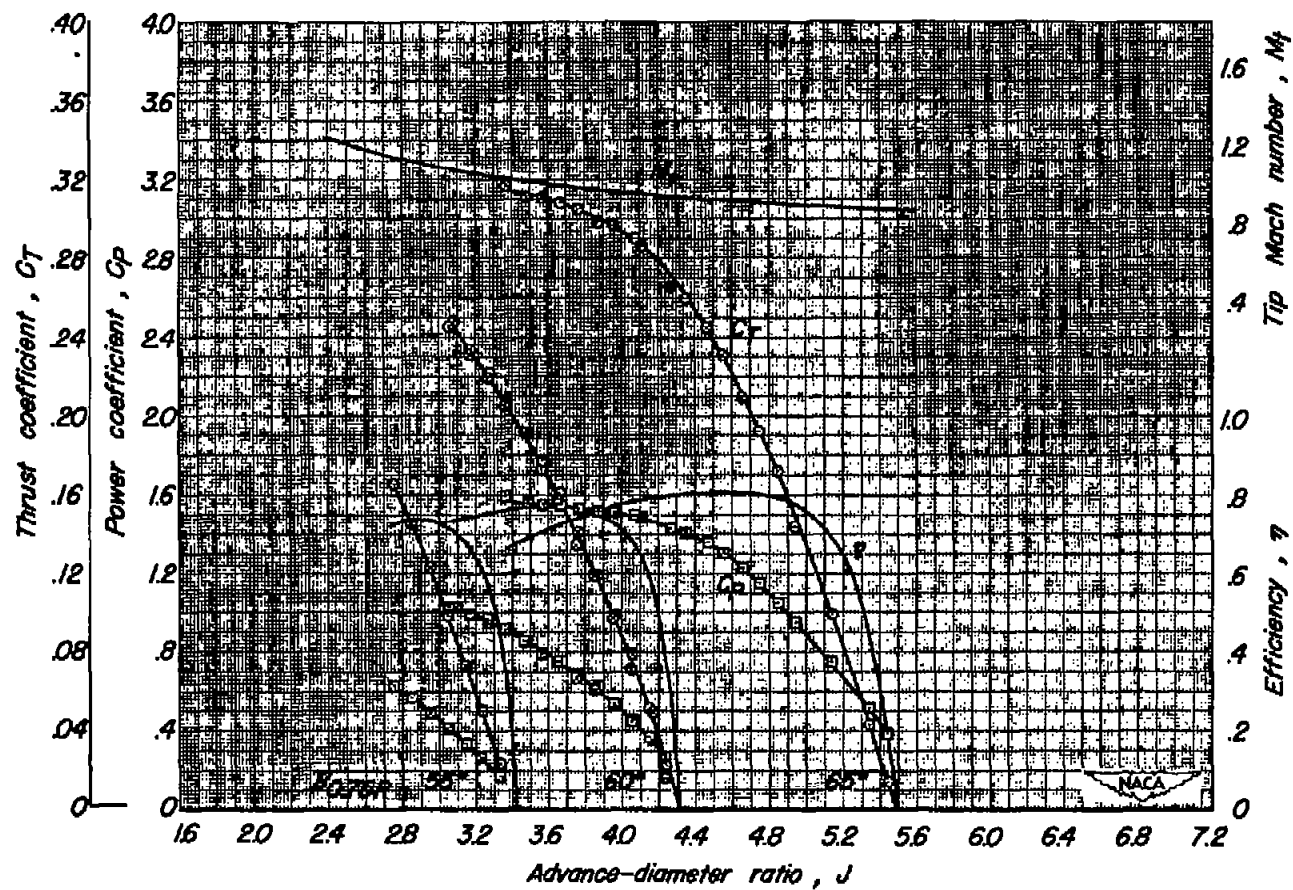


Figure 12 -Continued.

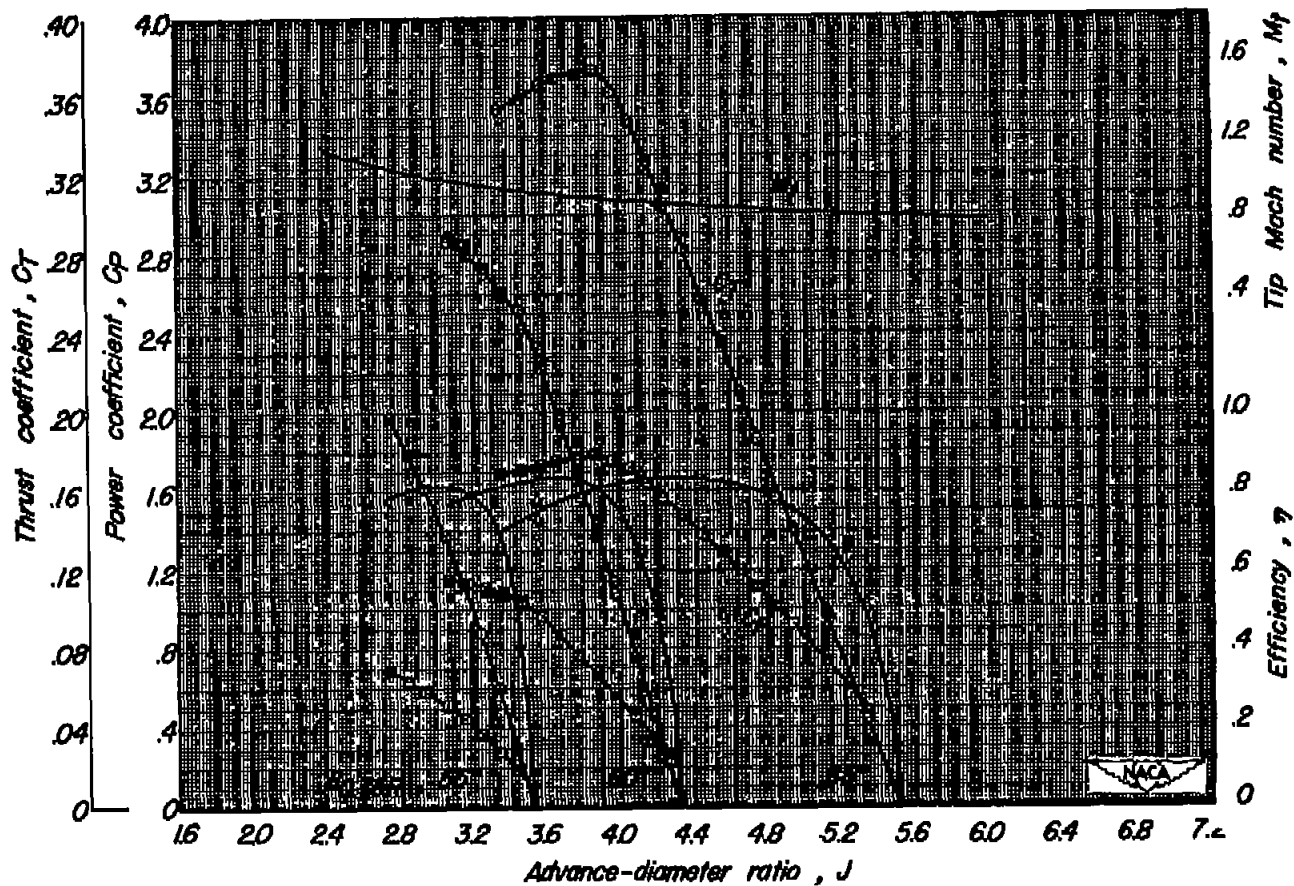
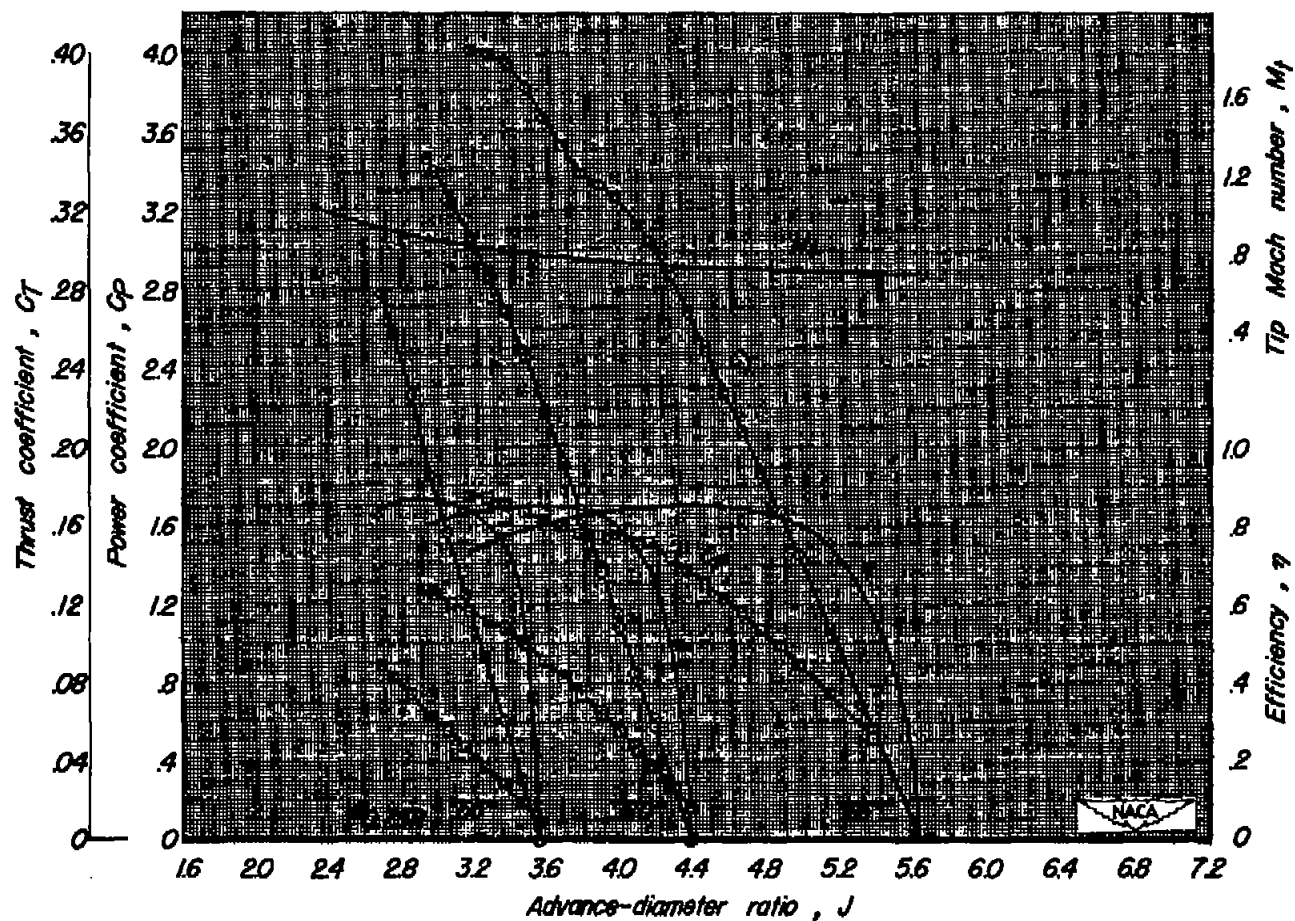


Figure 12.- Continued.



(e) $M_t = 0.59$

Figure 12 -Concluded.

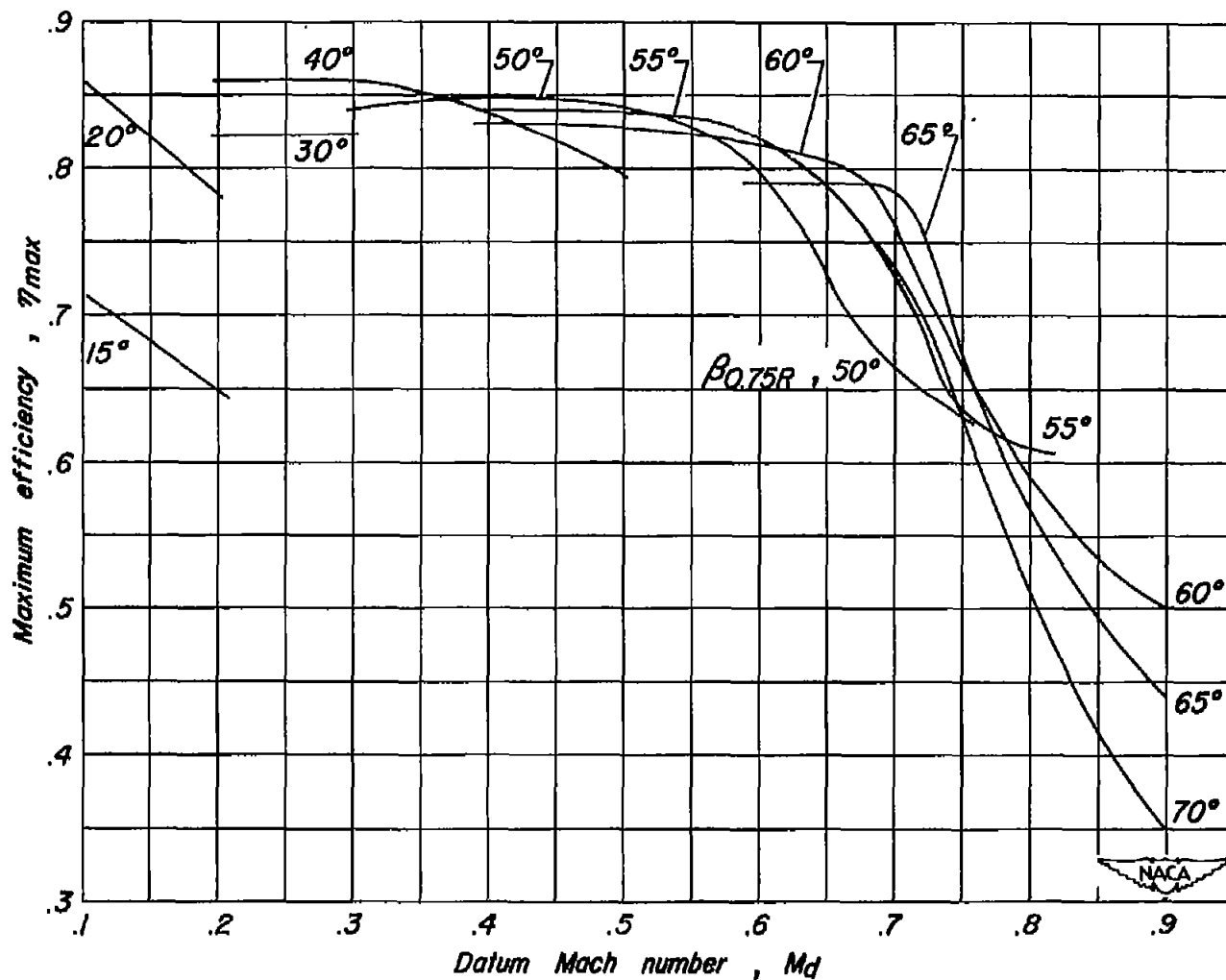


Figure 13.- The effect of blade angle and Mach number on the maximum efficiency of the NACA 4-(5)(05)-041 four-blade propeller with the 7.20-inch-diameter, 1-series spinner.

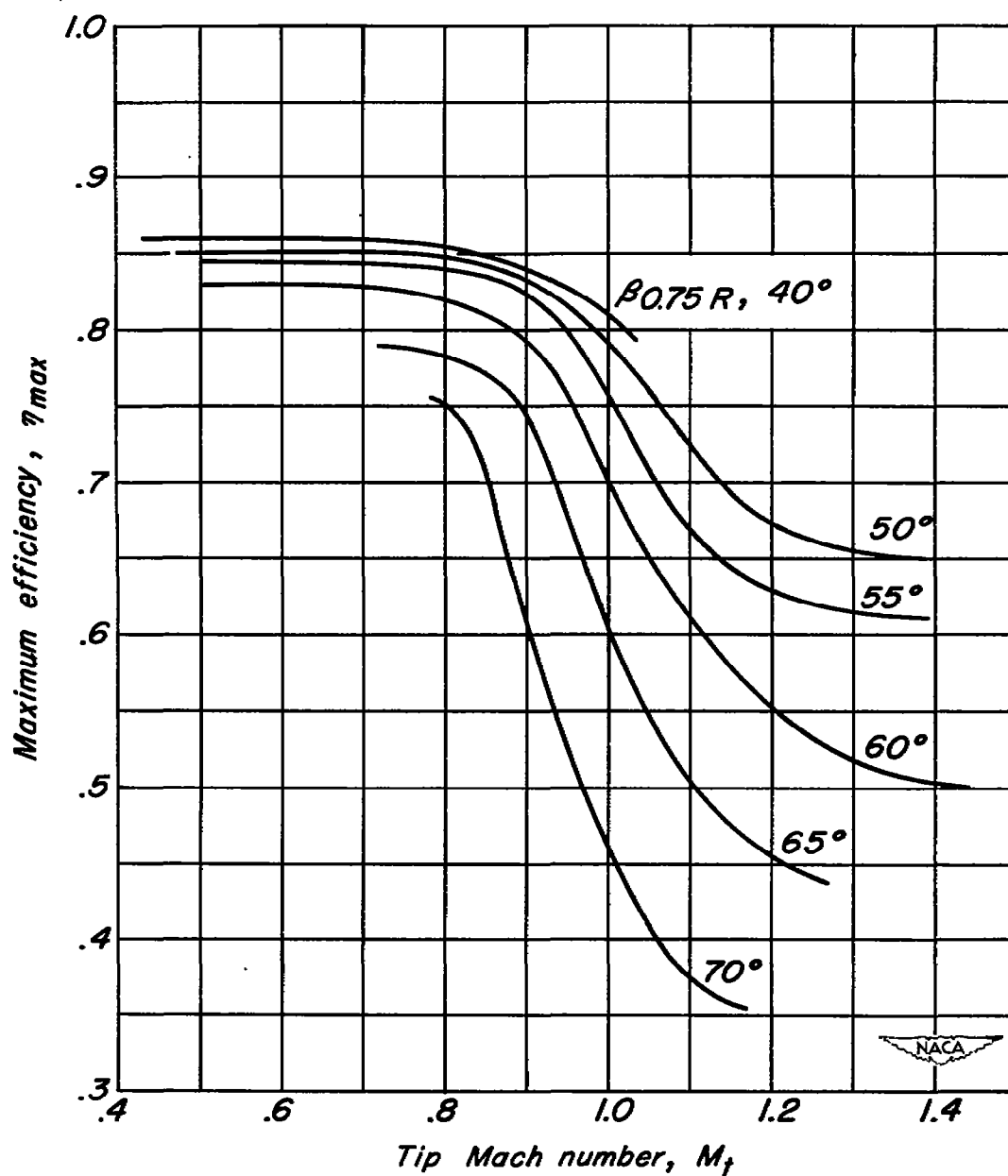


Figure 14.- The variation of maximum efficiency with tip Mach number, NACA 4-(5)(05)-041 propeller with the 7.20-inch-diameter, 1-series spinner.

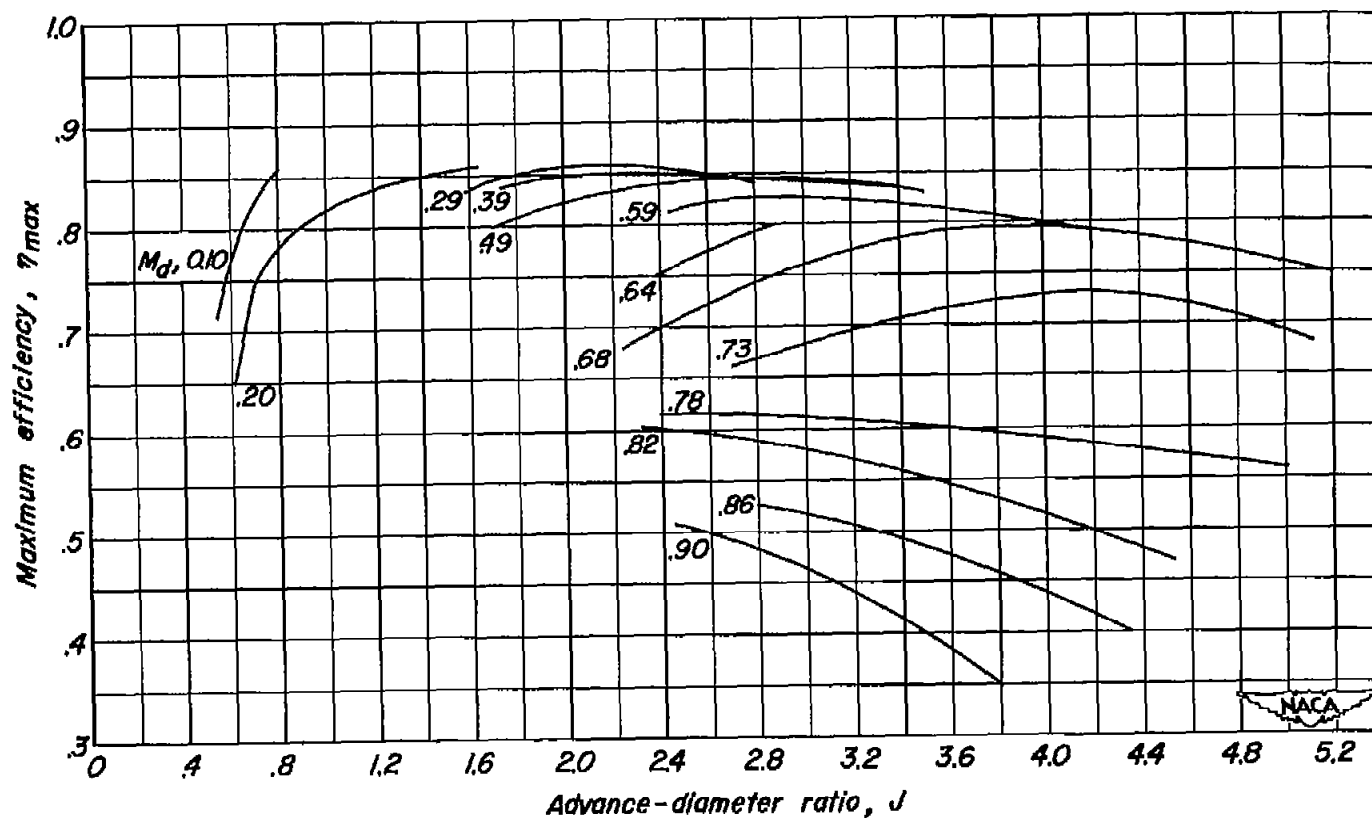
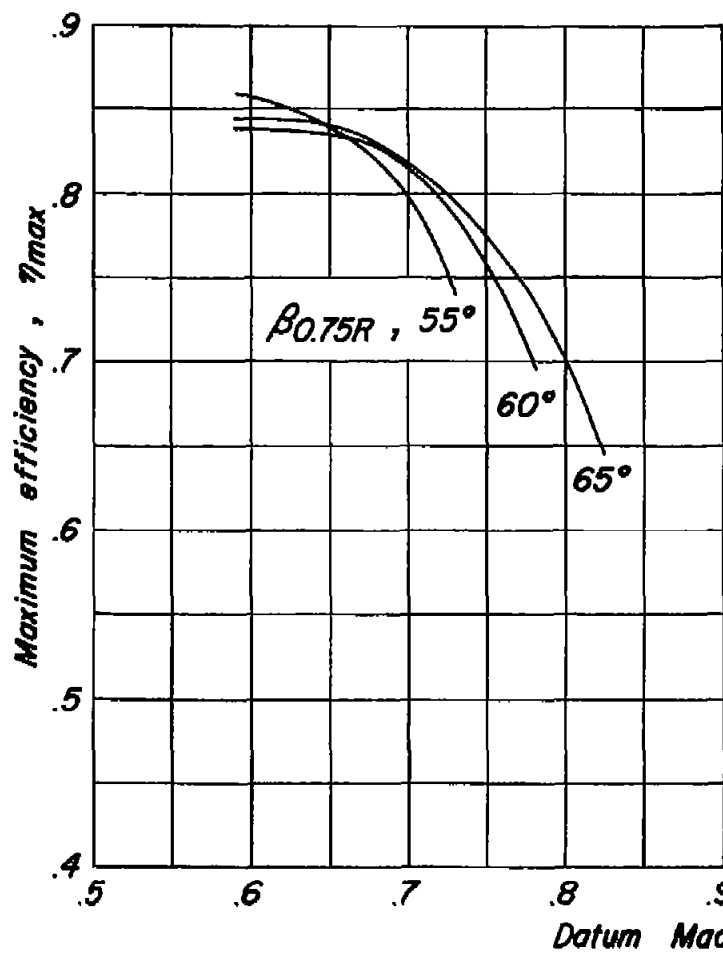
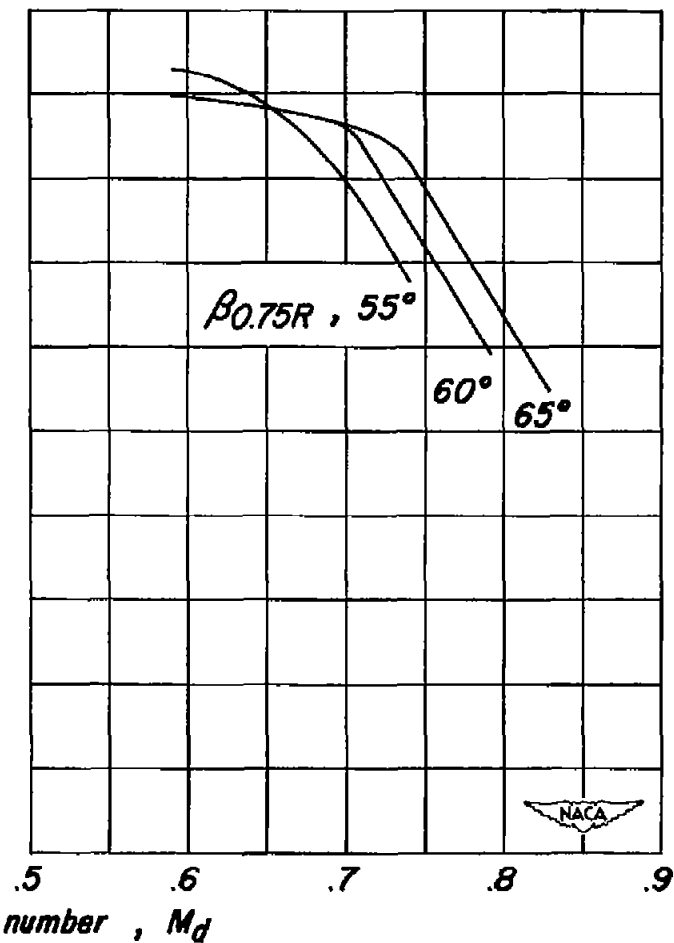


Figure 15.-The effect of Mach number and advance-diameter ratio on the maximum efficiency of the NACA 4-(5)05-041 four-blade propeller with the 7.20-inch-diameter, 1-series spinner.



(a) 7.20-inch diameter.



(b) 12.00-inch diameter.

Figure 16.-The effect of blade angle and Mach number on the maximum efficiency of the NACA 4-(5)(05)-041 four-blade propeller with the extended cylindrical spinners.

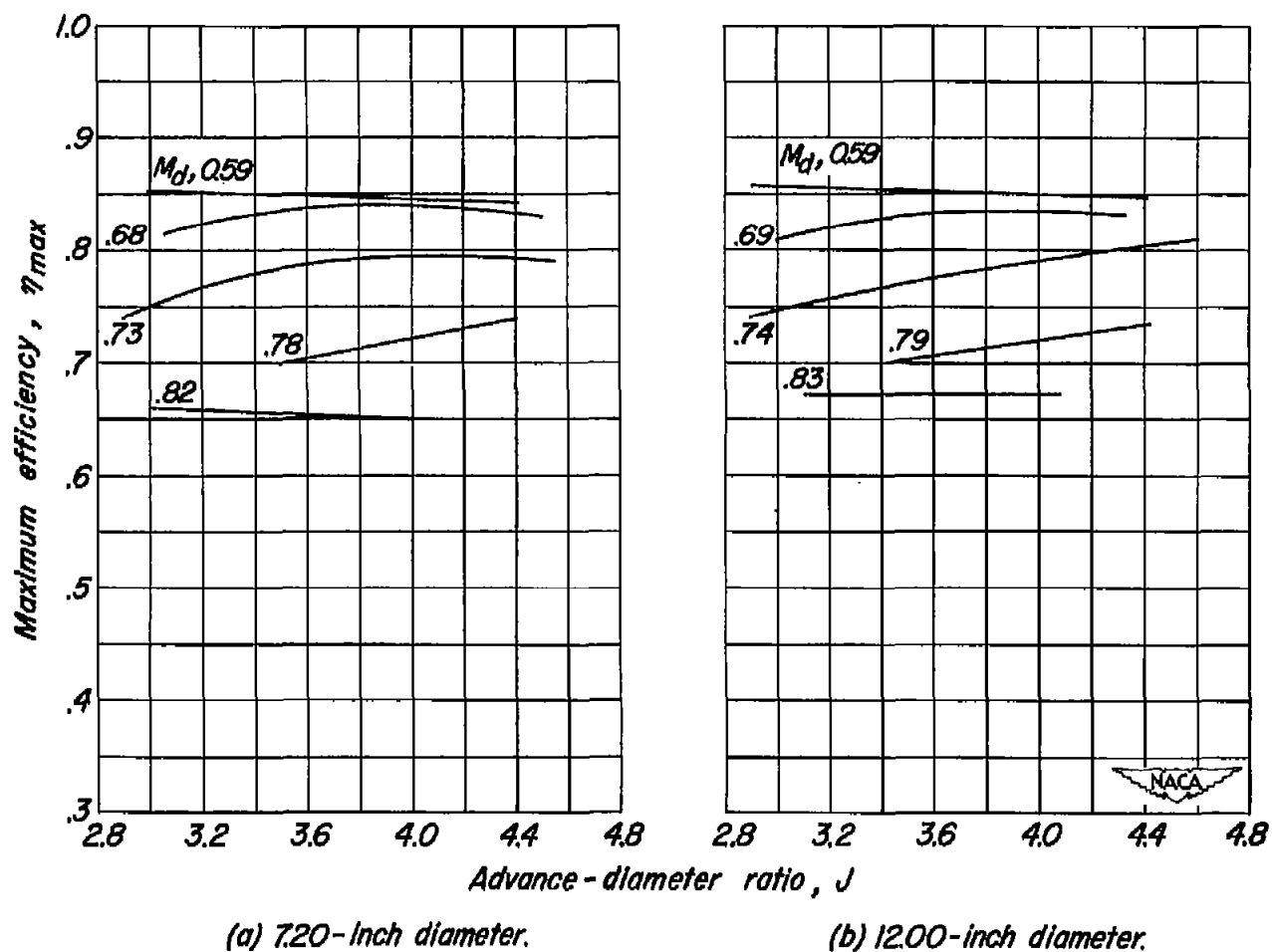


Figure 17.—The effect of Mach number and advance-diameter ratio on the maximum efficiency of the NACA 4-(5)(05)-041 four-blade propeller with the extended cylindrical spinners.

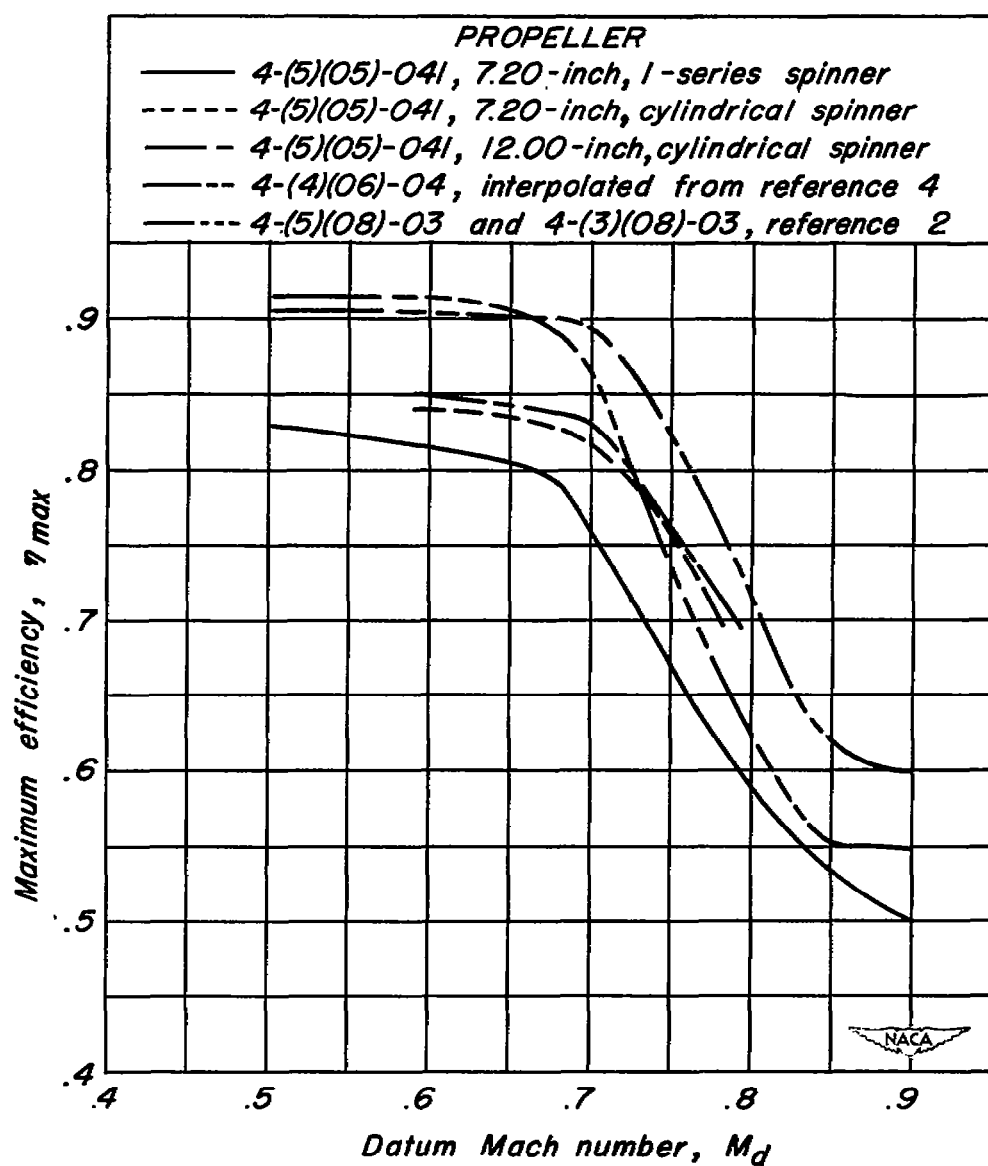
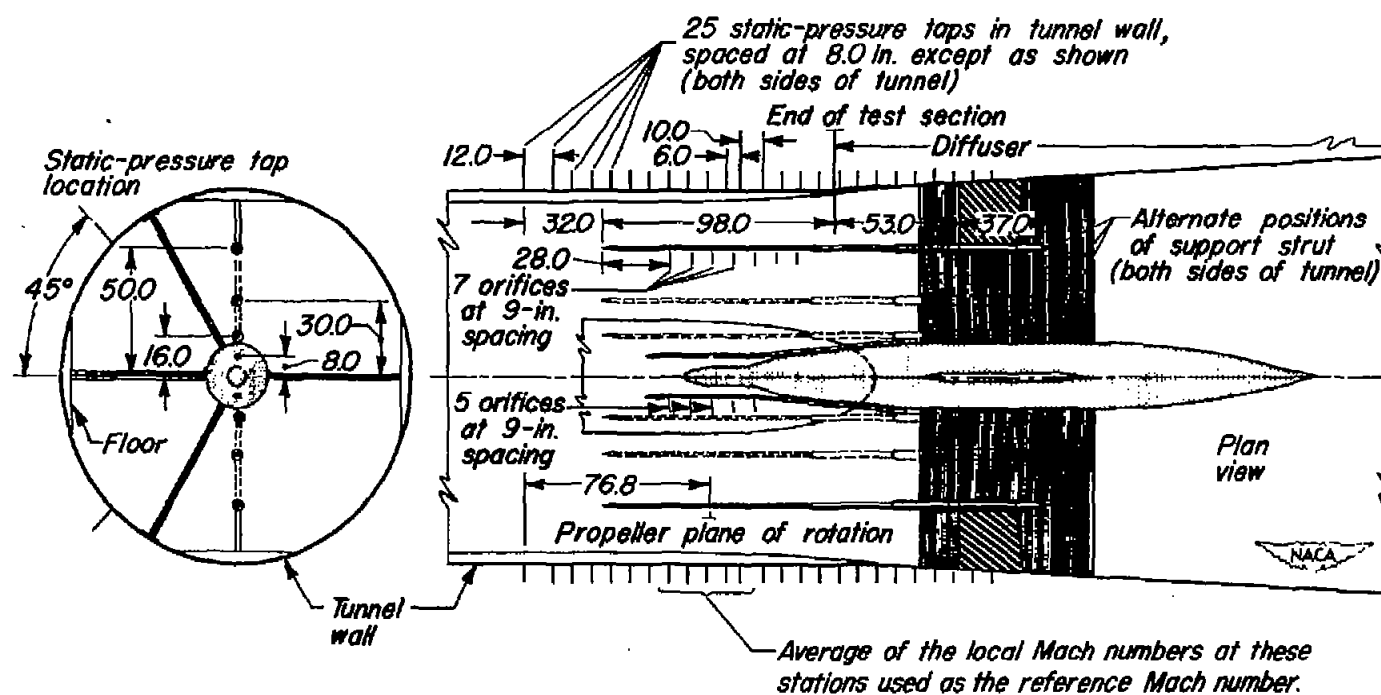


Figure 18.- The variation of maximum efficiency with Mach number for the NACA 4-(5)(05)-041 propeller as compared with the results of previous investigations. $\beta_{0.75 R} = 60^\circ$



Figure 19.- Cutaway view of the 1000-horsepower propeller dynamometer.



Note: Dimensions shown in inches

Figure 20- Installation of the stream survey-tubes with the 1000-horsepower propeller dynamometer.

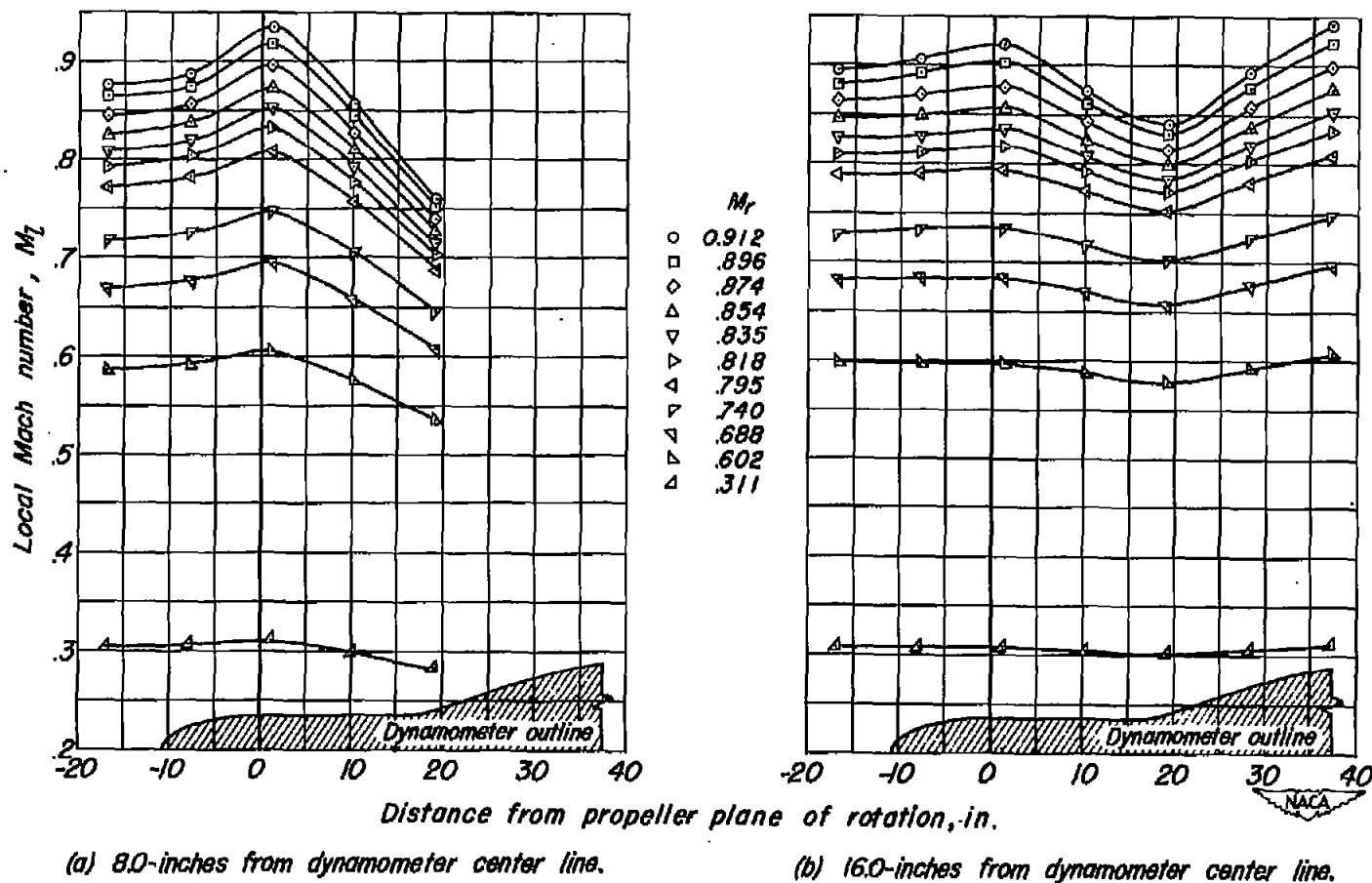
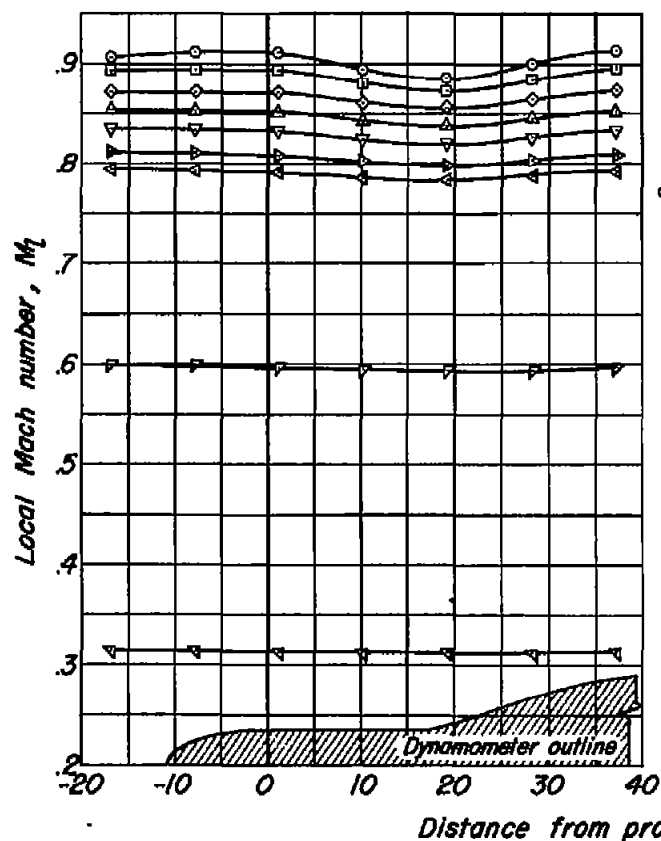
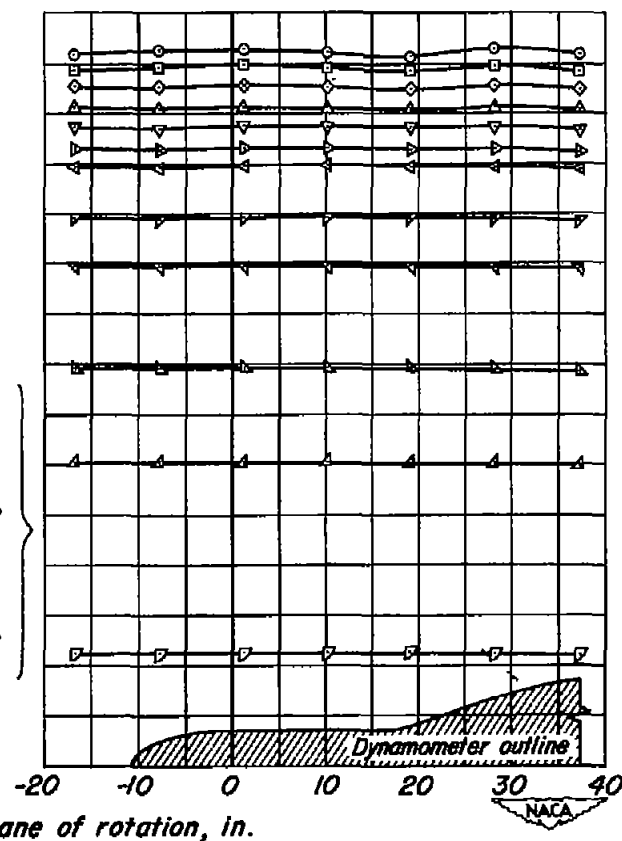


Figure 21.-The longitudinal variation of the local Mach number in the horizontal plane through the test-section center line for the dynamometer with the 7.20-inch-diameter, 1-series spinner.

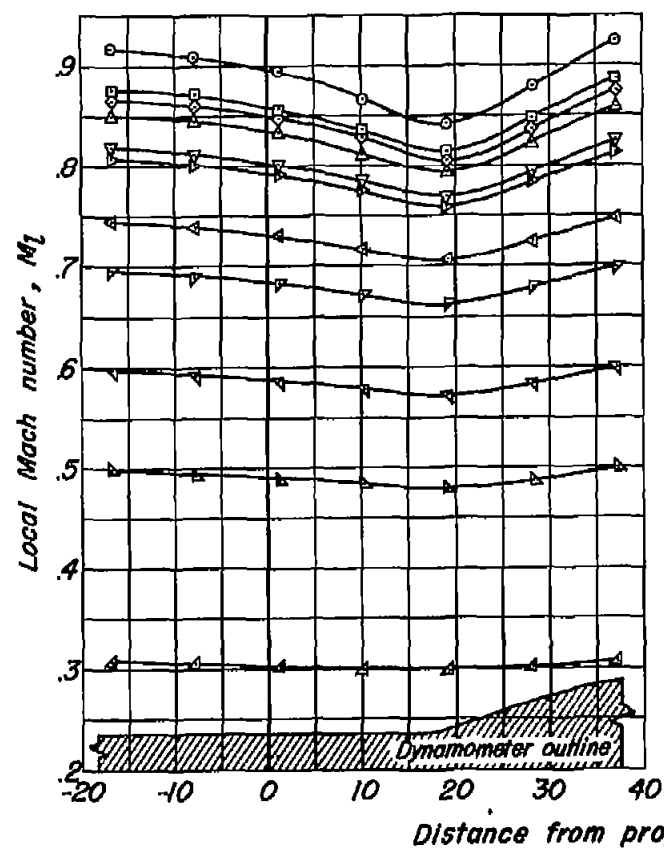


(c) 300-inches from dynamometer center line.



(d) 500-inches from dynamometer center line.

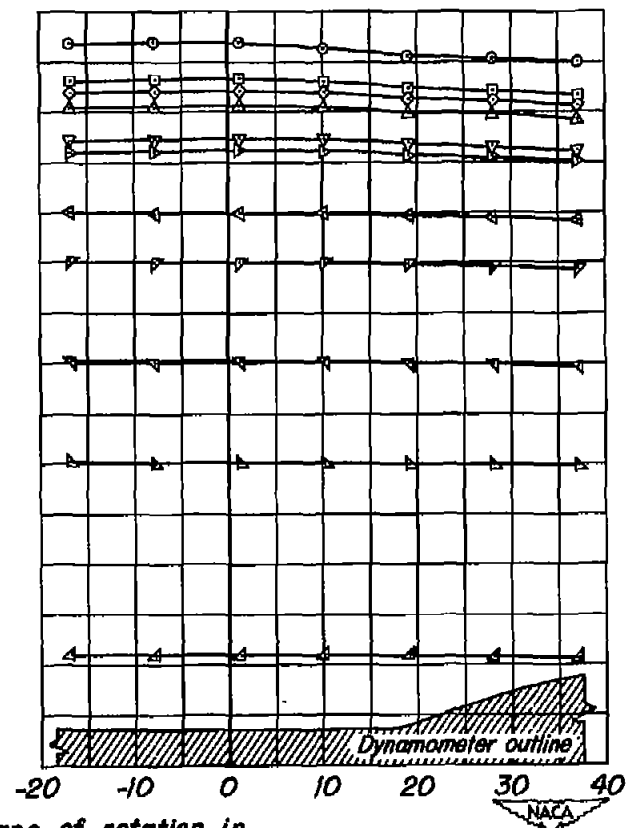
Figure 21 -Concluded.



(c) 16.0-inches from dynamometer center line.

M_r

- 0.909
- 0.872
- ◇ 0.860
- ◊ 0.847
- ▽ 0.815
- ▽ 0.805
- ▽ 0.743
- ▽ 0.695
- ▽ 0.597
- ▽ 0.497
- △ 0.307



(d) 50.0-inches from dynamometer center line.

Figure 22-Concluded.

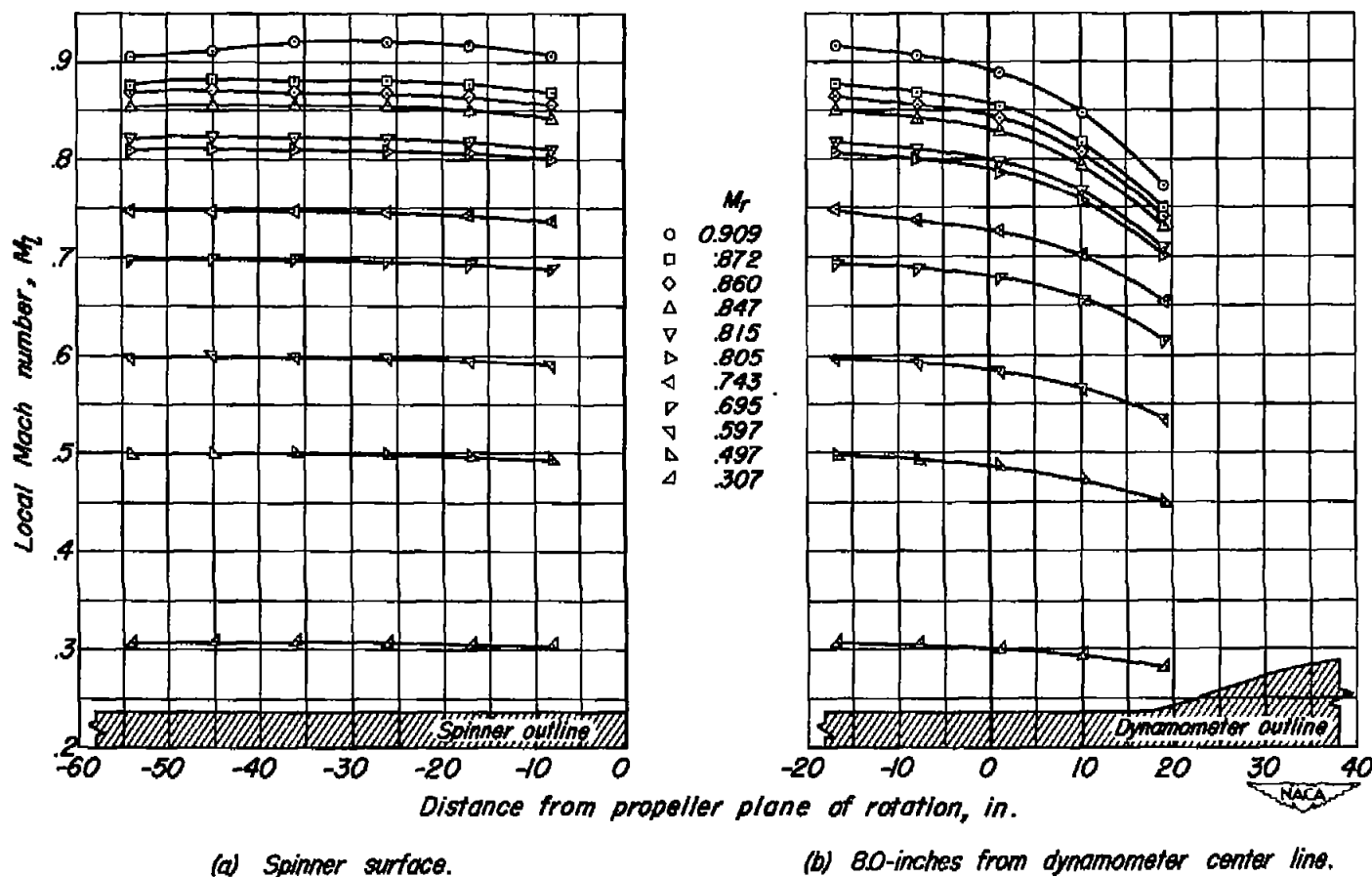


Figure 22.—The longitudinal variation of the local Mach number in the horizontal plane through the test-section center line for the dynamometer with the 7.20-inch-diameter, extended cylindrical spinner.

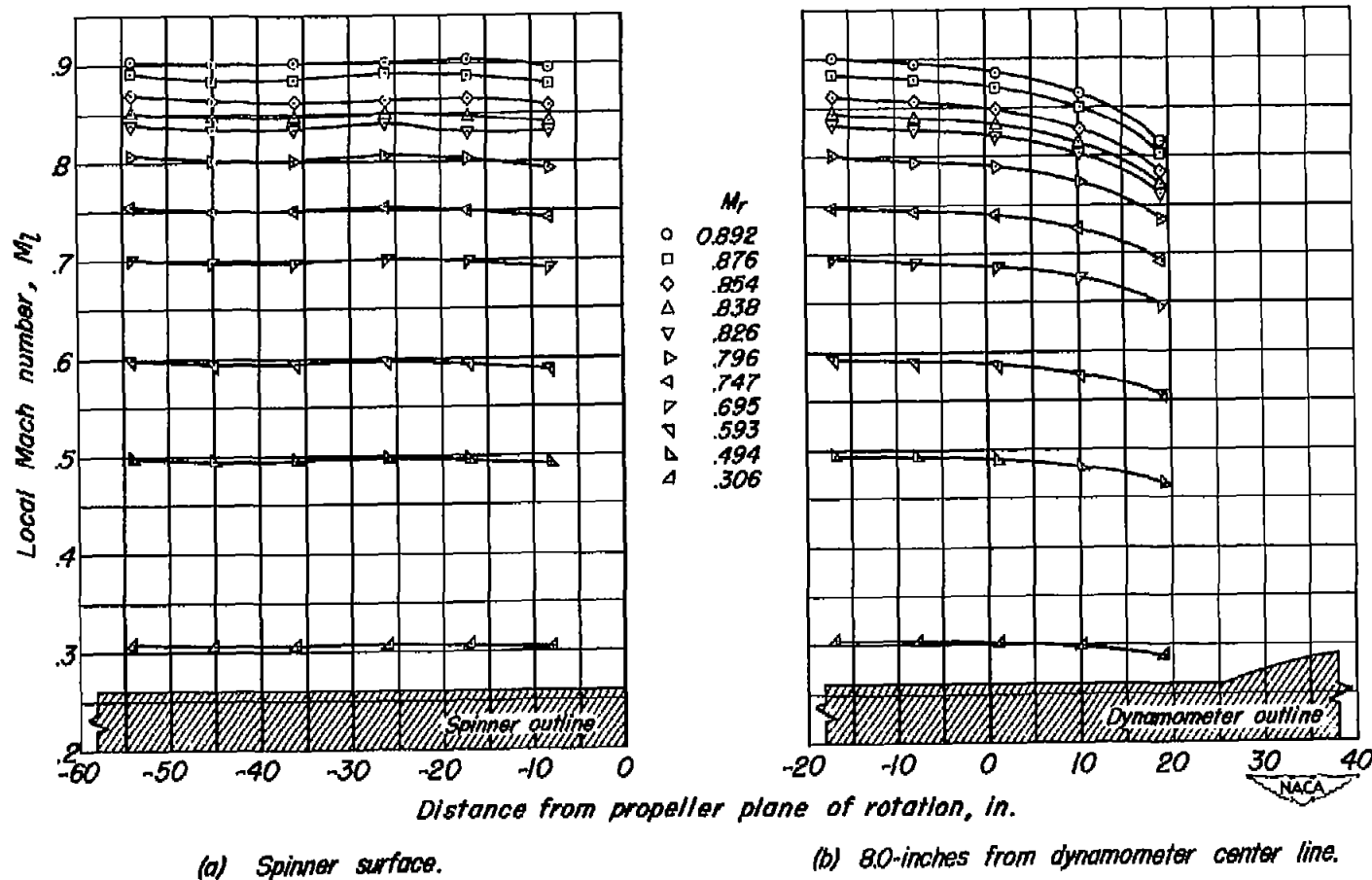
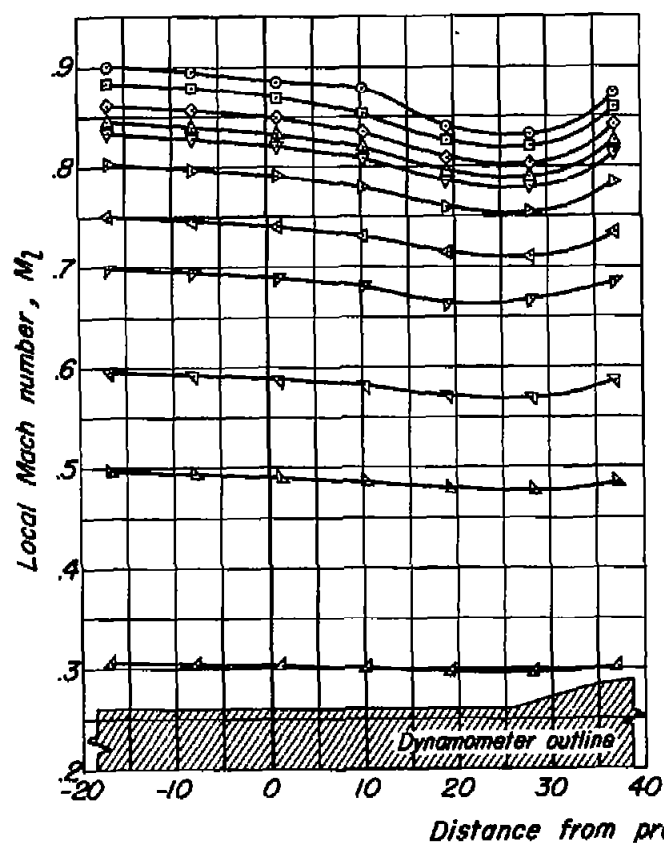
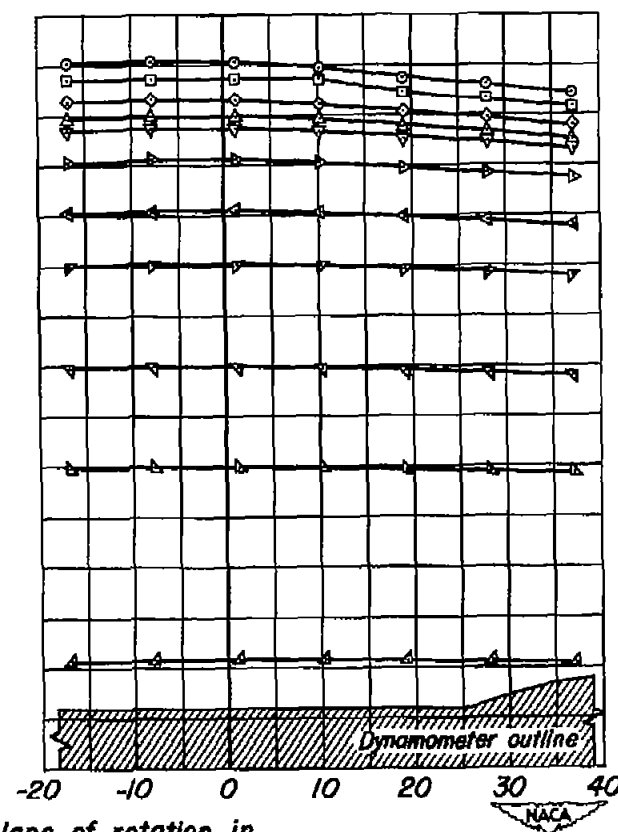


Figure 23.-The longitudinal variation of the local Mach number in the horizontal plane through the test-section center line for the dynamometer with the 12.00-inch-diameter, extended cylindrical spinner.



(c) 16.0-inches from dynamometer center line.



(d) 50.0-inches from dynamometer center line.

Figure 23-Concluded.

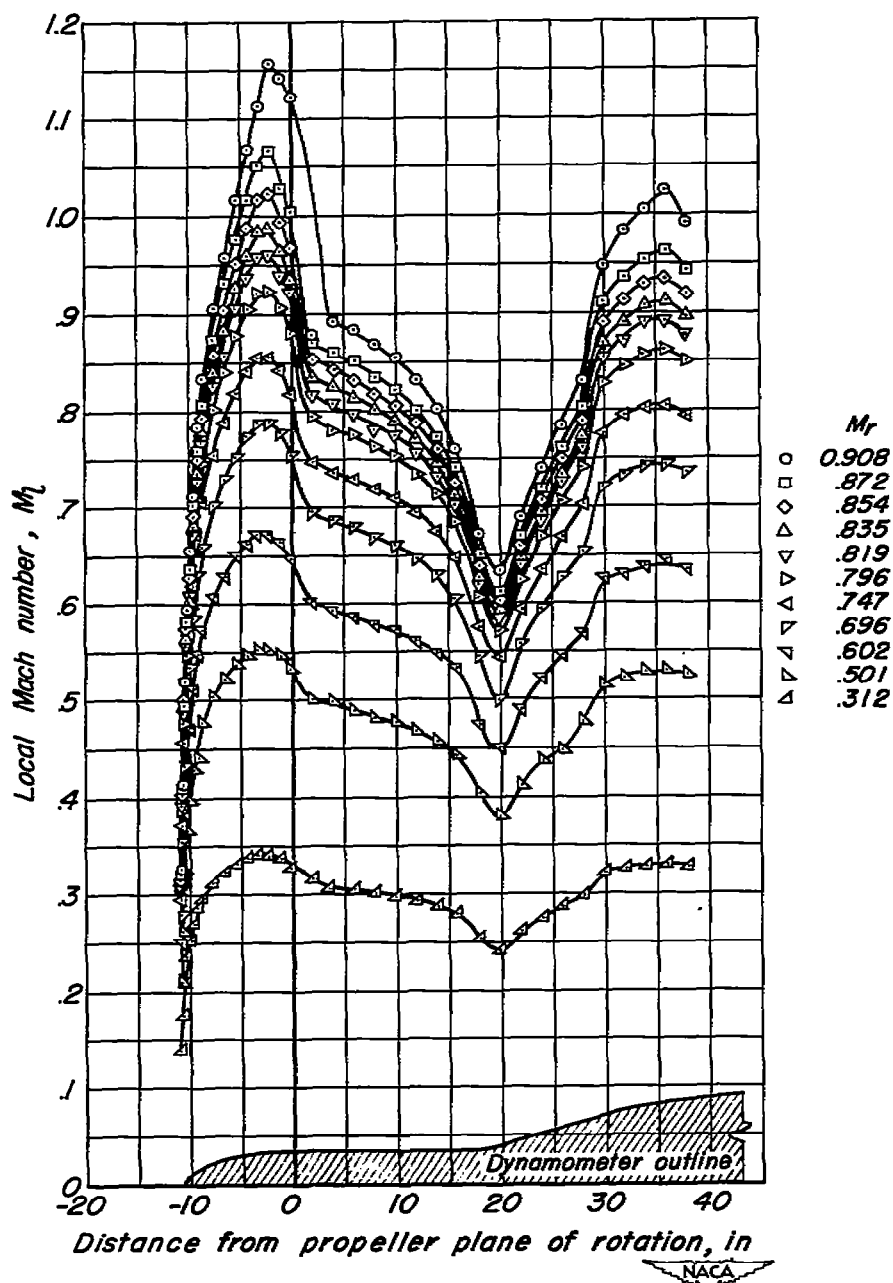


Figure 24.—The longitudinal variation of the local Mach number at the surface of the dynamometer mock-up with the 720-inch-diameter, I-series spinner.

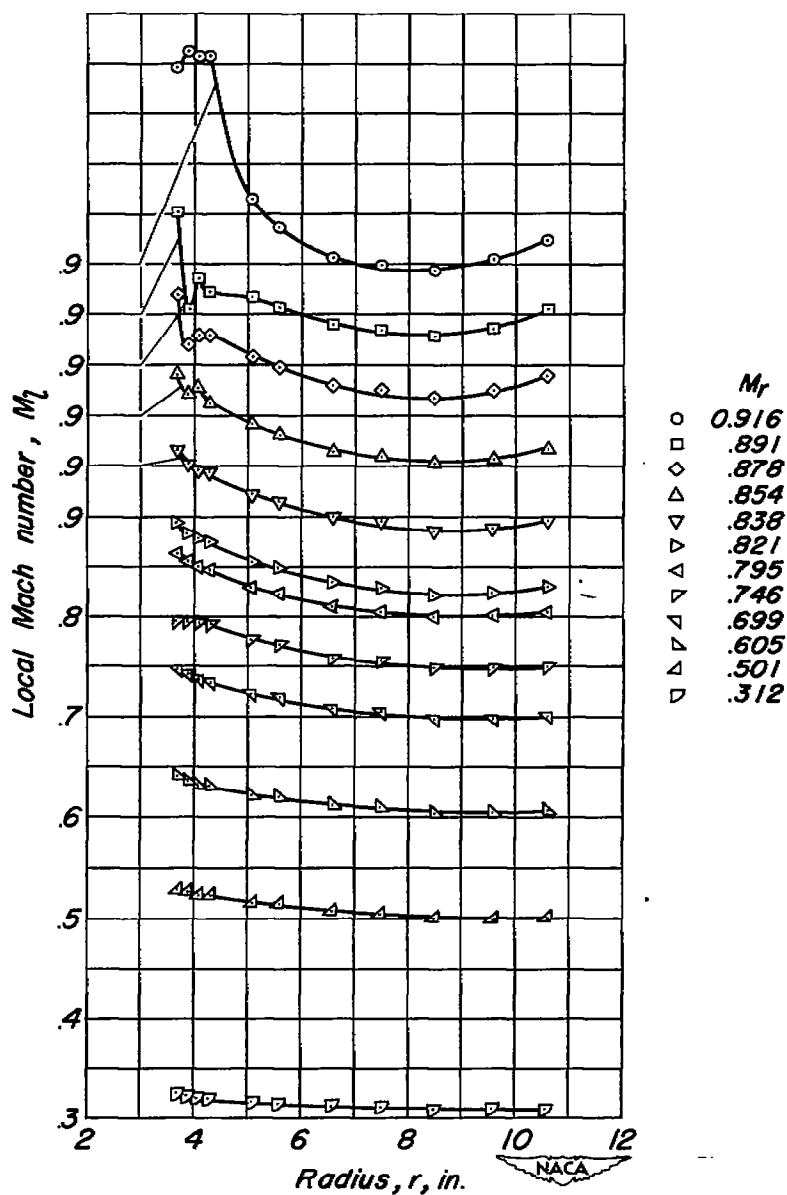


Figure 25.—The radial variation of the local Mach number at the propeller plane of rotation on the dynamometer mock-up with the 7.20-inch-diameter, I-series spinner.

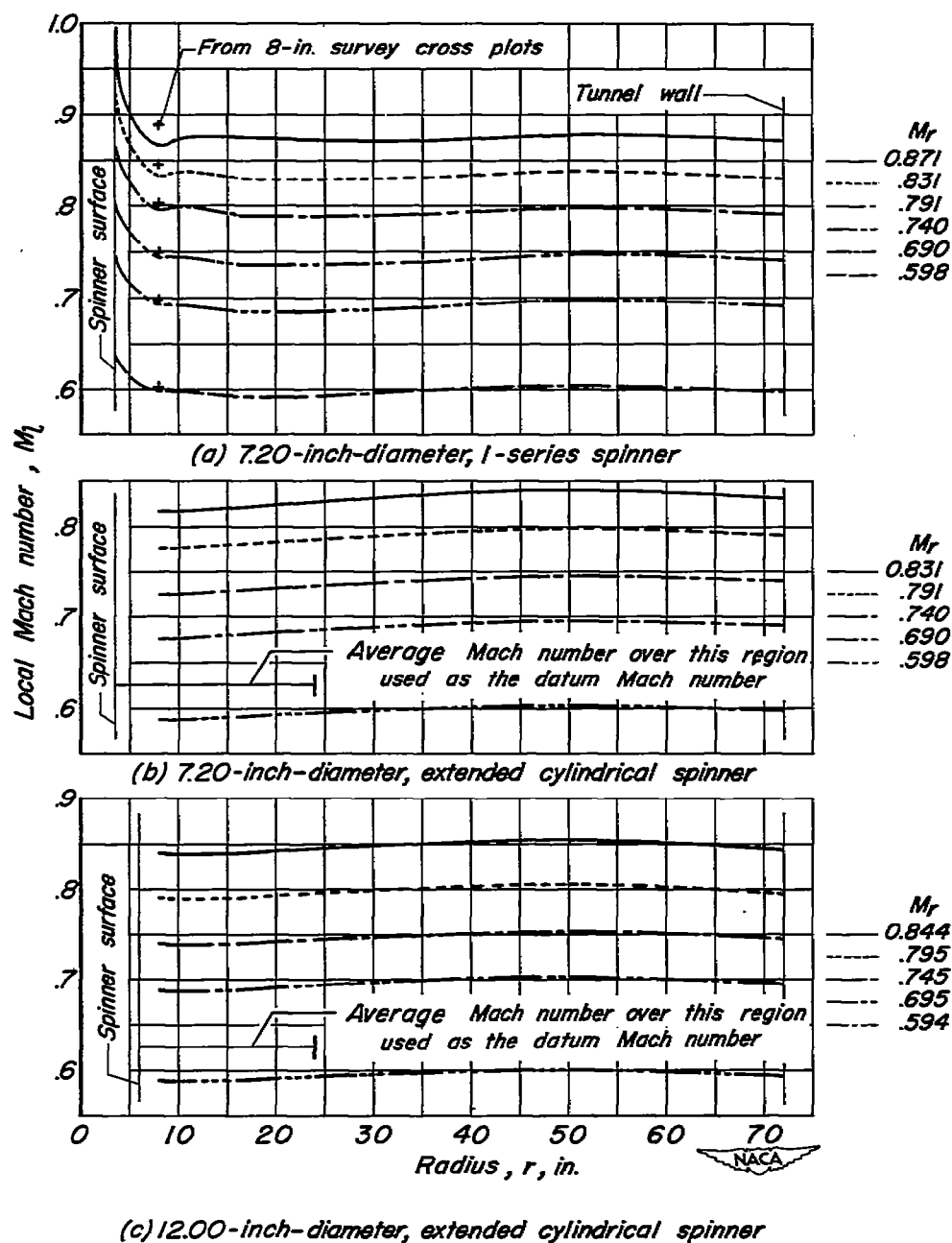


Figure 26.—The radial variation of the local Mach number at the propeller plane of rotation for various spinners.

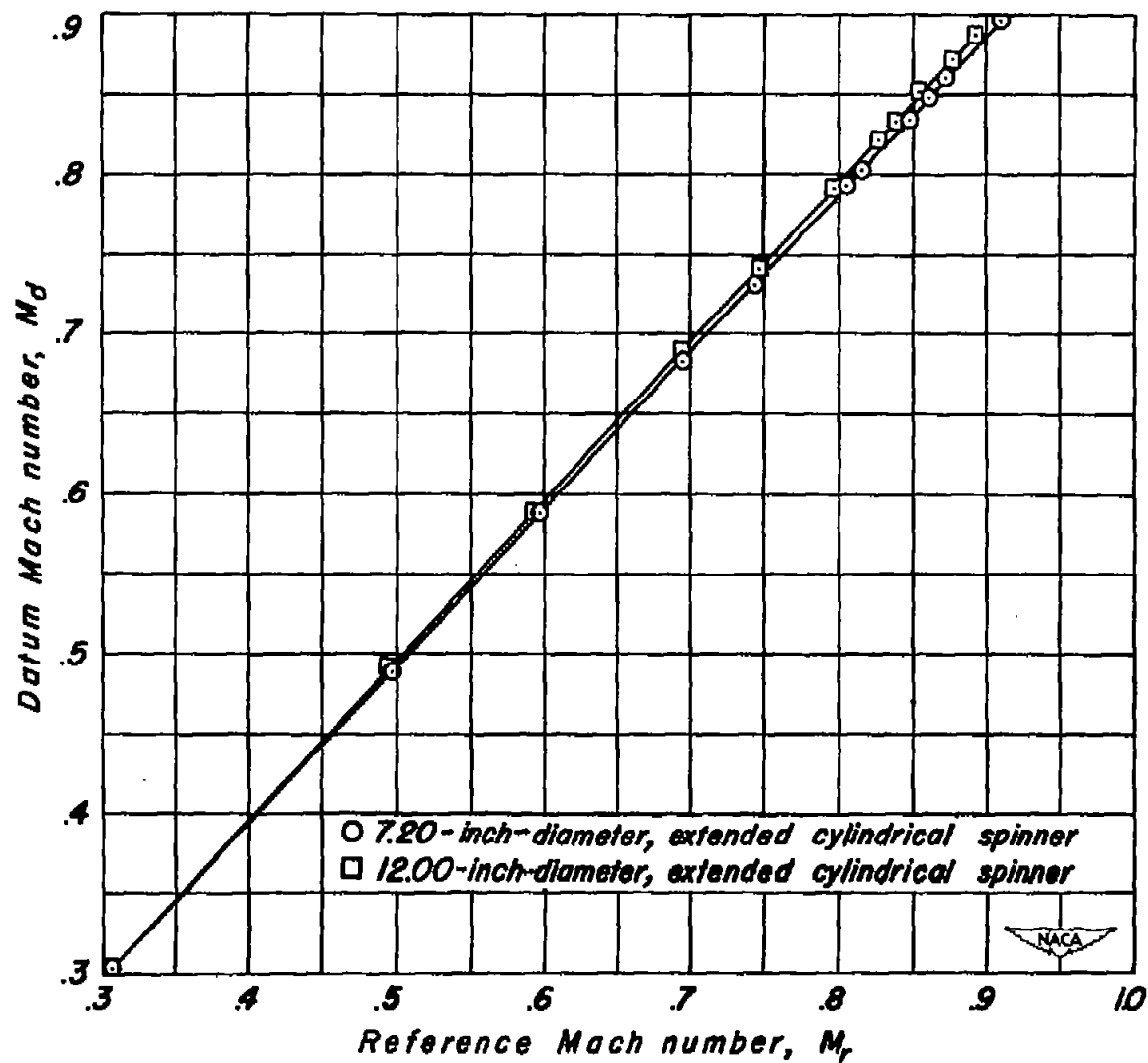


Figure 27.—The variation of the datum Mach number with the reference Mach number for the various spinners.

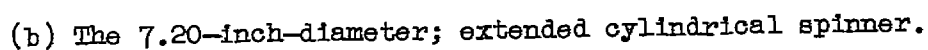


Figure 28.—Details of the flexible neoprene pressure seal, labyrinth, and static-pressure tap arrangement for the various spinners.

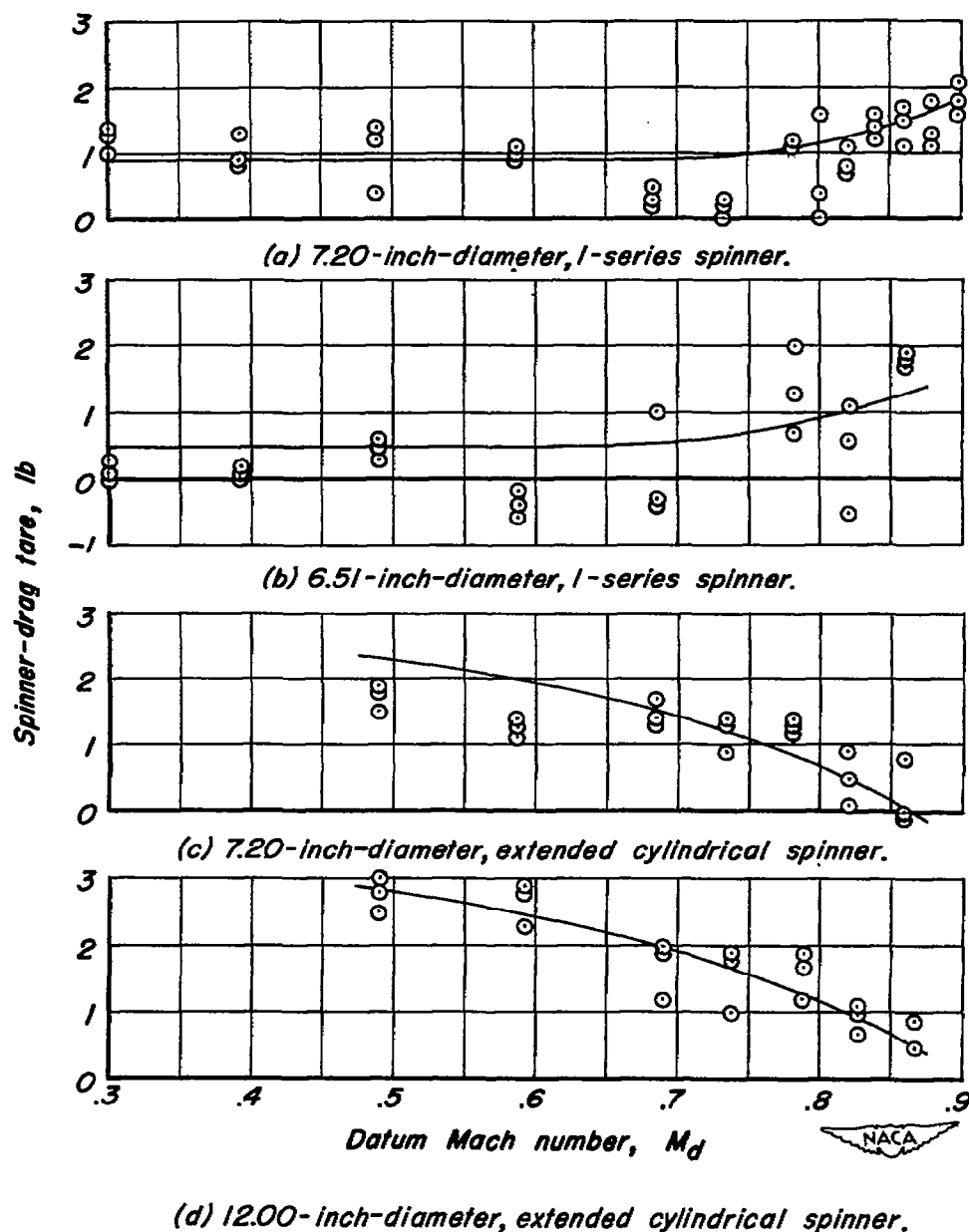


Figure 29.—The variation, with datum Mach number, of the spinner-drag tare corrections applied to the propeller thrust. $R_n, 1.5 \times 10^6$.